J-PARC

Japan Proton Accelerator Research Complex

Materials and Life Science Experimental Facility (MLF)

Contents

MLF neutron and muon instruments

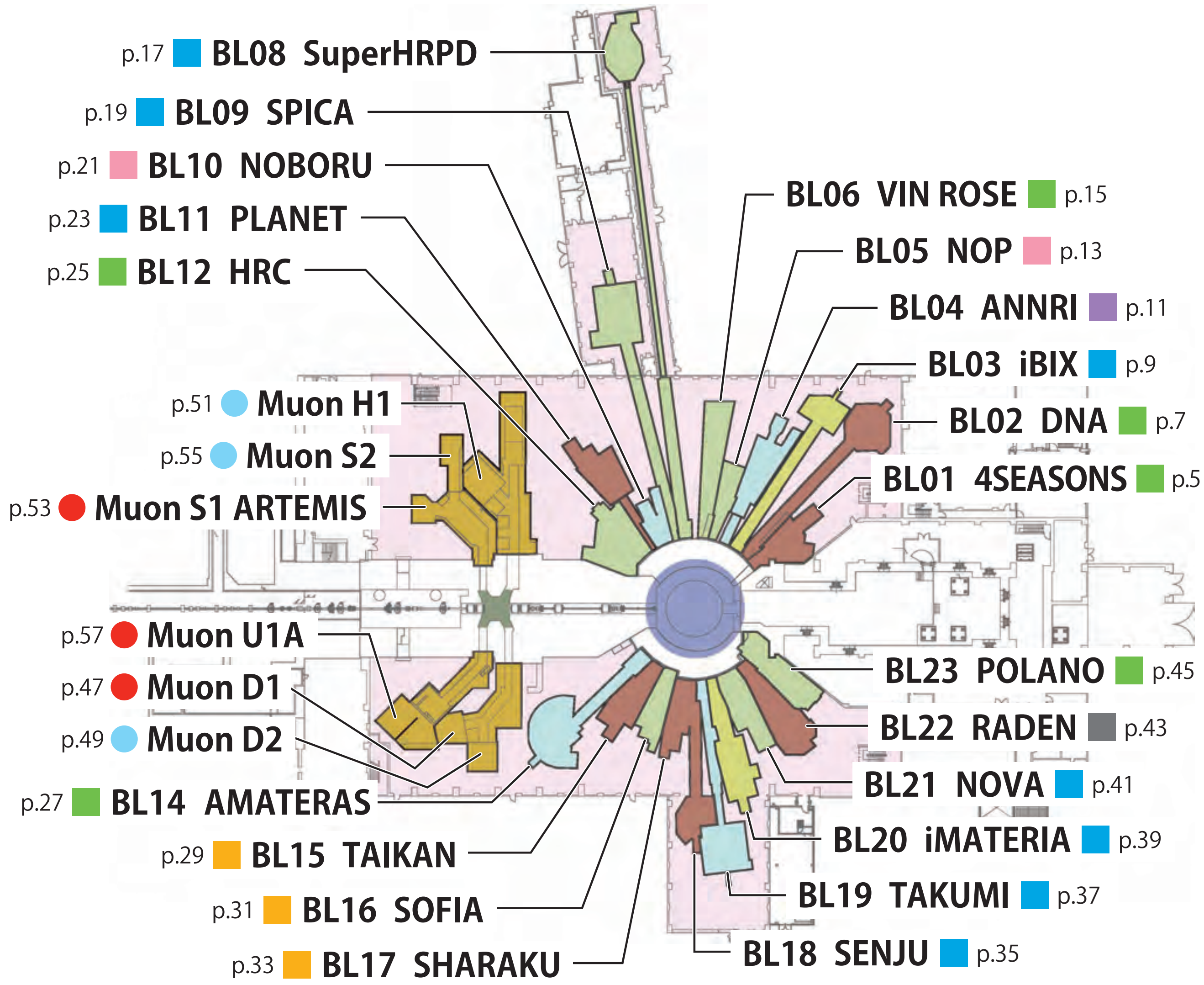

Measurement method of each instrument

- Quasi-elastic/inelastic neutron scattering
- Neutron diffraction
- Small-angle neutron scattering・Neutron reflectivity
- Neutron imaging
- Neutron-nuclear reaction/Prompt gamma-ray analysis
- Fundamental neutron physics/Neutron device development
- Muon spin rotation/relaxation/resonance
- Fundamental muon physics/Negative muon X-ray elemental analysis

Neutron instrument characteristics

The range covered by each instrument for (left) quasi-elastic / inelastic scattering and (right) diffraction. One could select an optimal instrument for ons's purpose.

Quasi-elastic/inelastic neutron scattering instruments

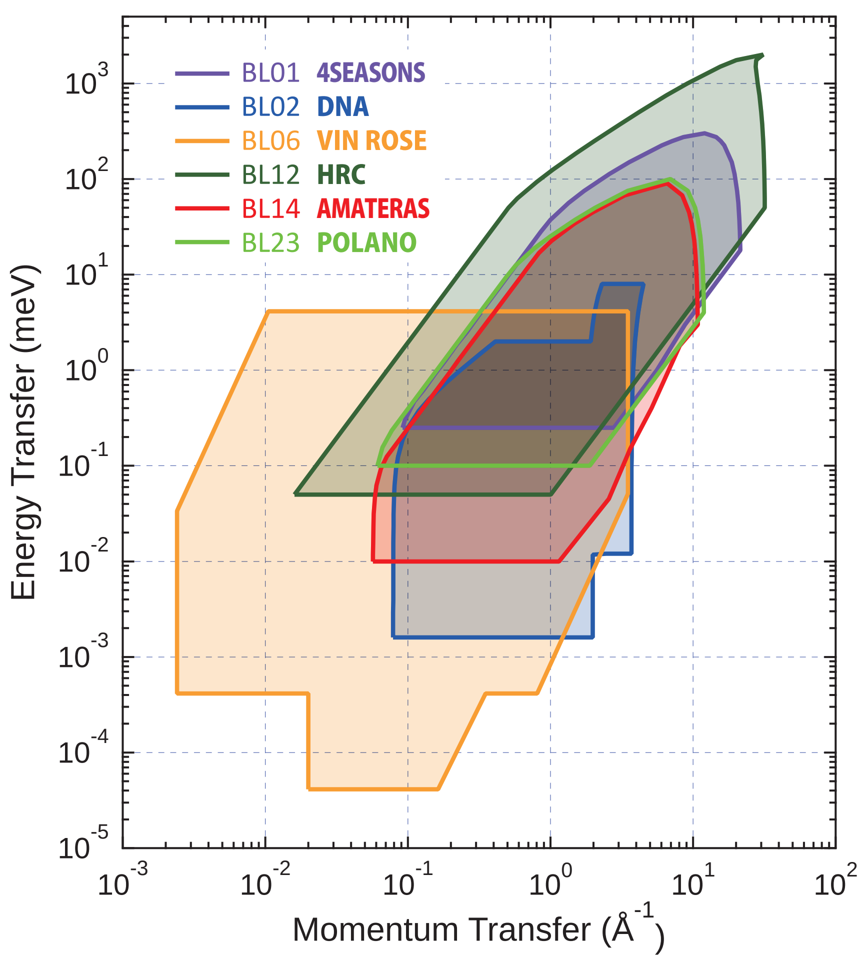

This figure is updated from the original figure of *Biochim. Biophys. Acta Gen. Subj.* 1861 (2017) 3651;
http://dx.doi.org/10.1016/j.bbagen.2016.04.025
(© 2016 The Authors. Published by Elsevier B.V.

Neutron diffractometers

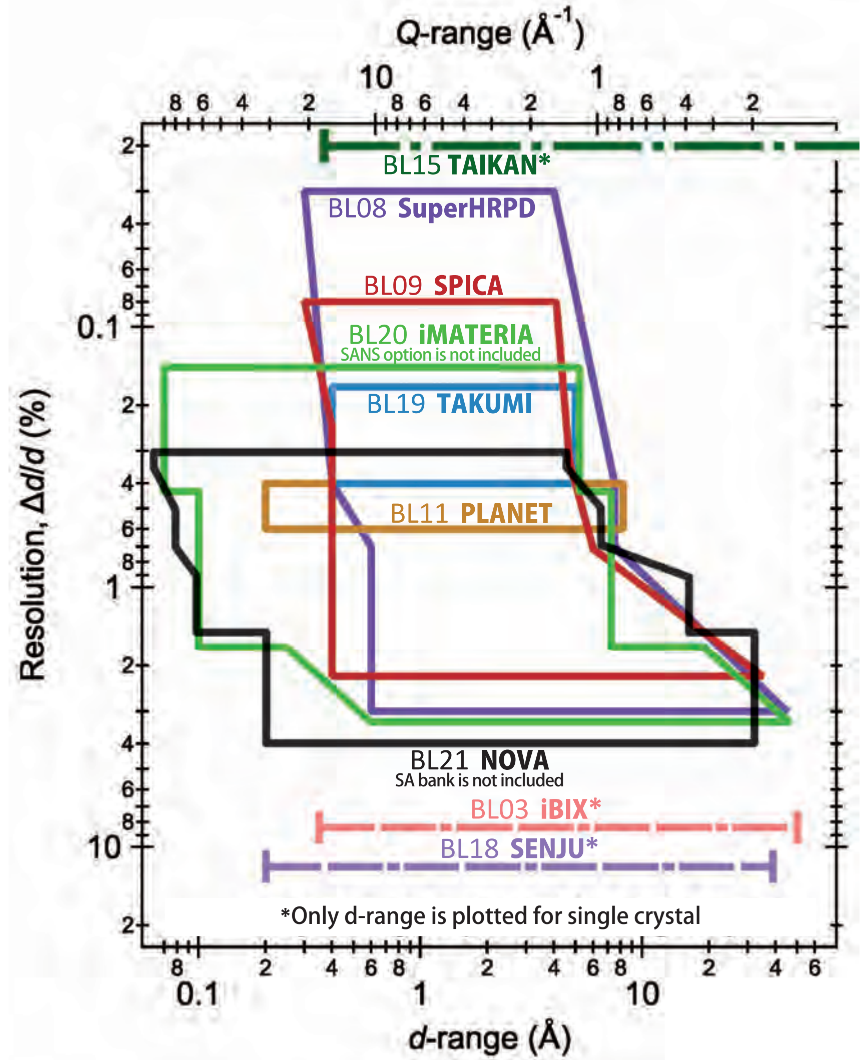

Data are added to the original figure of *Quantum Beam Sci.* 2017, 1(3), 9;
https://doi.org/10.3390/qubs1030009
(© 2017 The Authors. Licensee MDPI, Basel, Switzerland.)

List of neutron and muon instruments

Beamline number		Name of instrument	Capabilities	Page
■ Quasi-elastic/inelastic neutron scattering				
BL01	**4SEASONS**	4D-Space Access Neutron Spectrometer	Motion of spins, atoms, and molecules	5
BL02	**DNA**	Biomolecular Dynamics Spectrometer	Translational diffusion, rotation, vibration of atoms, molecules and spins	7
BL06	**VIN ROSE**	Village of Neutron Resonance Spin Echo Spectrometers	Atomic and molecular dynamics.	15
BL12	**HRC**	High Resolution Chopper Spectrometer	Spin, atoms, and molecular dynamics in solid state Spin wave dispersion measurements Phonon dispersion measurements of liquids	25
BL14	**AMATERAS**	Cold-Neutron Disk-Chopper Spectrometer	Lattice vibrations, magnetic excitations Diffusion and relaxation dynamics of atoms/molecules	27
BL23	**POLANO**	Polarized Neutron Spectrometer	Degrees of freedom in materials, such as atoms, molecules, spins, charges, and orbitals Cross-correlations of the degrees of freedom	45
■ Neutron diffraction				
BL03	**iBIX**	IBARAKI Biological Crystal Diffractometer	Crystal structure (single crystal)	9
BL08	**SuperHRPD**	Super High Resolution Powder Diffractometer	Crystal structure, magnetic structure	17
BL09	**SPICA**	Special Environment Powder Diffractometer	Crystal structure, magnetic structure	19
BL11	**PLANET**	High Pressure Neutron Diffractometer	Crystal structure, structure of liquid and amorphous (high pressure)	23
BL18	**SENJU**	Extreme Environment Single Crystal Neutron Diffractometer	Crystal structure, magnetic structure (single crystal)	35
BL19	**TAKUMI**	Engineering Materials Diffractometer	Crystal structure, lattice strain, crystal defects, crystal orientation (texture)	37
BL20	**iMATERIA**	IBARAKI Materials Design Diffractometer	Crystal structure, crystal orientation (texture), local structure of amorphous, nanostructure	39
BL21	**NOVA**	High Intensity Total Diffractometer	Local structure of liquids and amorphous, crystal structure, magnetic structure	41

Beamline number		Name of instrument	Capabilities	Page
■ Small-angel neutron scattering / Neutron reflectometry				
BL15	**TAIKAN**	Small and Wide Angle Neutron Scattering Instrument	Nanostructure, magnetic structure	29
BL16	**SOFIA**	Soft Interface Analyzer	Nanostructure of interface	31
BL17	**SHARAKU**	Polarized Neutron Reflectometer	Nanostructure, magnetic structure of interface	33
■ Neutron imaging				
BL22	**RADEN**	Energy Resolved Neutron Imaging System	2D transmission images, 3D tomography images, spatial distribution of crystal structure, magnetic field, nuclide, and temperature	43
■ Neutron-nuclear reaction, Prompt gamma-ray analysis				
BL04	**ANNRI**	Accurate Neutron-Nucleus Reaction Measurement Instrument	Basic properties of unstable isotopes elemental analysis elucidation of non-equilibrium phenomena	11
■ Fundamental neutron physics, Neutron device development				
BL05	**NOP**	Neutron Optics and Fundamental Physics	Basic properties of neutrons Neutron optics	13
BL10	**NOBORU**	NeutrOn Beam-line for Observation and Research Use	Test port for cold, epithermal, and high energy neutrons	21
● Muon spin rotation, relaxation and resonance				
D1	**Muon D1**	Muon Spectrometer for Materials and Life Science Experiments	Electronic states, magnetic states, dynamics of electrons, hydrogen, and ions	47
S1	**ARTEMIS**	General Purpose μSR Spectrometer	Electronic states, magnetic states, dynamics of electrons, hydrogen, and ions	53
U1A	**Muon U1A**	Ultra-Slow Muon Microscope	Electronic states, magnetic states, and dynamics of electrons, hydrogen, and ions at surfaces and interfaces	57
● Fundamental muon physics / Negative muon X-ray elemental analysis				
D2	**Muon D2**	Muon Experimental Area for Basic Science	Elementary particle reactions	49
H1	**Muon H1**	High-intensity Muon Beam for General Use	Fundamental physical quantities of muons, particle physics	51
S2	**Muon S2**	Muonium Laser Physics Apparatus	Fundamental physical quantities of muons	55

BL01

Quasi-elastic/inelastic neutron scattering

4D-Space Access Neutron Spectrometer (4SEASONS)

High-efficient observation of spin and lattice dynamics over four-dimensional momentum and energy space

Instrument Description

- Medium-resolution thermal-neutron spectrometer using a Fermi chopper
- High efficient measurements through a combination of efficient beam transport, large area detector, and use of multiple incident energies

Specifications

- Measurable energy: 1 to 300 meV
- Scattering angle range Horizontal : −35° to +130°
  Vertical : −25° to +27°
- Energy resolution: About 5% of incident energy
- Beam size (variable): Max. 45mm × 45mm
  Optimum 20mm × 20mm

Sample Environments

- Closed-cycle refrigerator
  (5 to 300 K; up to 600 K with high-temperature option)
- Radial collimator
  (Please inquire about the appropriate sample size)
- Other MLF-shared sample environment devices

Instrument Configurations

Beam transport guide tube

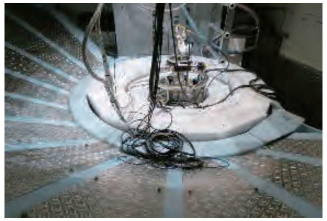

Vacuum scattering tank and refrigerator

Large-area neutron detector

CONTACT

Ryoichi KAJIMOTO
ryoichi.kajimoto@j-parc.jp
JAEA

Mitsutaka NAKAMURA
mitsutaka.nakamura@j-parc.jp
JAEA

Kazuya KAMAZAWA
k_kamazawa@cross.or.jp
CROSS

4D-Space Access Neutron Spectrometer (4SEASONS)

BL01

Capabilities

- Observation of motion of spins, atoms, and molecules in the momentum and energy range of 0.1 Å^{-1} to 20 Å^{-1} and 1 meV to several 100 meV
- Determination of the couplings between spins, atoms, and molecules, and their relationship to magnetic and structural properties

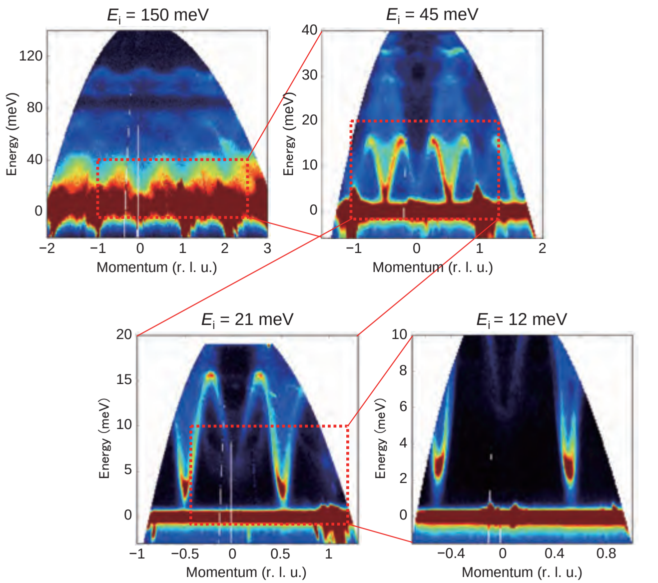

Excitation spectra of $CuGeO_3$ measured using multiple incident energies (E_is) simultaneously

Applications

- Magnetic excitations and lattice vibrations in superconductors
- Novel magnetism in quantum magnets, frustrated magnets [1], and itinerant magnets [2]
- Lattice vibrations in thermoelectric materials
- Excess excitations in glasses
- Lattice vibrations in catalysts

Superconductivity and polarity of magnetic excitation in an iron-based superconductor

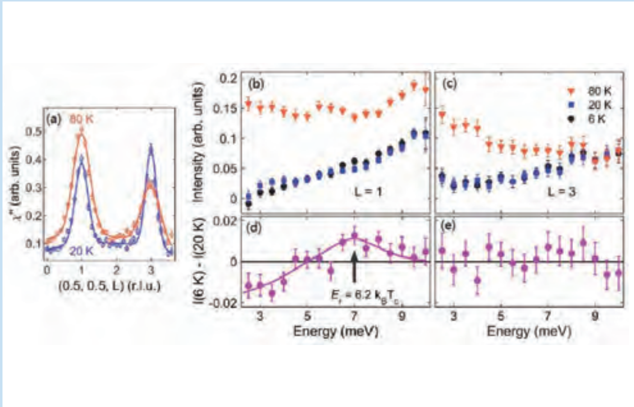

J. Guo *et al.*, *Phys. Rev. Lett.* **122**, 017001(2019) (© 2019 American Physical Society).

Topological spin excitations in a three-dimensional antiferromagnet

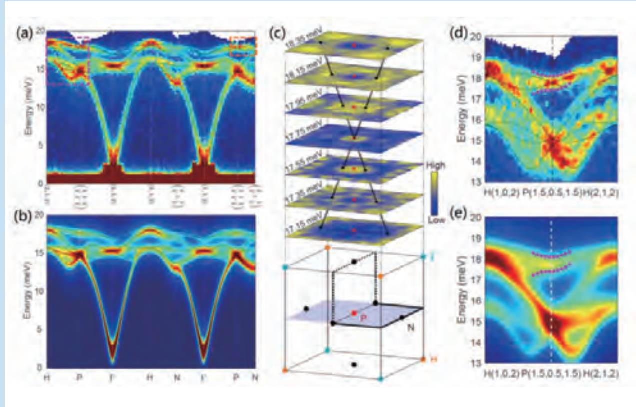

W. Yao *et al.*, *Nat. Phys.* **14**, 1011(2018) (© 2018 Nature Publishing Group).

For 1) and 2) , see Glossary (p.61)

BL02 Biomolecular Dynamics Spectrometer (DNA)

Quasi-elastic/inelastic neutron scattering

Elucidation of functional origins of materials by measuring atomic and molecular dynamics in nanosecond order

Instrument Description

- High energy resolution (~μeV) in a wide dynamic range (meV)
- Flexible energy resolution and dynamic range by changing pulse-shaping choppers
- High efficiency and high signal-to-noise ratio (~10^5) owing to back coated Si-analyzers

Specifications

- Dynamic range：–500 to 1500 μeV : Si(111), –2000 to 6000 μeV : Si(311)
- Q-range $0.08 < Q < 1.98$ [$Å^{-1}$] : Si(111), $1.79 < Q < 3.39$ [$Å^{-1}$] : Si(311)
- Energy resolution：
  Si111 1 cm slit : 2.2 μeV (300 Hz), 2.4 μeV (225 Hz)
  Si111 3 cm slit : 3.1 μeV (300 Hz), 3.6 μeV (225 Hz)
- Beam size：3 cm (vertical) × 2 cm (horizontal)

Sample Environments

- Top-loading cryofurnace (7 K < T < 650 K)
- Sample changer（3samples, 20samples）
- Liquid Pressure Cell (0.1 < P < 145[MPa], room temp.)
- Humidity control system
- High electric voltage cell（E < 1.5 kV, < 200℃）, High electric current cell（I < 5 A, < 200℃）

Instrument Configurations

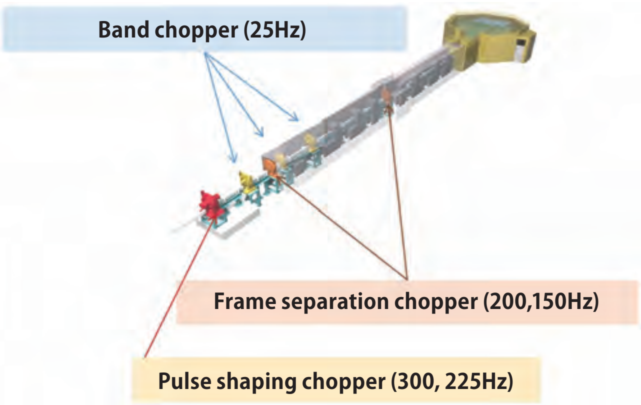

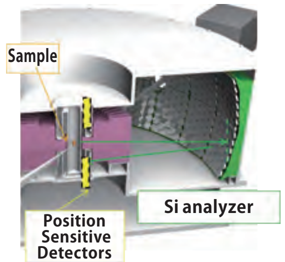

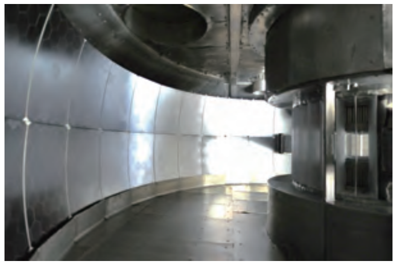

TOF-type near backscattering spectrometer using perfect Si111 and Si311 crystal analyzers

CONTACT

Masato MATSUURA CROSS

Hiromu TAMATSUKURI JAEA

Contact：mlf-bl02@ml.j-parc.jp

Biomolecular Dynamics Spectrometer (DNA)

BL02

Capabilities

- Dynamics of atoms, molecules, ions, and spins in wide dynamic range from pico to nano seconds
- Translational diffusion, rotation, vibration, spin gap

Applications

- Biomacromolecules (proteins, lipids, foods)
- Soft materials (polymers, ionic liquids, hydrated water, rubbers)
- Functional materials (batteries, catalyst, ferroelectrics)
- Magnetism

Rotational tunneling spectra of methyl groups of N-γ-picoline

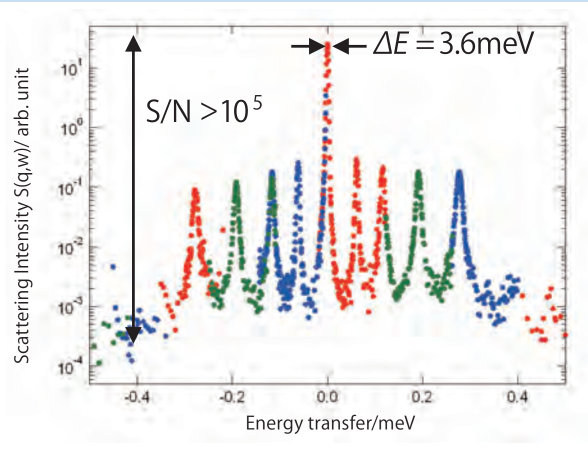

Dynamics of water in fuel cell catalyst

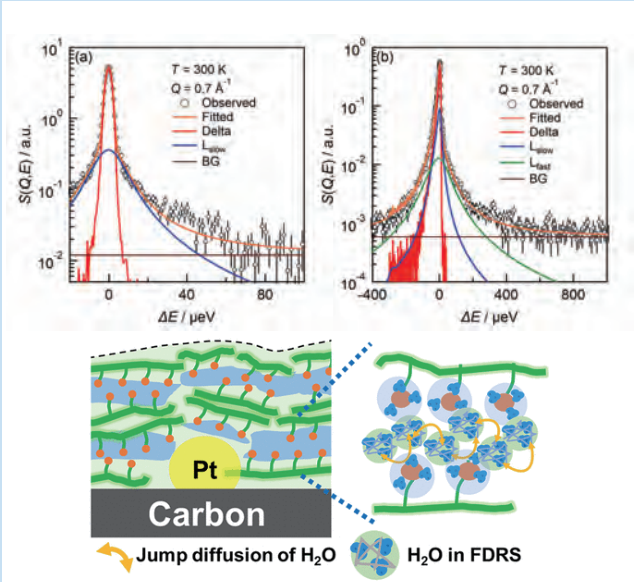

Reveal the hierarchical dynamics of water in fuel cell catalyst

K. Ito, *et al.*, J. Phys. Chem. C 125, 12645 (2021).
(©2021American Chemical Society)

Magnetic anisotropy gap in multiferroic $Ba_2MnGe_2O_7$

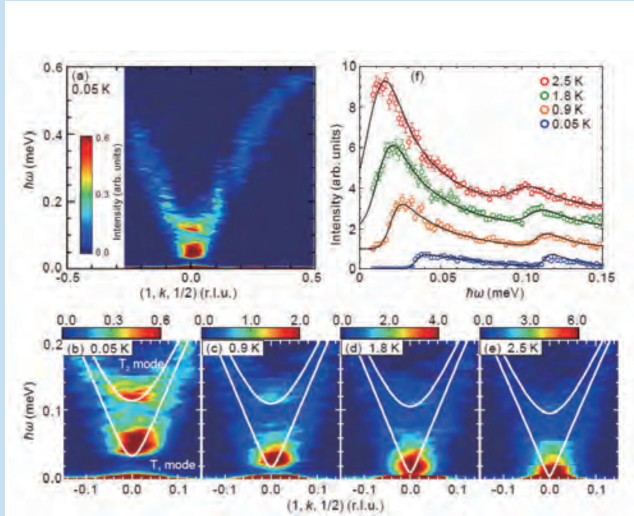

Reveal tiny spin gaps due to spin-nematic interactions equivalent to the interactions of electric polarization

S. Hasegawa *et al.*, Phys. Rev. Research 3, L032023 (2021).
(©2021American Physical Society)

BL03 IBARAKI Biological Crystal Diffractometer (iBIX)

Neutron diffraction

Single crystal neutron diffractometer for observation of hydrogen and hydration structure of macromolecules and organic compounds with high efficiency and high resolution

Instrument Description

- High measurement efficiency by a wide wavelength range. The development of a high-resolution two-dimensional detector enables highly efficient measurement of protein structure analysis data.
- The open space around the sample allows for the free placement of various sample environment.

Specifications

Specification （@1MW）

- Max. Cell dimension：135 × 135 × 135 Å^3 (Demonstrated by single crystal structure nalysis of manganese catalase, which has the largest crystal lattice volume)
- Sample volume：< 1 mm^3
- Measurement time ：4 days

Sample Environments

- Gas flow type cooling system （100 - 300 K）
- Heating device（300 - 600 K）
- Stretching device （Max. load：200 N, Max. stretching length：90 mm, Speed：1 - 1000 µm/sec）


Stretching device

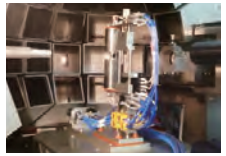
Heating device

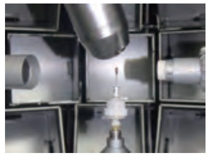
Gas flow type cooling system

Instrument Configurations

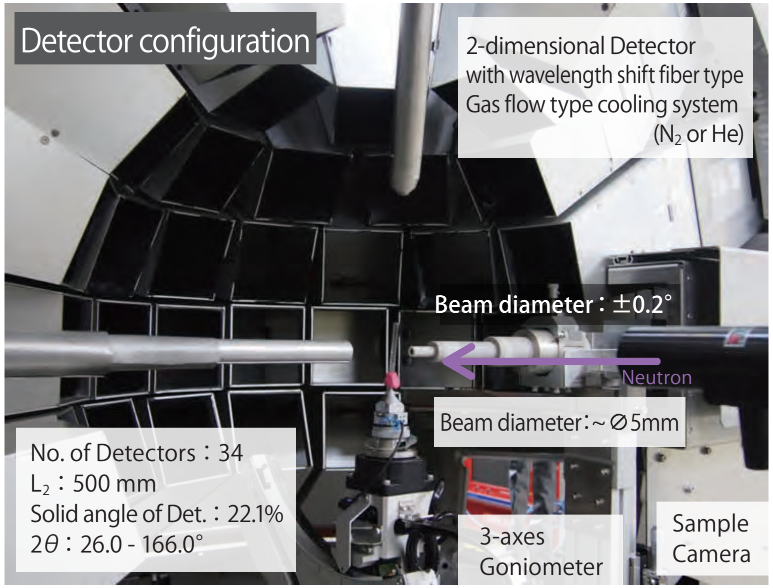

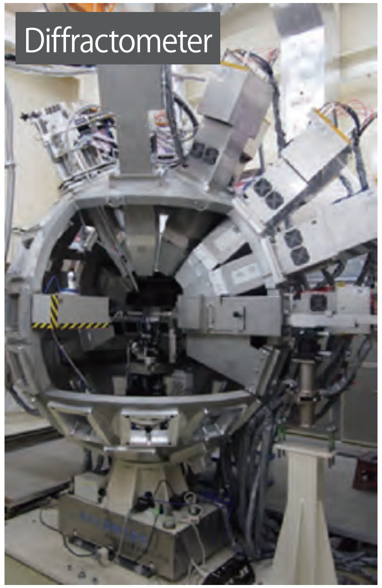

CONTACT

Katsuhiro KUSAKA
k_kusaka@cross.or.jp

Terutoshi SAKAKURA
t_sakakura@cross.or.jp

Haruki SUGIYAMA
h_sugiyama@cross.or.jp

IBARAKI Biological Crystal Diffractometer (iBIX)

J-PARC MLF

J-PARC

BL03

Capabilities

- The presence or absence of hydrogen bonds between proteins and inhibitors, and proton tautomerism, based on the positions of hydrogen atoms in proteins
- Positions of hydrogen atoms of OH, NH, and NH_2 in the side chains of amino acid residues
- The presence of water molecules expected from the existence of the exchangeable hydrogen by heavy water.
- Positions of hydrogen atoms around heavy elements, which are difficult to detect using X-rays
- Protein structure at room temperature with minimal radiation damage
- Undamaged structure of oxidoreductase that undergoes structural changes in X-rays
- Information on hydrogen bonds and hydrophobic interactions in protein-compound interactions

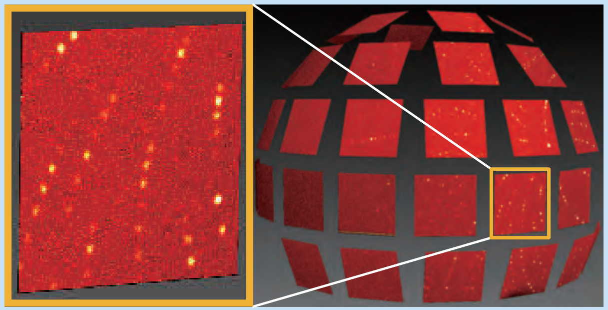

TOF diffraction pattrern of a protein crystal

Applications

- Observation of hydrogen-bond network caused the stabilization of transthyretin tetramer associated with human amyloidosis.
- Visualization of newton's cradle proton relay with amide-imidic acid tautomerization in Hydrolysis process of cellulase that catalyze cellulolysis.
- Two hydrogenation states and structural features of the bilin reductase PcyA that synthesizes photoreceptor pigment and substrate complex.
- Neutron crystal structure of catalase with the largest unit cell volume (135X135X135Å) of all neutrons structure analyses.
- Observation of keto/enolate interconversion of the quinone cofactor and unusual proton sharing between the cofactor and the catalytic base in copper amine oxidase
- Experimental evidence of the electron transfer pathway in the catalytic reaction of the copper-containing nitrite reductase play an important role for the Earth's nitrogen cycle.

The ingenious mechanism of enzyme catalysis revealed by unusual proton sharing by successful high-resolution neutron crystallography of a large protein

Background

- Copper amine oxidase : An enzyme that decompose primary amines into aldehydes and ammonia. Containing a Cu^{2+} ion and the protein-derived quinone cofactor topa quinone (TPQ). This enzyme in human serum is also involved in the onset of diabetes.
- Visualization of hydrogen atom positions is necessary to understand the details of the enzyme reaction mechanism of copper amine oxidase.

Breakthrough in this research

- Successfully performed neutron crystal structure analysis of a large protein (molecular weight:70,600) far exceeding previous records
- Revealing the precise position of hydrogen ions, essential for elucidating the mechanism of enzyme reactions

The huge crystal used in neutron crystallography

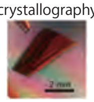

Neutron crystal structure of AGAO

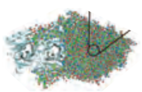

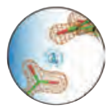

Unusual proton sharing between the cofactor and the catalytic base

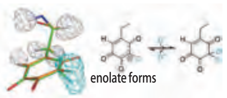

The equilibrium between the enolate and the keto forms of TPQ. It was previously assumed to be an enolate form.

Contributions by iBIX

High-precision, high-resolution neutron structure analysis data for copper amine oxidase could be obtained and successfully determined its three-dimensional structure, including hydrogen atoms

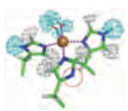

Active-site H-bond network and Cu^{2+}-coordination structure.
His is exist as an imidazolate anion (fully deprotonated form)

Significance of research results

- The result of this study will greatly expand the scope of application of neutron crystal structure analysis. It is expected that this will lead to the determination of the three-dimensional structures including hydrogen atoms for high-molecular-weight proteins and target proteins for Drug Discovery.
- This results demonstrate that neutron crystal structure analysis can reveal the existence of previously unsuspected structures and reaction mechanism.

The reaction mechanism of an enzyme play an important role for the Earth's nitrogen cycle

– High-precision determination of the all-atom structure of copper-containing nitrite reductase (CuNIR) –

Background

- CuNIR: Copper-containing nitrite reductases (CuNIRs) transform nitrite to gaseous nitric oxide, which is a key process in the global nitrogen cycle.
- To understand the details of the CuNIR chemical reaction (the process in which hydrogen ions are transferred to nitrite ions), it is necessary to determine the hydrogen atom positions.

Breakthrough in this research

- It is found that a hydroxide ion can exist as a ligand to the catalytic Cu atom in the resting state
- The results of this sutudy indicates the possibility of correctly rewriting the chemical reaction mechanism proposed by previous experiments, and succeeded in obtaining experimental evidence for the pathway through which electrons necessary for the reaction within the protein.

Neutron crystal structure of CuNIR

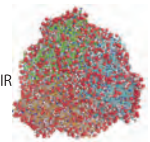

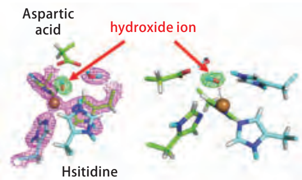

Hydroxide ions bound to copper ions (brown spheres) observed in CuNIR

Contributions by iBIX

Obtained high-precision, high-resolution neutron structure analysis data from CuNIR and successfully determined the three-dimensional structure including hydrogen atoms

Future development

- Industrial applications: Use of microorganisms with enhanced denitrification activity, development of artificial enzymes
- Reduction of nitrous oxide gas (greenhouse gas) = Contribution to improving the air quality, reduction of excess nitrogen compounds that flow into the environment as fertilizer = Contribution to improving environmental pollution

Accurate Neutron-Nucleus Reaction Measurement Instrument (ANNRI)

Instrument precisely measuring prompt γ-rays produced in neutron capture reactions for research related to nuclear science, such as nuclear data measurement, elemental analysis, and astrophysics.

Instrument Description

- Several γ-ray detectors are available for precise measurement:
  - Ge cluster detectors with high energy resolution,
  - Large NaI(Tl) detectors with good time resolution,
  - $LaBr_3$ detector with low dead time.
- Li-glass detectors capable of measuring transmission neutrons.

Specifications

- Neutron energy range: $E_n > 0.0015$ eV
- γ-ray detector : Ge spectrometer (Flight path: 21.5 m)
  :NaI (Tl) detector (Flight path: 28 m)
  :$LaBr_3$ detector (Flight path: 28.5 m)
- Neutron detector: Li-glass detector
  (Flight path: 28.5 m)

Peripheral Equipment

- Variable Collimator
  Adjustable beam sizes: ∅22, 15, 7, 6mm
- Automatic sample changer
  ～ Automatic exchange of up to 200 samples
- Double disk chopper
  cuts lapsed low-energy neutrons
- Movable neutron filter
  (Pb, Mn+Co+In+Ag, Cd)
  Reduction of γ-rays on neutron beam
  Adjustment of Neutron beam intensity, B.G. estimation

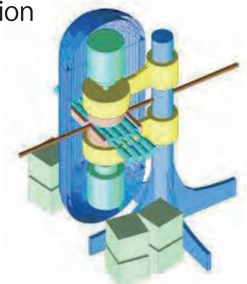

Instrument Configurations

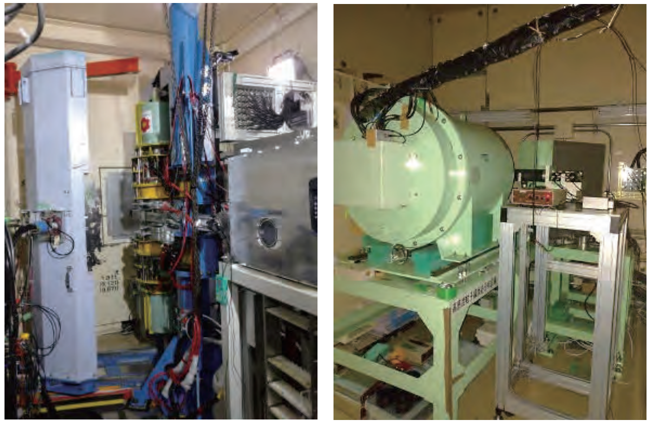

ANNRI
Ge spectrometer (left), and NaI and Li -glass detectors (right)

Development of Radiation Detector

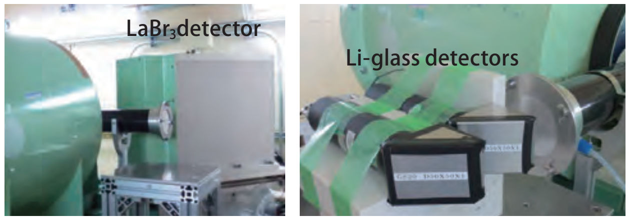

Development of Data Acquisition (DAQ) System

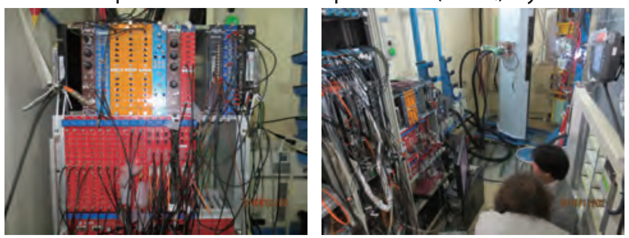

DAQ System(CAEN modules)   System Development

CONTACT

Atsushi KIMURA
kimura.atsushi04@jaea.go.jp

Mariko SEGAWA
segawa.mariko@jaea.go.jp

Accurate Neutron-Nucleus Reaction Measurement Instrument (ANNRI)

Capabilities

Capture cross section measurement for ^{244}Cm(half-life 18 years)

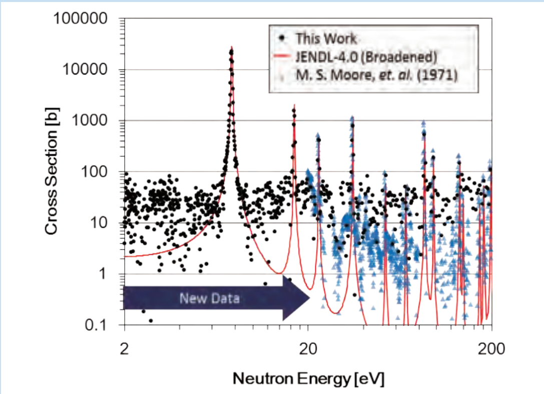

A. Kimura et al. J. Nucl. Sci. Technol. 2012, vol. 49, 708-724
(© 2012 Taylor and Francis Group)

Total cross section measurement for ^{241}Am

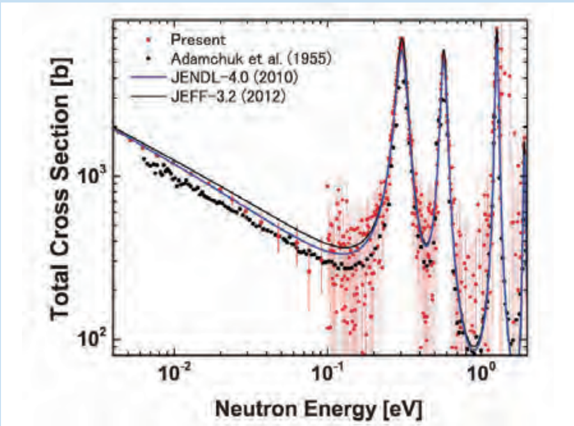

K. Terada et al. J. Nucl. Sci. Technol. 2018, vol. 55, 1198-1211
(© 2018 Taylor and Francis Group)

Applications

- Neutron capture cross section studies of Minor actinides (Cm isotopes, Am isotopes, ^{237}Np, etc.) using the Ge spectrometer and the large NaI spectrometer
- Measurements of total neutron cross sections of Am isotopes using the Li-Glass Detectors
- Development of a new prompt gamma-ray analysis method using the time-of-flight method
- Study of ^{112}Cd(n,γ) reaction for astronomical origin of ^{115}Sn
- CP violation in compound nuclear resonance

Nuclear data research for nuclear transmutation

Transmutation is a method of convert nuclear waste nuclides such as minor actinides (MAs) and long-lived fission products (LLFPs) into stable nuclides through nuclear reactions.

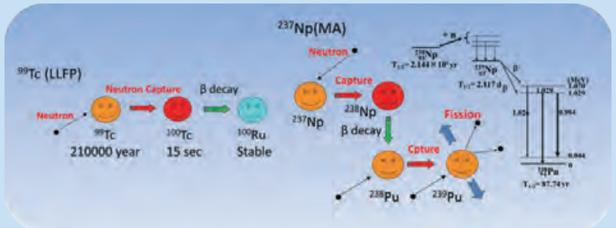

For the design study of transmutation systems, it is essential to improve the accuracy of the neutron capture reaction cross section, i.e., the ease of neutron capture reaction (red arrow).

A neutron-nuclear reaction measurement instrument (ANNRI) has been installed at MLF, and research is being conducted to improve the accuracy of nuclear data such as neutron capture reaction cross sections.

Prompt gamma-ray analysis using the TOF

By using the world's most intense pulsed neutron beam, high-efficiency Ge detectors, high speed DAQ and high-efficiency shielding, we succeeded for the first time in the world in developing a new analytical method that combines two non-destructive elemental analysis methods.
The synergistic effect of the fusion of the new analytical methods has demonstrated that even elements that are difficult to analyze using either method can be analyzed accurately.

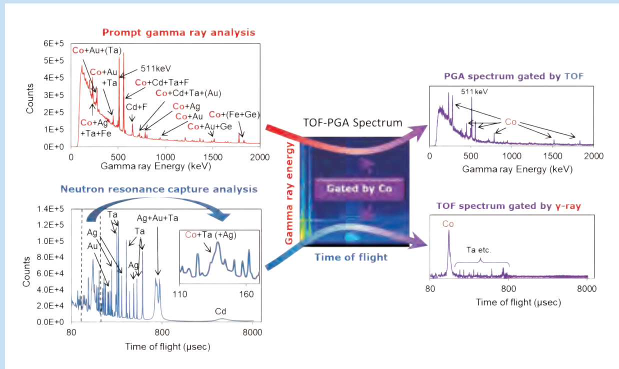

BL05

Fundamental neutron physics/
Neutron device development

Neutron Optics and Fundamental Physics (NOP)

Beamlines for fundamental physics experiments using state-of-the-art neutron optics technology to explore the origins of matter and the universe.

Instrument Description

- The beamline is branched into three branches using neutron benders upstream.
- Fast neutrons are shielded upstream and only slow neutrons are available.
- Each of the three branches has its own characteristic beam.

Specifications

The beamline is branched into the following three branches. Each has the following characteristics

- Unpolarised: high intensity
- Polarised: 94 - 96% polarisation
- Low divergence: low divergence and high luminosity

Auxiliary equipment

- Position sensitive 2D detector
  Resolution 0.5 mm
- Doppler shifter [3] type Ultra-cold neutron (UCN) source
  Pulsed UCNs are available.
- Multi-layer type neutron interferometer
  Coherent scattering length measurements
  Sensitivity with 20 mrad/20 min

Instrument Configurations

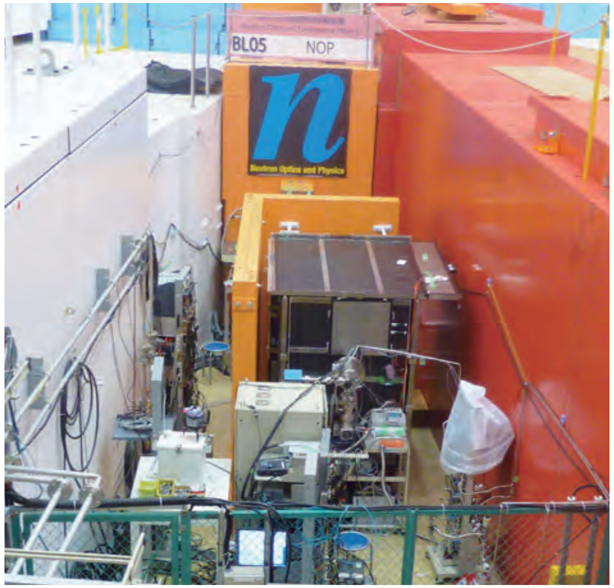

CONTACT

Kenji MISHIMA
kmishima@kmi.nagoya-u.ac.jp

Takashi INO
takashi.ino@kek.jp

Go ICHIKAWA
go.ichikawa@kek.jp

Neutron Optics and Fundamental Physics (NOP)

J-PARC MLF

J-PARC

BL05

Capabilities

- 3 Characteristic beams come in three branches
- Independent experiments can be carried out in parallel on each
  - Neutron decay
  - Neutron-matter interactions
  - Development of UCN devices

BL05 Beam conditions for each branch

Branch	Unpolarized	Polarized	Low-Divergence
Cross section (Y × X mm^2)	50 × 40	120 × 60	80 × 20
Beam Divergence (Y × X mrad^2)	V_{xy} < 14 m/s	23 × 9.4	0.23 × 0.23
Beam flux (cm^{-2}s^{-1}@1 MW)	(3.8 ± 0.3) × 10^8	(4.0 ± 0.3) × 10^7	(5.4 ± 0.5) × 10^4
Polarization	–	94~96%	–

Applications

- Precise measurement of neutron lifetime
- Pulsed super-cooled neutron generation using a Doppler shifter
- Neutron scattering of rare gases to search for unknown interactions
- Cold neutron interferometry
- Ultra-high resolution neutron detector development

Muti-layer type neutron interferometer

Schematic for the interferometer. The multi-layer neutron mirrors are on beam splitting etalons. Neutron beams are spitted at one etalon and merged on another one.

Setup of the neutron interferometer at Low-divergence beam branch

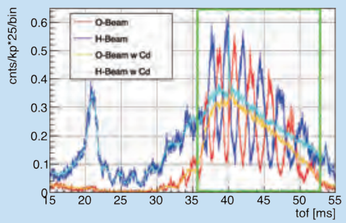

Oscillation of two beam paths. In case one path covered, oscillation disappears.

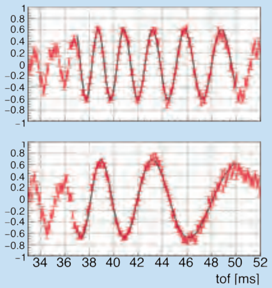

Oscillation without (top) and with sample (bottom)

T. Fujiie *et al.*, *Phys. Rev*. Lett. **132**, 023402 (2024) (© 2024 American Physical Society).

neutron emulsion detector with spacial resolution of 100 nm

Nuclear emulsion is a type of a photographic film used as a tracking device in particle physics, which features high spatial resolution. We succeeded in developing a neutron detector which realizes a spatial resolution of 11-99 nm in a selected condition by using an emulsion.

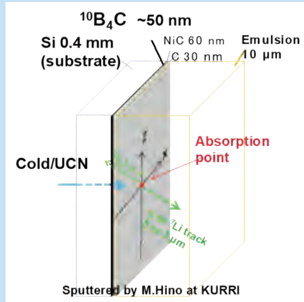

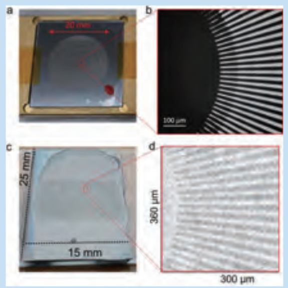

Images of photograph by cameras(a&c), microscope(b), and neutron emulsion(d) of the Siemens star test pattern made by Gd. Spacial resolution of less than 1 um is available.

A. Muneem *et al.*, J. Appl. Phys. **133**, 054902 (2023) (© 2023 AIP Publishing LLC).

For 3) , see Glossary (p.61)

BL06

Quasi-elastic/inelastic neutron scattering

Village of Neutron Resonance Spin Echo Spectrometers (VIN ROSE)

Dynamical behaviors of materials from ps to sub-μs

Instrument Description

- Neutron spin echo spectrometers (NRSE and MIEZE) with neutron resonance spin flippers.
- Direct observation of intermediate scattering function is possible from ps to ns to investigate atomic and molecular dynamics.

Specifications

- Fourier time：1 ps - 2 ns （Sample to Detector Length: Max. 2 m, Max. MIEZE Flequncy：400 kHz)
- Scattering Angle $2\theta = 0 - 15°$
- Possible Neutron Reflectivity: $R > 1.0^{-5}$
- MIEZE instrument is currently available for user programs.（Option: Neutron Polarization Analyses) Please contact the responsible persons.

Sample Environments

- 4 K GM Cryostat

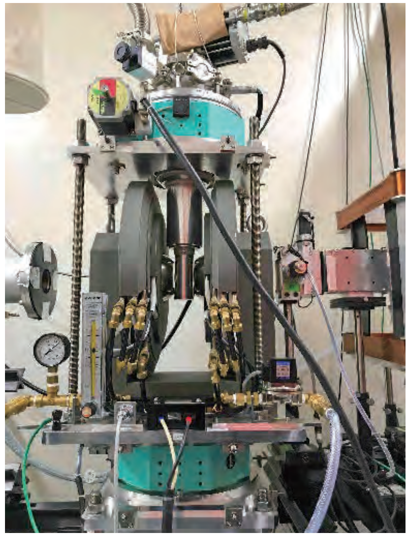

Instrument Configurations

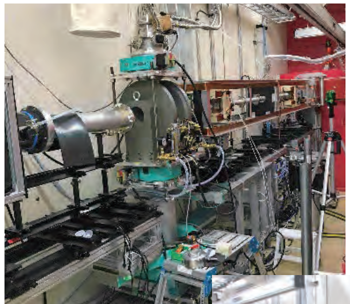

MIEZE Instrument

NRSE Instrument

CONTACT

Hitoshi ENDO
hitendo@post.j-parc.jp

Hideki SETO
hideki.seto@kek.jp

Village of Neutron Resonance Spin Echo Spectrometers (VIN ROSE)

J-PARC MLF

J-PARC

BL06

Capabilities

- Dynamics of atoms and molecules in nano-second order.
- Neutron polarization analyses are available.

Spectro meter	Wave-length [A]	Q range [Å^{-1}]	Fourier Time
NRSE	$5 < \lambda < 20$	$0.02 < Q < 0.65$	0.1 [ns] < t < 0.1 [μs]
MIEZE	$3 < \lambda < 13$	$0.002 < Q < 3.5$	1 [ps] < t < 2 [ns]

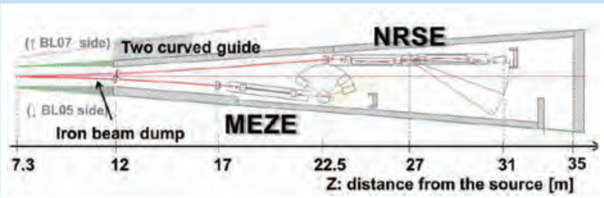

Schematic view of BL06 VIN ROSE

Applications

- Slow dynamics of soft matters, such as polymers, proteins, membranes, colloids, etc.
- Neutron polarization analyses for investigation of super paramagnetism in magnetic nanoparticles [4).
- Investigation of viscoelastic properties of plastics with molecular scale.
- Study of spin dynamics in magnetic materials.

NRSE (a) & MIEZE (b) neutron spin echo spectrometers

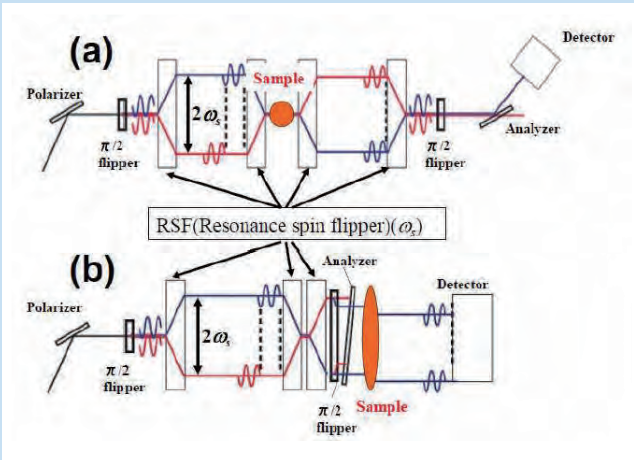

M. Hino *et al.*, *Physics Procedia* **42**, 136 (2013) (©2013 Elsevier).

Spin dynamics of magnetic Skyrmion in MnSi

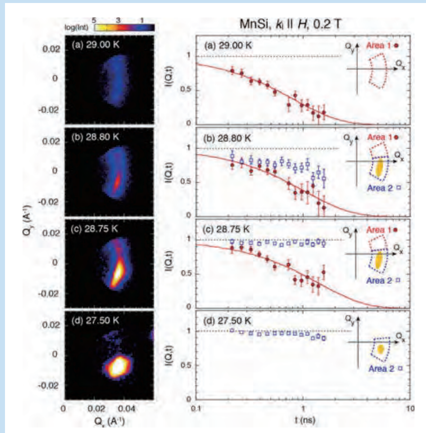

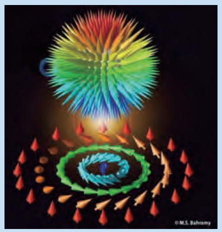

T. Nakajima *et al.*, *Phys. Rev. Res.* **2**, 043393 (2020). (©2020 American Physical Society).

For 4) , see Glossary (p.61)

BL08

Neutron diffraction

Super High Resolution Powder Diffractometer (SuperHRPD)

Observation of slight structure distortion with high precision

Instrument Description

- A number of reflection intensities with distinct peaks can be observed
- A slight peak split with phase transition can be observed
- Hydrogen atom position can be determined
- Enables the development of new structural analysis methods by complementing X-ray in intensity and resolution

Specifications

◦ *d* –range (standard setting)
0.3 - 3.75 Å (High-angle bank: $150° \le 2\theta \le 175°$)
0.4 - 5.2 Å (90 degree bank: $60° \le 2\theta \le 120°$)
0.6 - 15 Å (Low-angle bank: $10° \le 2\theta \le 40°$)

◦ Resolution ($\Delta d/d$)
Optimal resolution 0.0365% (@ $2\theta > 172°$)
≧ 0.08% (High-angle bank)
≧ 0.35% (90degree bank)
≧ 0.7% (Low-angle bank)

Sample Environments

- Auto sample changer (RT, 10 samples)
- 4 K closed cycle refrigerator (4 - 300 K)
- Cryo furnace (5 - 800 K)
- High temperature furnace (< 1223 K)
- 1 K closed cycle refrigerator (0.9 - 300 K)
- 14 Tesla Magnet

Instrument Configurations

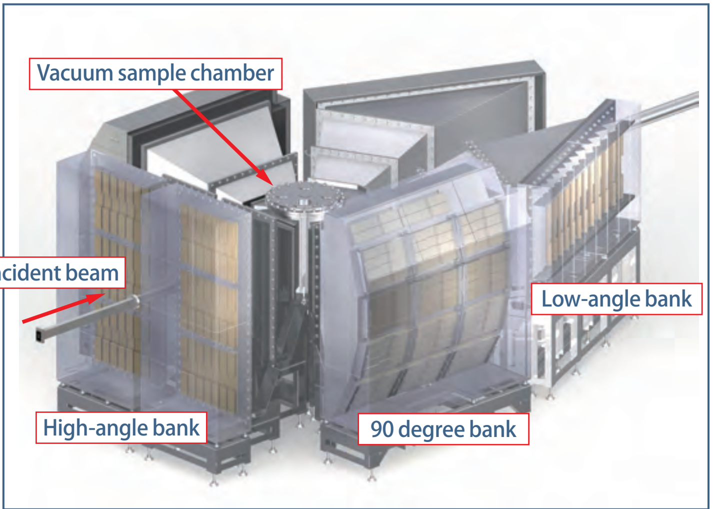

High angle detector bank and high resolution detector unit with 8mm PSD

CONTACT

Shuki TORII
torii@post.kek.jp

Takashi SAITO
saitot@post.kek.jp

Super High Resolution Powder Diffractometer (SuperHRPD)

J-PARC MLF

BL08

Capabilities

- High resolution crystal and magnetic structure refinement
- Detection of extremely small structural distortions

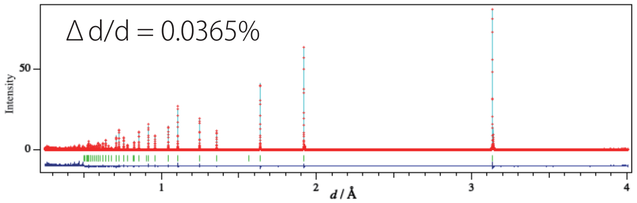

Neutron diffraction data of powder silicon measured by high-resolution mode and crystal structure analysis results using Z-Rietveld

Applications

- Spin-state transition and giant magnetovolume effect in cobalt oxides [5)]
- High temperature structural analysis of high sodium ion conductors
- Lattice distortion associated with magnetic phase transitions in 4d transition metal oxides
- Negative thermal expansion of perovskite-type cobalt oxides near room temperature [5)]

Observation of minimal changes in crystal structure

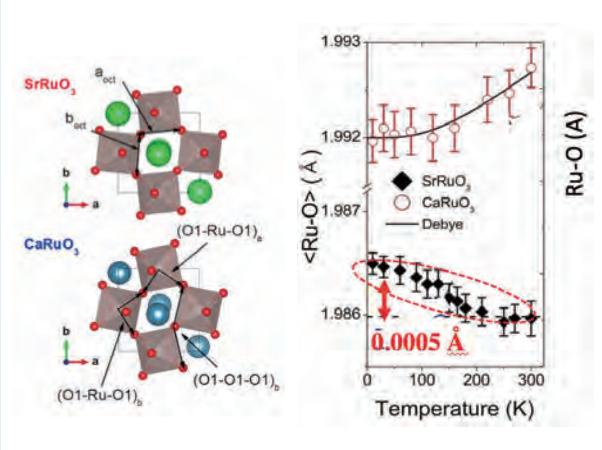

We were the first to successfully detect a slight increase in the Ru-O bond length (0.0005 Å) associated with magnetic ordering in the 4d magnet $SrRuO_3$.

Lee *et al.*, J. Phys.: Cond. Mat. 25, 465601(2013) (© 2013 IOP Publishing)

Observation of crystal structure in a magnetic field

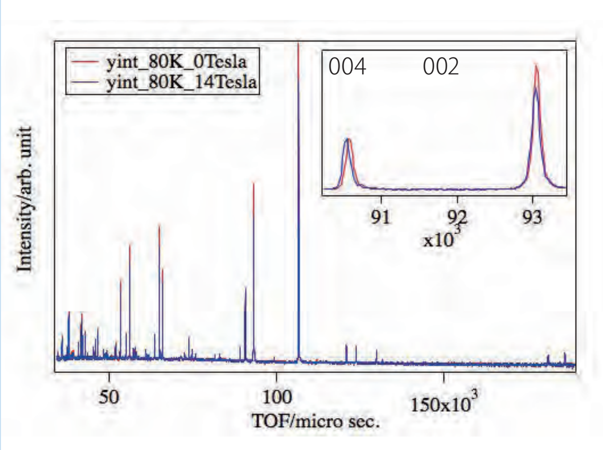

Diffraction patterns of perovskite cobalt oxides showing negative thermal expansion at 0 and 14 Tesla.
The 004 reflection was shifted by 0.05% by the magnetic field and the 200 reflection was reduced in intensity by 20%.

For 5）, see Glossary (p.61)

BL09

Neutron diffraction

Special Environment Powder Diffractometer (SPICA)

Real-time observation of structure and its change of functional materials and non-equilibrium reaction in practical devices

Instrument Description

- SPICA is dedicated to structural investigations for next-generation rechargeable batteries
- SPICA focuses on neutron diffraction experiments in special environment –particularly in charge–discharge operations (i.e., operando measurements)
- SPICA is used in experiments in various fields, including physics, chemistry, materials science, archeology, environmental science, and battery science

Specifications

- Range of *d*–spacing
  - 0.3 - 3.7 Å (High-angle bank)
  - 0.4 - 5.0 Å (90-degree bank)
  - 0.5 - 11.0 Å (Low-angle bank)
- Resolution ($\Delta d/d$)
  - 0.09% (Optimal resolution)
  - 0.12% (High-angle bank)
  - 0.47% (90-degree bank)
  - 1.27% (Low-angle bank)

Sample Environments

- Auto sample changer (RT, 40 samples)
- Top-loading 4K-type cryostat (4 - 300 K)
- Top-loading cryo-furnace (30 - 700 K)
- Potentiostat, Temperature control system, etc.

Instrument Configurations

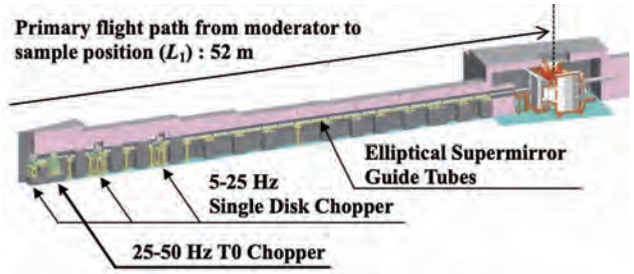

Neutron diffraction data

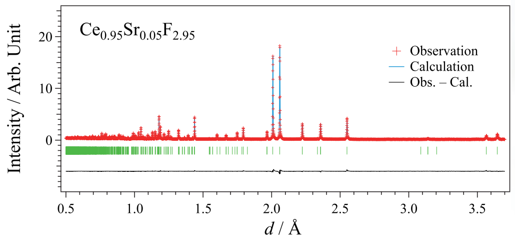

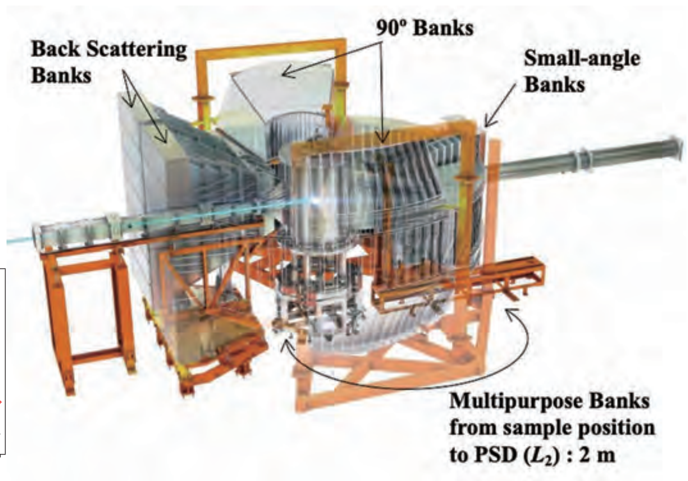

Credit：J-PARC center

CONTACT

Kazuhiro MORI
kmori@post.kek.jp

Takashi SAITO
takashi.saito@kek.jp

Seungyub SONG
song@post.kek.jp

Special Environment Powder Diffractometer (SPICA)

BL09

Capabilities

- Neutron diffraction data with high resolution & intensity in the wide *d* (or *Q*) range
- Operando neutron diffraction measurements
- Annex building for SPICA is available to prepare samples for neutron diffraction experiments, assemble rechargeable batteries, and perform charge–discharge evaluations before and/or after operando measurements

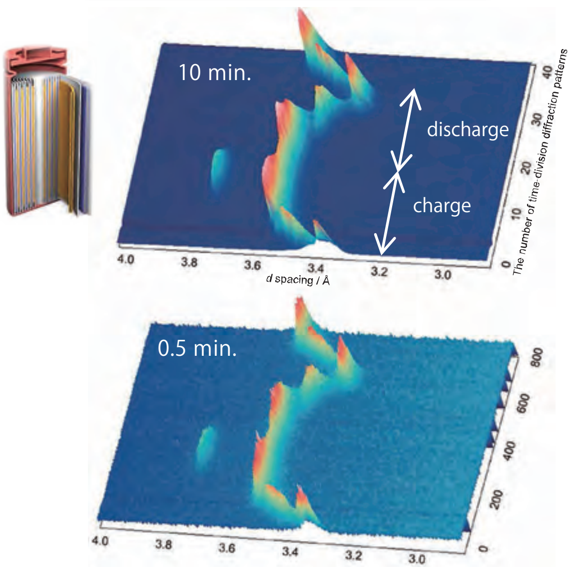

Operando neutron diffraction measurements

Applications

Direct observation of battery reactions through operando neutron diffraction measurements

Elucidating the reaction mechanisms that occur during practical operation is crucial for the development of battery technologies. An operando diffraction technique uses high-intensity neutrons to detect reactions in non-equilibrium states driven by high-current operation in commercial batteries. This technique provides valuable information for developing advanced batteries.

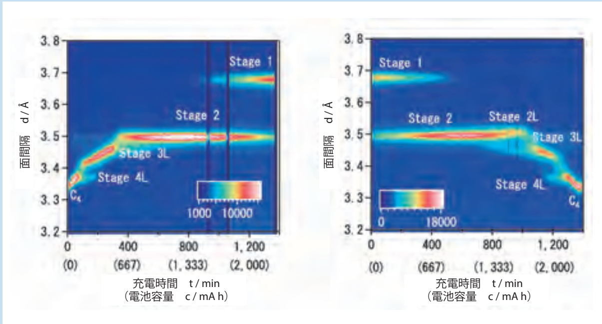

"Real-time observations of lithium battery reactions - operando neutron diffraction analysis during practical operation"
S. Taminato *et al.*, *Scientific Reports*, **6** (2016)28843
(©2016 Nature Publishing Group)

Structural investigations of hydride-ion-conducting materials using neutron diffraction

Various hydride-ion-conducting materials have been found and developed nowadays. Neutron diffraction is a powerful tool to determine precisely the atomic positions of hydride ions.

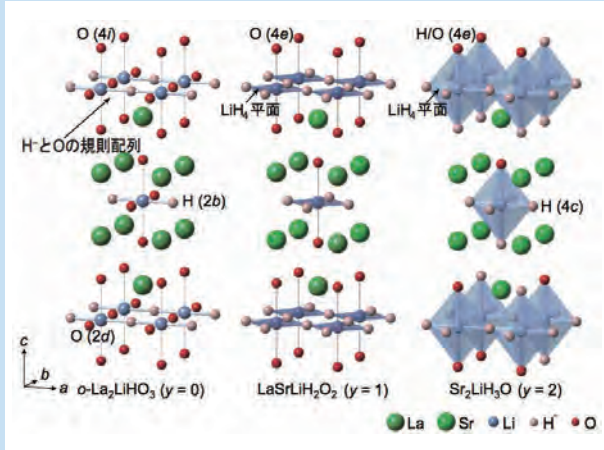

"Pure H^- conduction in oxyhydrides"
G. Kobayashi *et al.*, *Science*, **351 (6279)**, (2016), 1314–1317
(© 2016 AAAS)

BL10

Fundamental neutron physics/
Neutron device development

NeutrOn Beam-line for Observation and Research Use (NOBORU)

Serving a versatile neutron field for characterizing the neutron source as well as for R&D on various devices, irradiation and analysis of materials, etc.

Instrument Description

- Robust shielded cave and tough experiment table for massive sample/device testing.
- Closest irradiation position to the source of MLF, which can provide high-energy (above 10 MeV) to low-energy neutrons (below 1 meV).
- Simple and stable beamline device/optics.

Specifications

- L1 (moderator to sample pos.) : 14.0 m
- Max. beam size : 100 mm × 100 mm
- Inside room : W 2.5 m × L 3.5 m × H 3.0 m
- Neutron flux @ 14 m, 1 MW
  - < 0.4 eV : 4.8×10^7 [n/s/cm^2]
  - > 1 MeV : 1.2×10^7 [n/s/cm^2]
  - > 10 MeV : 1.2×10^6 [n/s/cm^2]

Sample Environments

- Each user builds the environment for each experiment.

Instrument Configurations

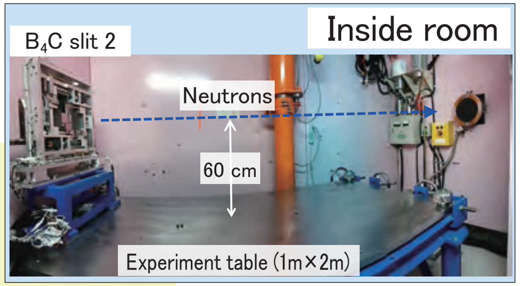

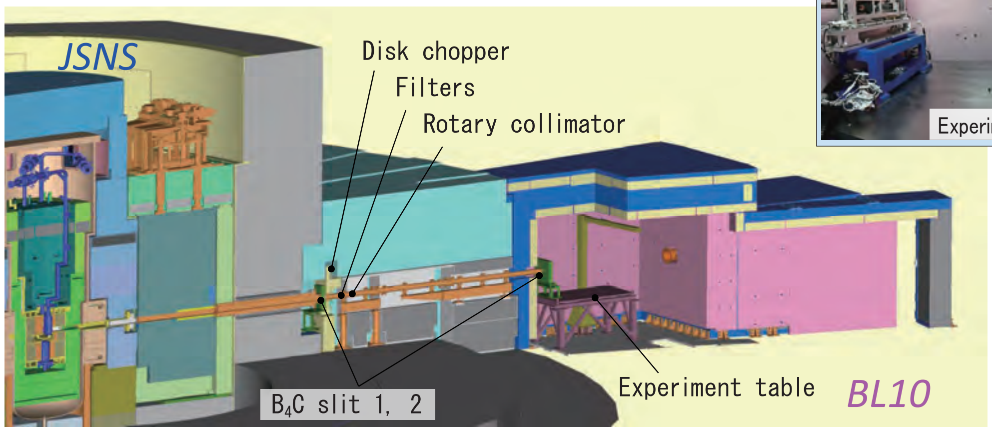

CONTACT

Kenichi OIKAWA
kenichi.oikawa@j-parc.jp
JAEA

Masahide HARADA
harada.masahide@jaea.go.jp
JAEA

NeutrOn Beam-line for Observation and Research Use (NOBORU)

J-PARC MLF

J-PARC

Capabilities

- Measurement and diagnosis of neutron source properties.
- Serves as a test port for neutron optics, detector development, etc.
- Provides a high-intensity, high-energy neutron irradiation field.

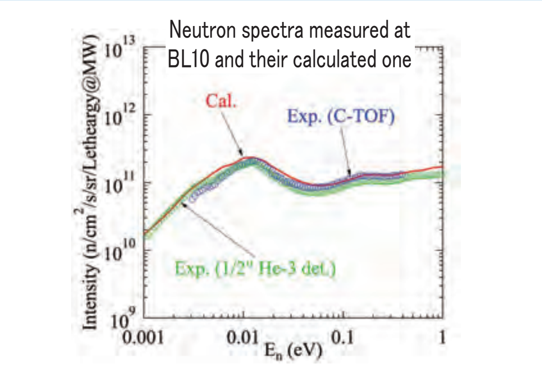

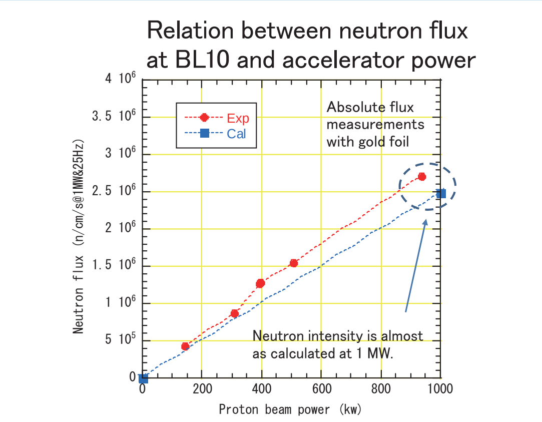

Applications

- Demonstrated world's highest neutron performance, fixed-point observation
- Element selective studies of local structures around dopants by white neutron holography.
- Development of SEOP 6) -type polarized neutron devices and experiments.
- Micron-order imaging with high-resolution 2D neutron detector using superconducting device.
- Evaluation of semiconductor device and plant mutagenesis by high-energy neutron irradiation.

Spatial distribution of elements using prompt γ-ray analysis

Synchronized measurement of XY-stage and HPGe detector.

Scanning measurement with a beam dia. of several mm.
⇒2D distribution measurement
⇒Identification and quantification of element(s)

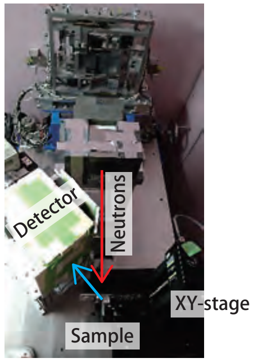

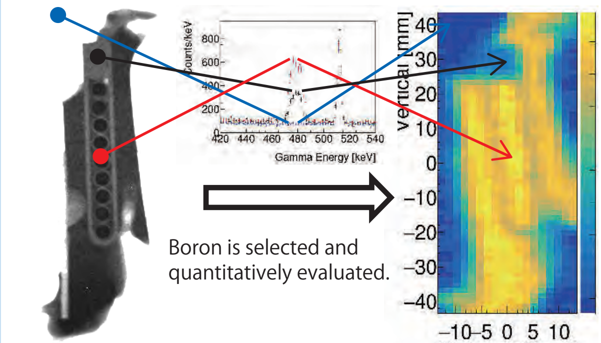

Simulated fuel debris of the F1NPS

Cosmic ray tolerance of power semiconductors

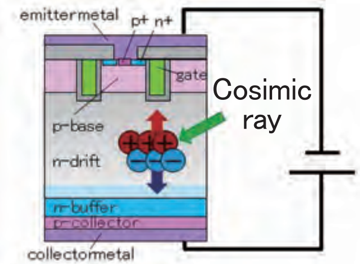

Cross-sectional model of insulated gate bipolar transistor

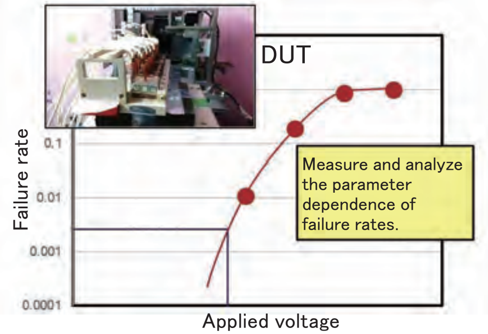

Calculate failure rates from acceleration experiments using neutron irradiation.

For 6), see Glossary (p.61)

BL11

Neutron diffraction

High Pressure Neutron Diffractometer (PLANET)

Accurately determine structures of crystalline, liquid, and glass over a wide pressure and temperature range.

Instrument Description

- High pressure and high temperature experiments up to 14 GPa and 2,000K with the 6-axis press, ATSUHIME
- High quality diffraction patterns free from contaminant peaks from sample surrounding materials via narrow incident slits pressure and radial collimators

Specifications

Diffraction

Resolution: $\Delta d/d = 0.6\%$, *d*-range: 0.2-4.2Å

Beam size: 1-15mm square.

Radial collimator gauge size: 0.5, 1.1, 2.8 mm

Radiography

Resolution: 200 μm, Field of view: 14 mm square

Sample Environments

High-pressure presses and available *PT* range

- Paris-Edinburgh cell: 40 GPa & 300 - 373 K
- 6-axis press : 14 GPa & 300 - 2,000 K
- Mito System : 5 GPa & 30 - 273 K
- Piston cylinder cell : 2 GPa & 4 - 300 K

Instrument Configurations

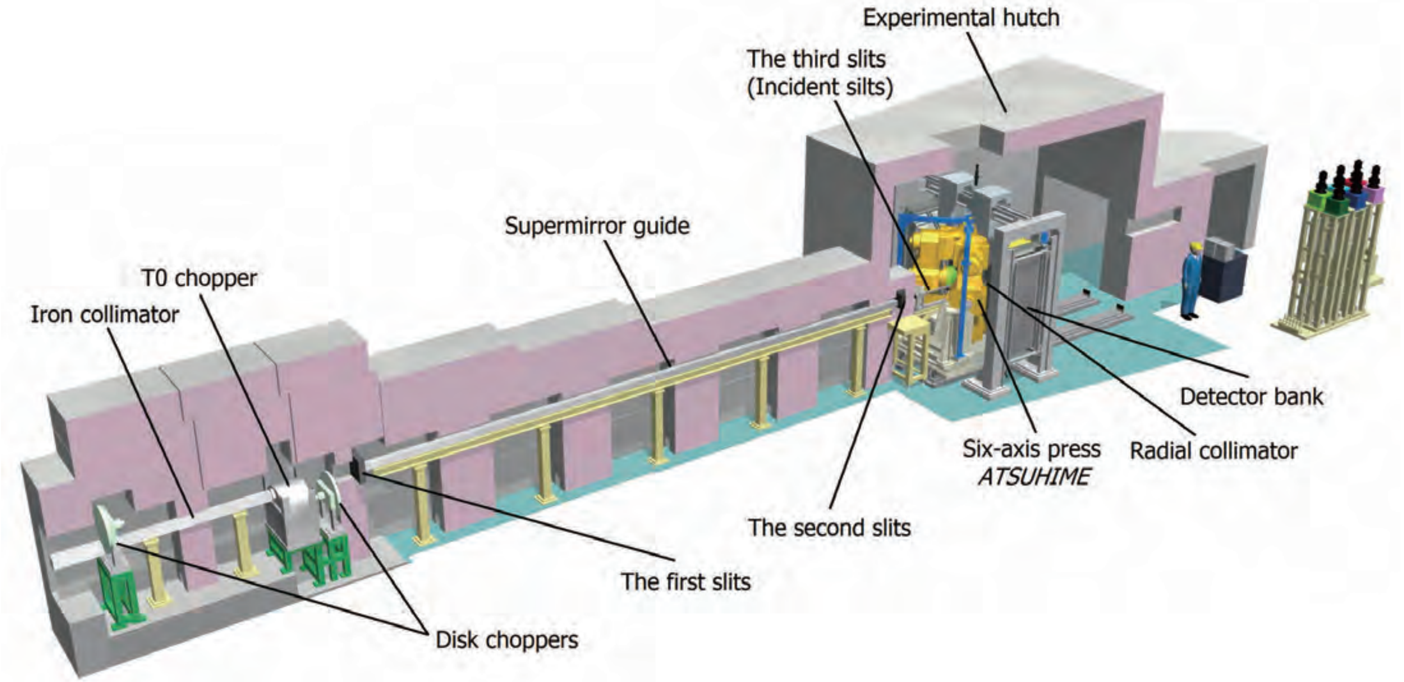

CONTACT

Takanori HATTORI
takanori@post.j-parc.jp
JAEA

Asami SANO
sanoasa@post.j-parc.jp
JAEA

High-Pressure Neutron Diffractometer (PLANET)

BL11

Capabilities

- Atomic and magnetic structures of crystals and liquid/glass under high pressure
- Transmission image of the sample under high pressure

Applications

- Estimation of light elements in the Earth's core.
- Exploration of new ice polymorphs
- Hydrogen bond symmetrization of OH including minerals
- Pressure induced structural changes in liquid and glasses

Hydrogen distribution in ice polymorph

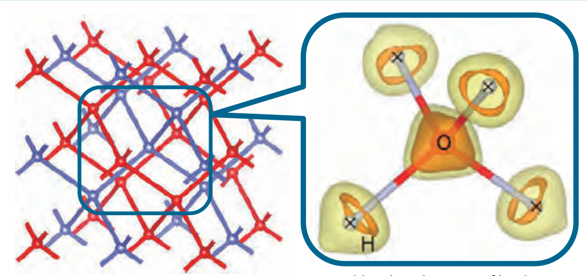

Ice VII (Only oxygen lattice is shown)

Ring-like distribution of hydrogen (No distribution at X position)

K. Yamashita *et al.*, PNAS **119**, e2208717119 (2022) (©2022 National Academy of Science)

H-D interdiffusion of brucite at high PT

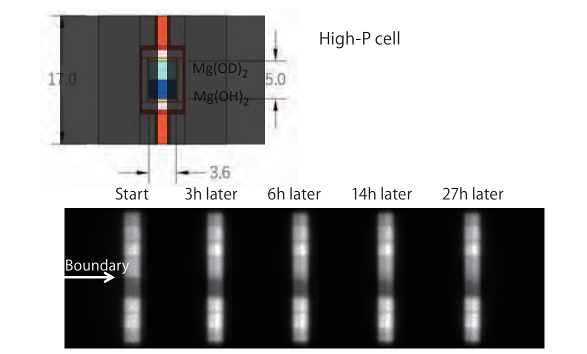

Discovery of new ice polymorph, XIX

Ice takes various crystal structures depending on the PT condition. This study revealed that the ice VI transformed into the new hydrogen ordered form (XIX) on cooling. The discovery of the new phase is the first in two years, since 2019, and will help in the comprehensive understanding of ice polymorphism in the future.

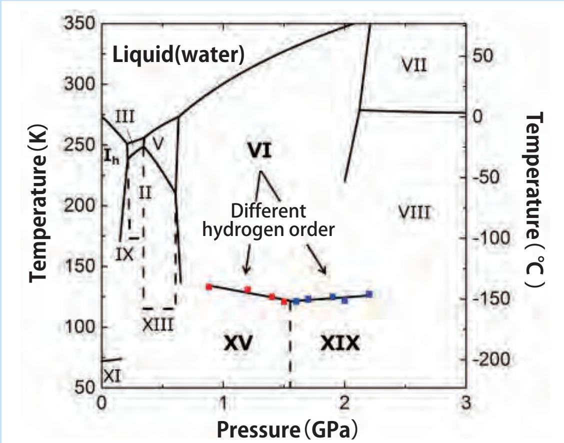

Temperature-pressure phase diagram of ice and the stable region of ice XIX discovered in this study.

R. Yamane *et al., Nature Commun.* **12**, 1129 (2021) (©2021 Springer Nature)

New graphitic material synthesized by compression of CS_2

CS_2 instantly decomposes into sulfur and C_2S at about 10 GPa. Annealing of the recovered C_2S further decomposed into sp^2 graphite sheets bound to sulfur. Since they can be synthesized in large quantities under high pressure, they will be useful for the design of electronic devices based on graphite sheets.

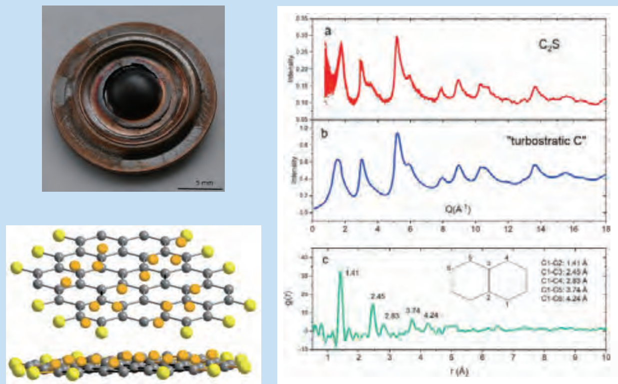

(Left) Sample recovered from high pressure and its estimated structure. (Right upper) Comparison of diffraction patterns between the recovered sample and layered carbon. (Right lower) Pair distribution function of the recovered sample. C-C interatomic distance characteristic to the carbon sheet are observed.

S. Klotz *et al., Carbon* **185**, 491 (2021) (©2021 Elsevier Ltd.)

BL12 High Resolution Chopper Spectrometer (HRC)

Quasi-elastic/inelastic neutron scattering

HRC enables us to access the wide momentum (*Q*) and energy (*E*) for conducting forefront researches on dynamical properties in material with the best resolution ever!

Instrument Description

- High resolution Fermi chopper and high speed T0 chopper for high energy measurements
- Supermirror guide tubes and large-area detectors increase the number of neutrons detected
- Neutron Brillouin scattering measurement is realized by a detector with a minimum scattering angle of 0.6°

Specifications

Neutron energy：$3 < E_i < 500$ meV

Scattering :Horizontal: 3°~ 62° ($L_2 = 4$ m),
-31°~ -13° ($L_2 = 4$ m),
-5.1°~ -0.6° ($L_2 = 5.2$ m)
Vertical: ± 20 ° ($L_2 = 4$ m),
± 4 ° ($L_2 = 5.2$ m)

Neutron intensity: (@sample position @1MW)
1×10^5 n/s/cm^2 ($\Delta E/E_i = 2.5\%$)

Energy resolution: $\Delta E/E_i \geq 2\%$ (@E= 0 meV)

Maximum sample size: 4 × 4 cm^2

Sample Environments

- Closed cycle refrigerator (4-300 K)
- 1 K refrigerator (1-300 K)
- ^{3}He refrigerator (0.3-300 K)
- Superconducting magnet (Max. 5 T, 2 K – 300 K)
- Pressure cell (Cylinder type, Max 1.2 GPa)

Instrument Configurations

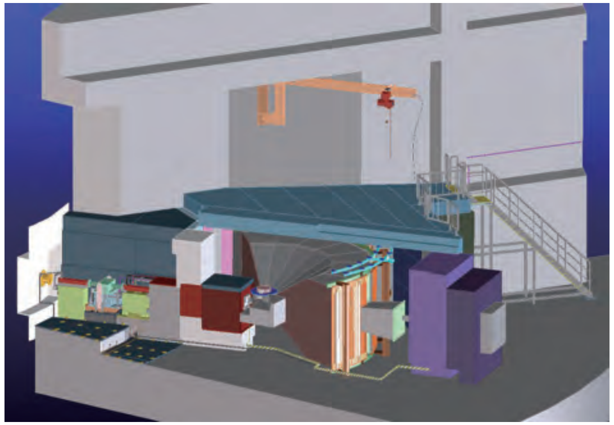

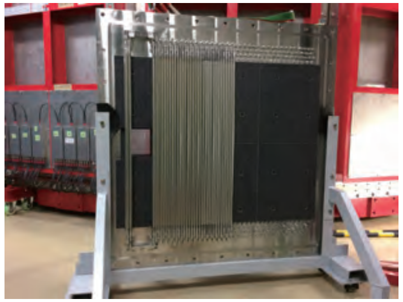

Small-angle area detectors

Vacuum Scattering Chamber

CONTACT

Daichi UETA
dueta@post.kek.jp

Shinichi ITOH
shinichi.itoh@kek.jp

Takatsugu MASUDA
masuda@issp.u-tokyo.ac.jp
東京大学 THE UNIVERSITY OF TOKYO

High Resolution Chopper Spectrometer (HRC)

BL12

Capabilities

- Spin, atoms, and molecular dynamics in solid state
- Spin wave dispersion measurements from ferromagnetic powder samples
- Phonon dispersion measurements of liquids

Applications

- Magnetic excitations in metallic ferromagnets
- Pressure-induced quantum phase transitions and magnetic states
- Magnetic excitations in multiferroic materials [7)]
- Magnetic excitations in one-dimensional quantum spin systems
- Magnetic excitations in layered transition metal oxides
- Magnetic excitations in skutterudite systems [8)]
- Magnetic excitations in metallic antiferromagnets
- Lattice vibrations in liquid and polycrystalline systems

Spin wave dispersion of one-dimensional spin system $CsVCl_3$

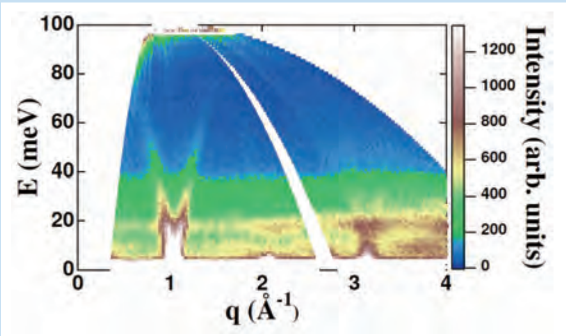

S. Itoh *et al.*, *J. Phys. Soc. Jpn.* **82** (2013) SA033 (© 2013 The Physical Society of Japan)

Neutron Brillouin scattering study measurement with a detector system down to 0.6° of scattering angle

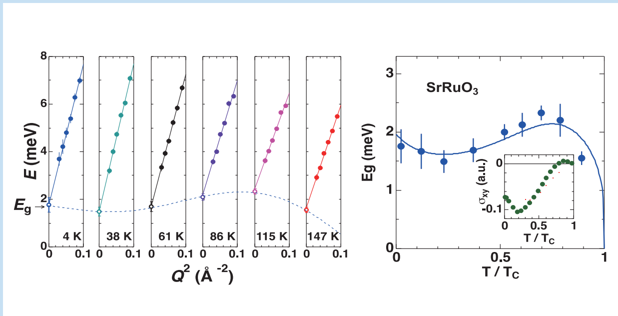

S. Itoh *et al.*, *Nature Commun.* 7, 11788 (2016). (© 2016 SPringer Nature)

Novel excitations near quantum criticality in geometrically frustrated antiferromagnet [1)] $CsFeCl_3$

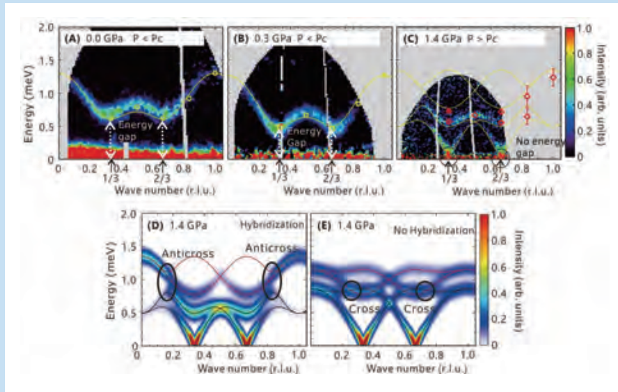

S. Hayashida *et al.*, *Sci. Adv.* 5, eaaw5639 (2019). (© 2019 AAAS).

For 1), 7) and 8), see Glossary (p.61-62).

BL14

Quasi-elastic/inelastic neutron scattering

Cold-neutron disk-chopper spectrometer (AMATERAS)

A low-energy dedicated inelastic/quasi-elastic scattering instrument designed to offer fine and tunable energy resolution and high neutron flux meeting the needs of a wide range of research fields, such as magnetic systems, amorphous substances, and liquids

Instrument Description

- Dynamics measurements in the energy range from 10^{-2} to 10^{2} meV
- High-efficiency beam transport, detectors with a large solid angle, and multi-Ei technique are available
- Highly efficient measurement detects weak signals from dynamical motions of atoms and spins that could not be captured before

Specifications

- Incident energy：1 < 80 meV
- Energy resolution：$\Delta E/E_i > 1\%$ ($E_i < 3$ meV)
  $\Delta E/E_i > 2 - 3\%$ ($E_i < 20$ meV)
  $\Delta E/E_i > 4 - 5\%$ ($E_i < 80$ meV)
- Detector coverage： 3.4° - 116° (horizontal), –16° - 23° (vertical)
- Optimal sample size ∅1×2 cm^3

Sample Environments

- Bottom-loading closed-cycle refrigerator (5 - 300 K)
- Top-loading closed-cycle refrigerator (7 - 500 K)
- High-temperature stick ($T < 680$ K)
- Other equipment is also available. Some of equipment cannot be used in full-spec. Please inquire of the BL14 staff members about more detail.

Instrument Configurations

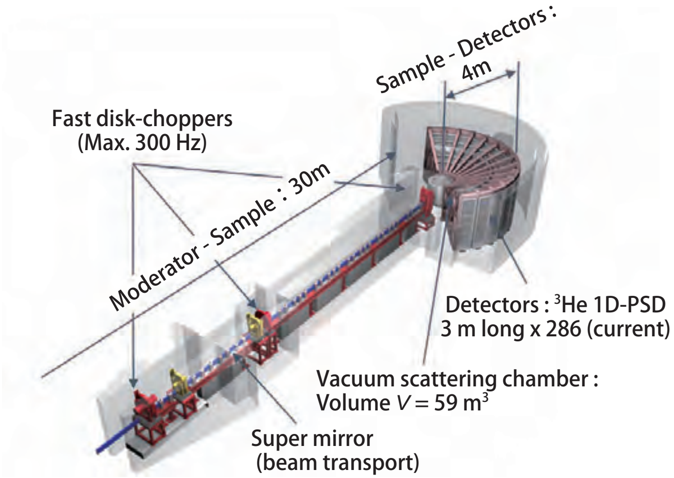

Fask disk-chopper

Vacuum scattering chamber and detectors

CONTACT

Seiko OHIRA-KAWAMURA
seiko.kawamura@j-parc.jp
JAEA

Maiko KOFU
maiko.kofu@j-parc.jp
JAEA

Cold-Neutron Disk-Chopper Spectrometer (AMATERAS)

J-PARC MLF

J-PARC

BL14

Capabilities

- Observation of lattice vibrations and magnetic excitations from 0.1 meV to several 10 meV on spatial scales on the order of Å
- Investigation of diffusion and relaxation of atoms/molecules moving in the time range of 0.05 - 50 ps and spatial range of 2 - 20 Å, and their relationship to structure

Applications

- Magnetic excitations and lattice vibrations in strongly correlated electron systems and quantum spin systems
- Vibration and diffusion phenomena in liquids and low-energy dynamics in amorphous materials
- Lattice dynamics of functional materials such as thermoelectric materials
- Molecular motion and flexibility in polymers and biomaterials

Elucidation of dynamics of polymers and fillers composing rubber

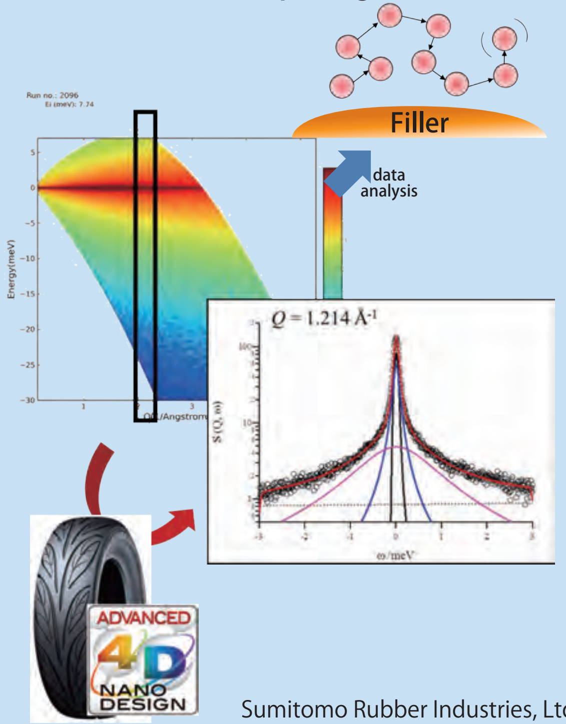

Sumitomo Rubber Industries, Ltd.

Colossal barocaloric [9] material for pressure-induced solid-state refrigeration

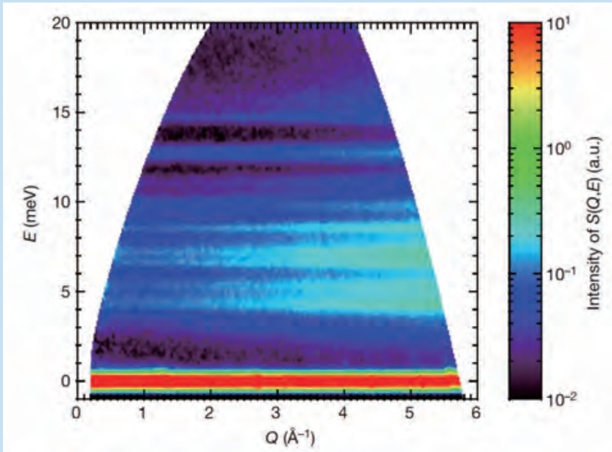

Anharmonic lattice vibration of neopentylglycol

B. Li *et al., Nature* **567**, 506 (2019) (©2019 Springer Nature).

Triplon band splitting and topological edge states ($Ba_2CuSi_2O_6Cl_2$)

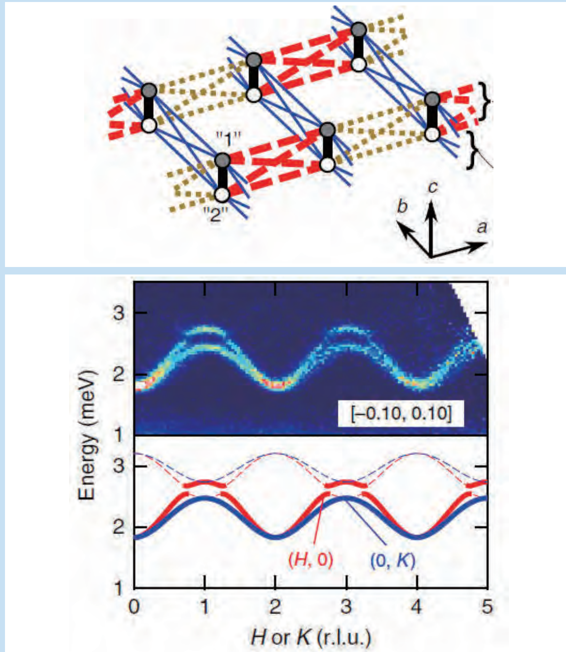

K. Nawa *et al., Nature Commun.* **10**, 2096 (2019) (©2019 Springer Nature).

For 9) , see Glossary (p.62)

BL15

Small angle neutron scattering

Small and Wide Angle Neutron Scattering Instrument (TAIKAN)

Structural information with a wide spatial range, from sub-nanometer to micron scales, is obtained for analyzing the structures and non-equilibrium phenomena of various materials such as metals, magnetic materials, superconductors, soft matter, biopolymers, and composites

Instrument Description

High-resolution and high-efficiency measurements over a wide range of spatial scales, both small-angle and wide-angle, enable hierarchical structural analysis. In-situ observation measurements using a variety of sample environment devices are possible.

Specifications

Range of wavelength：
- 0.08 - 0.78 nm （unpolarized）
- 0.25 - 0.78 nm （polarized）

Range of q：
- 7×10^{-3} - 170 nm^{-1} （unpolarized）
- 7×10^{-3} - 25 nm^{-1} （polarized）

Sample Environments

Sample changer, 3 K/4 K refrigerator, 1 T magnet, 4 T cryo magnet, 10 T magnet, Rheometer, tensile tester, humidity controller, laser furnace, gas/vapor adsorption equipment, etc.

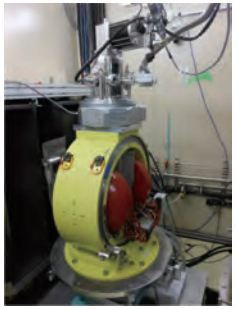
1 T magnet and 4K refrigerator


Humidity-Gas generator


Rheometer

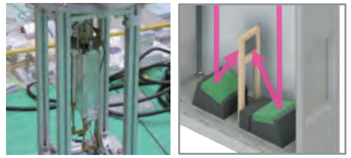
Laser heating furnace (chamber section) and heating image

Instrument Configurations

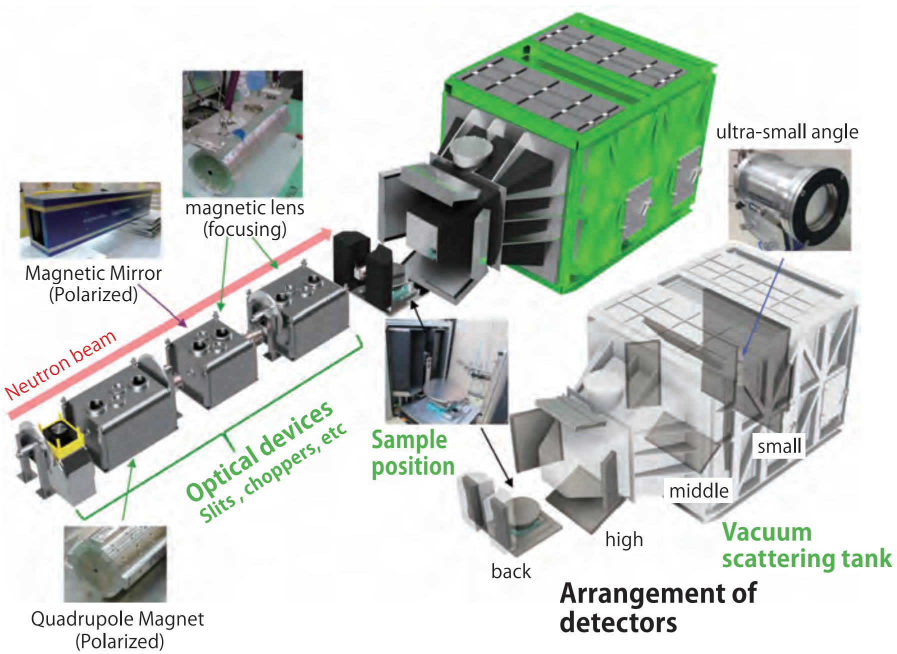

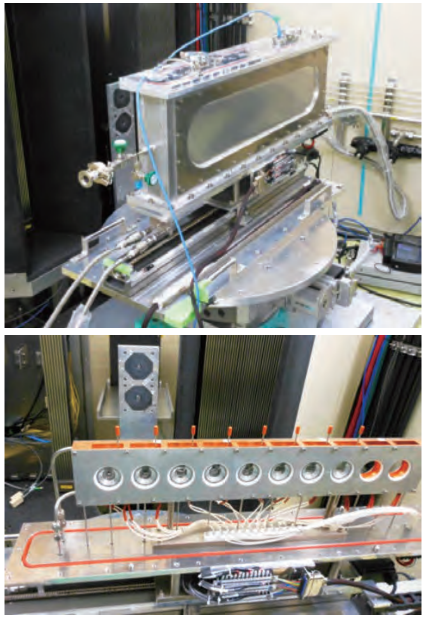
Sample changer

CONTACT

Shin-ichi TAKATA
shinichi.takata@j-parc.jp
JAEA

Kousuke HIROI
kosuke.hiroi@j-parc.jp
JAEA

Kazuki OHISHI
k_ohishi@cross.or.jp
CROSS

Small and Wide Angle Neutron Scattering Instrument (TAIKAN)

Capabilities

- Structural information from sub-nanometer to micron scale
- Structural analysis of nanomagnetic materials, biomaterials, and composites
- Analysis of non-equilibrium phenomena

Applications

- Analysis of the hierarchical structure of gluten in flour products
- Heterogeneous structure analysis of phenol resin during gelation process
- Nanostructural Analysis of Tire Rubber Material (Hydrogen Nuclear Spin Polarization)
- Study of solid polymer materials for fuel cell electrodes
- Analysis of micro precipitates in steel materials
- Magnetic-structural analysis in nano-scale

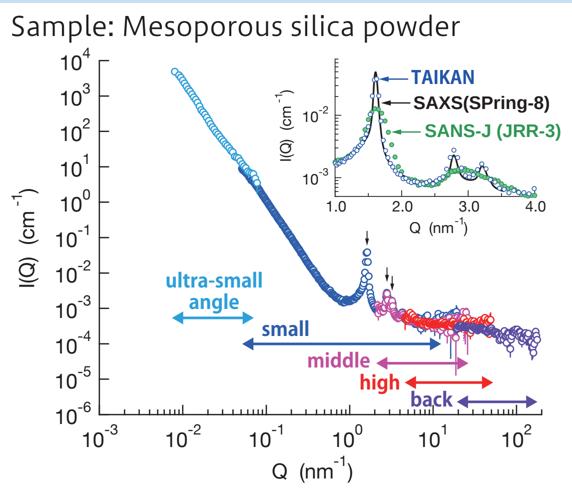

Measurement q-range of TAIKAN

H. Iwase, *Oleoscience* **16**, 10 (2016)
(© 2016 Japan oil chemists' society)

Magnetic structure analysis by polarized neutron analysis experiment

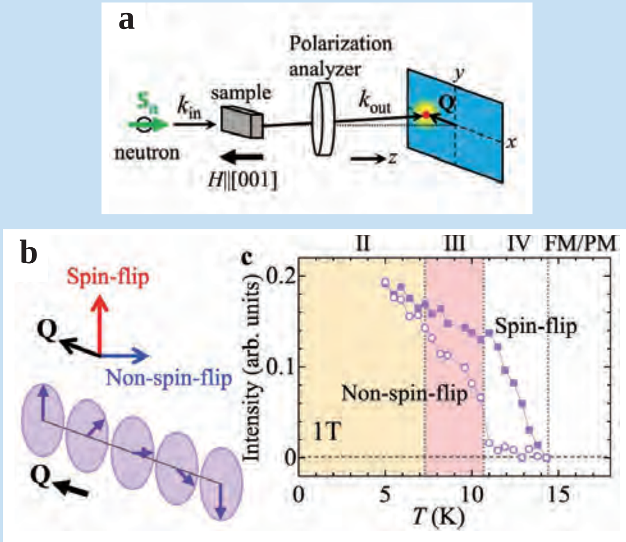

The magnetic structure is determined by measuring spin-flip and non-spin-flip scattering, because the spin state of the scattered neutrons depends on the direction of the magnetic moment of the material.

R. Takagi *et al.*, *Nat. Commun.* **13**, 1472 (2022). (©2022 SPringer Nature).

Structural analysis of sulfonated hydrocarbon films in humid environments

Study of proton conductivity trends (QP > MP > BP) and structural connectivity of water clusters

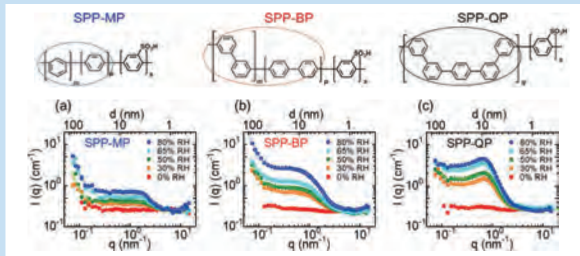

SANS profiles of (a) SPP-MP, (b) SPP-BP, and (c) SPP-QP films under 0 to 80% RH in D2O humidity at 80° C. Solid lines show the results of fitting with model functions.

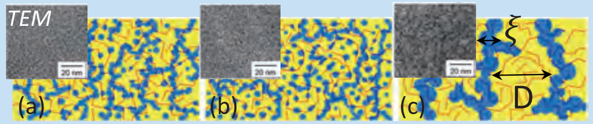

Morphology model of SPP-MP, SPP-BP, and SPP-QP membranes at 80° C and 80% RH

K. Shiino, *et al.*, *ACS Appl. Polym. Mater.* **2020**, 2 (12), 5558. (©2020 American Chemical Society).

BL16

Neutron reflectometry

Soft Interface Analyzer (SOFIA)

Horizontal sample geometry Neutron Reflectometer suitable for soft condensed matters

Instrument Description

- The high penetrability of neutrons and their ability to distinguish isotopes are used to investigate nanostructures at interfaces that cannot be observed by conventional methods.
- By injecting the beam downward, free surfaces such as gas/liquid and liquid/liquid interfaces as well as the solid interface can be investigated.

Specifications

- Rapid measurements by using the high-intensity incident neutron beam
- Wavelength range: 0.2 – 0.88 nm (single frame)
  0.2-1.76 nm (double frame)
- Incident angle: < 3.5 degrees
- Sample size < 50mm^{W} x 100mm^{D}
  (typically 2 to 3 inch wafers)
- low background : $R > 10^{-7}$
- Simultaneous time-slice measurements at wide-Q range possible: Δt~s to 10 min
- Estimated measurement time for all-Q region (at beam power 850kW, as of June 2024)
  - ○Gas/solid : 30 min (∅50 mm)
  - ○Liquid/solid: 30 min (∅75 mm)
  - ○Gas/liquid : 10 min (40×40 mm^2)
  - ○Liquid/ liquid : 3 hrs (20×40 mm^2)

Sample Environments

- Temperature control : RT–250℃/ 0 - 100℃/ RT –300℃ (Rapid heating by laser irradiation)
- Solid/Liquid interface measurement cells (Remote injection available)
- Gas/Liquid interface measurement cells (Langmuir trough available)
- Liquid/Liquid interface measurement cells

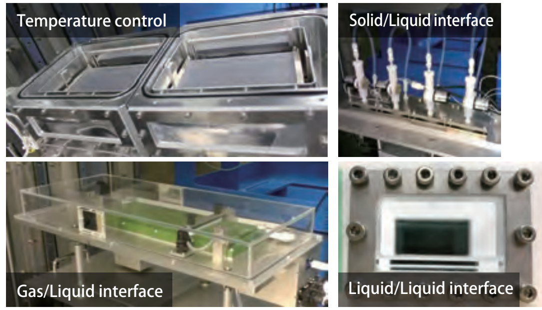

Instrument Setup

©HAYASHI Yuki

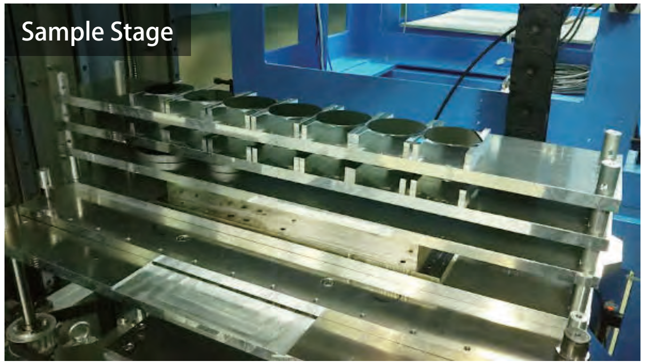

CONTACT

Hideki SETO
hideki.seto@kek.jp

Masako YAMADA
masako.yamada@kek.jp

Norifumi L. YAMADA
norifumi.yamada@kek.jp

Soft Interface Analyzer (SOFIA)

J-PARC MLF

J-PARC

BL16

Capabilities

- Evaluation of film thickness and roughness at various interfaces such as solid/solid, solid/liquid and gas/liquid.
- The average structure can be observed over a scale of a few nanometers to submicrometers in depth.

Liquid Crystal

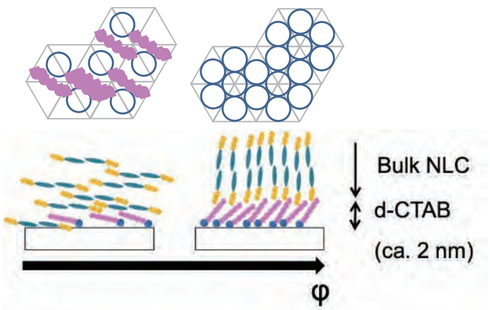

Alignment of nematic liquid crystal on glass surface was investigated.

Soft Matter, 18, 545 (2022).

©2022 Royal Society of Chemistry

Tribology

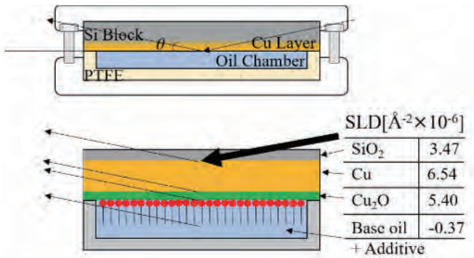

The effect of fhe friction-reduction of automotive engine oil was elucidated.

Tribol. Int., 167 (2022) 107365. ©2022 Elsevier.

Applications

- Swelling behavior of functional polymers in solvents.
- Observation of interfaces of organic devices with stacked structures.
- Structural changes in polymer thin films in annealing processes.
- Electrode interface of lithium-ion batteries.

Solar cell

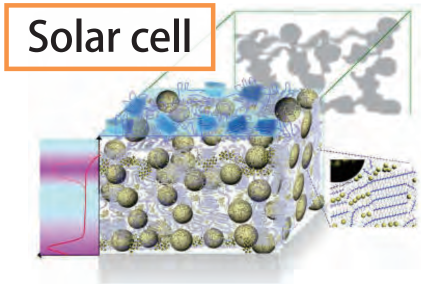

Phase separation behavior of organic solar cell thin films by complementary use of neutron and X-ray.

Soft Matter 7 (2011) 9276–9282.

©2010 Royal Society of Chemistry

Battery

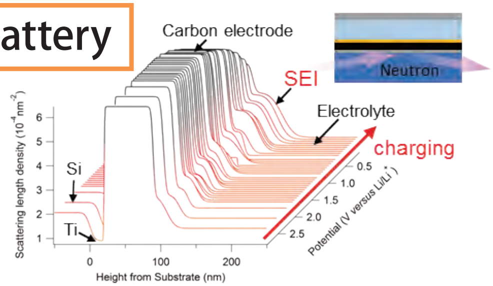

Operando measurement of film formation process on anode surface of Li-ion batteries on charging and discharging.

ACS Appl. Mater. Interfaces 8 (2016) 9540–9544.

©2016 American Chemical Society

Nafion

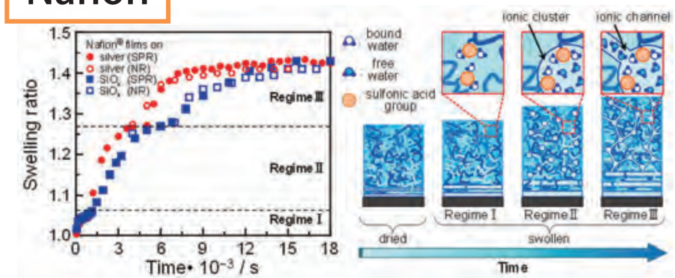

Time-lapse measurements of the process of network structure formation on swelling of proton conducting membranes.

Langmuir 34 (2018) 15483–15489.

©2018 American Chemical Society

OLED

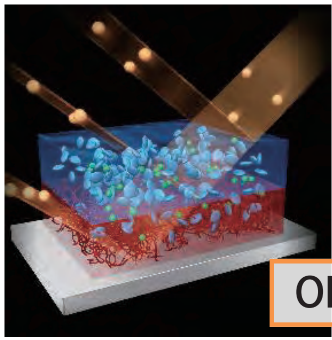

Differences in luminescence performance depending on the deposition process of OLEDs are explained by differences in the interface structure.

Adv. Mater. Interfaces 1 (2014) 1400097.

©2014 Wiley-VCH GmbH, Weinheim

BL17

Neutron reflectometry

Polarized Neutron Reflectometer (SHARAKU)

Polarized neutrons reveal the magnetic structure in a thin film.

Instrument Description

- The nanometric structure of the surface and interfaces in a thin film is examined by the reflection profile of a neutron beam incident at a small angle less than a few degrees.
- The direction and spatial distribution of the magnetic moment is analyzed by the reflection profiles dependent on the spin direction of the polarized neutrons.

Specifications

1.Specification

- Observed q range 0.05 - 17.9 nm^{-1} (unpolarized)
  0.1 - 8.19 nm^{-1} (polarized)
- Polarization ratio up to 97 %
- ^{3}He point detector
- MWPC-type two dimensional detector (detection area of 128 x 128 mm^2)

2.Measurement conditions

- Magnetic field up to 7 T
- Temperature from 4 to 500 K
- Measurement in vacuum, air, and liquids

Sample Environments

- Electro-magnets (1, 4, and 7 T)
- 4K-refrigerator
- Heater stage up to 500 K
- Electro-chemical cell
- Liquid immersion cell
- Temperature and humidity control chamber (Temperature 5 - 85℃, Humidity: 0 < 85%RH)

Instrument Configurations

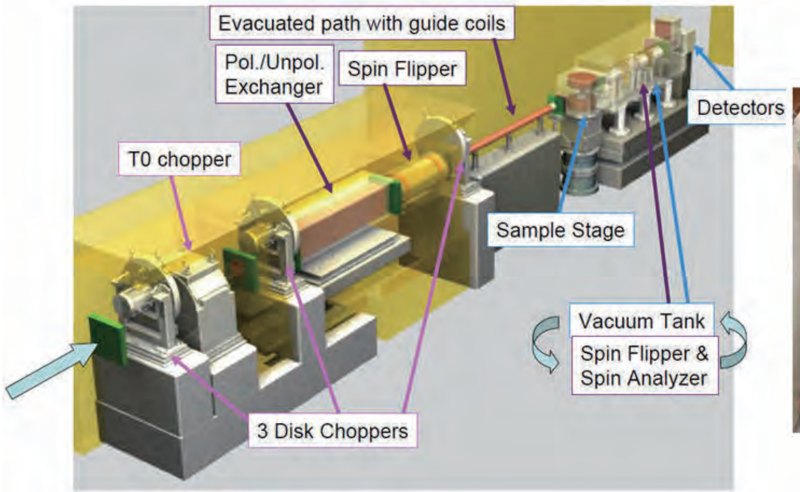

Humidity generator

Temperature and humidity control chamber

CONTACT

Hiroyuki AOKI
hiroyuki.aoki@j-parc.jp
JAEA

Takayasu HANASHIMA
t_hanashima@cross.or.jp
CROSS

Polarized Neutron Reflectometer (SHARAKU)

BL17

Capabilities

- Spatial distribution of chemicals normal to the interfaces of materials at length scales from nanometer to micrometer.
- Depth distribution of the magnetic moment in a magnetic thin film

Applications

- Analysis of moisture absorption process in polymer films
- Elucidation of proton-conduction pathway in polymer electrolytes
- Magnetic structure analysis for topological insulators and interfaces in ferromagnetic materials
- Structure analysis of electronic double layers at the interface of electrodes

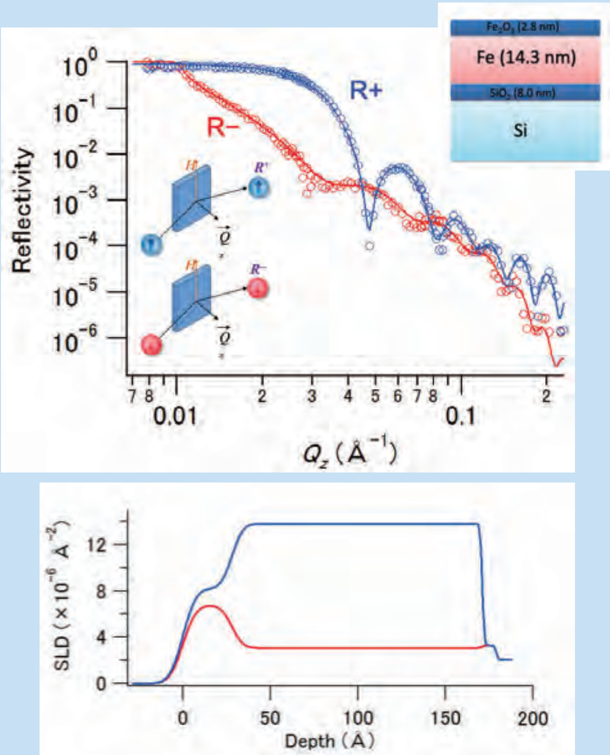

Scattering length density profile reconstructed from the reflection profiles

Structure Analysis in High Humidity

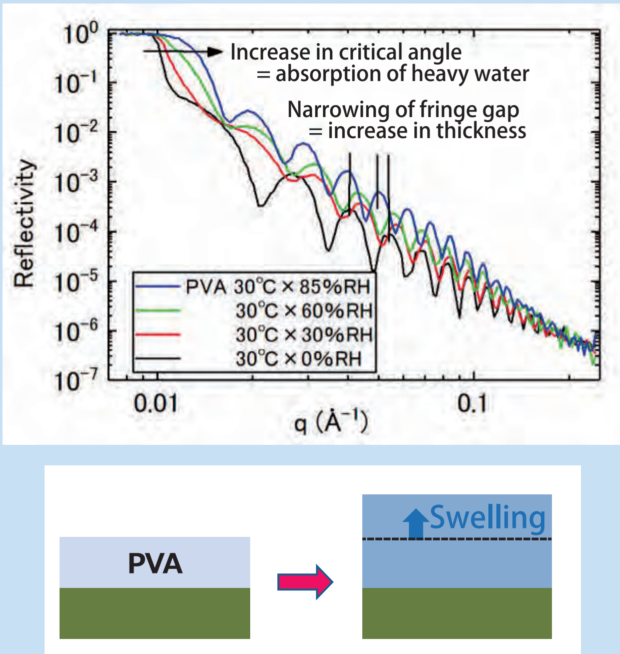

Swelling behavior of poly(vinyl alcohol) (PVA) thin film in humid atmosphere

Magnetic Structure of a Ni/FeMn Interface

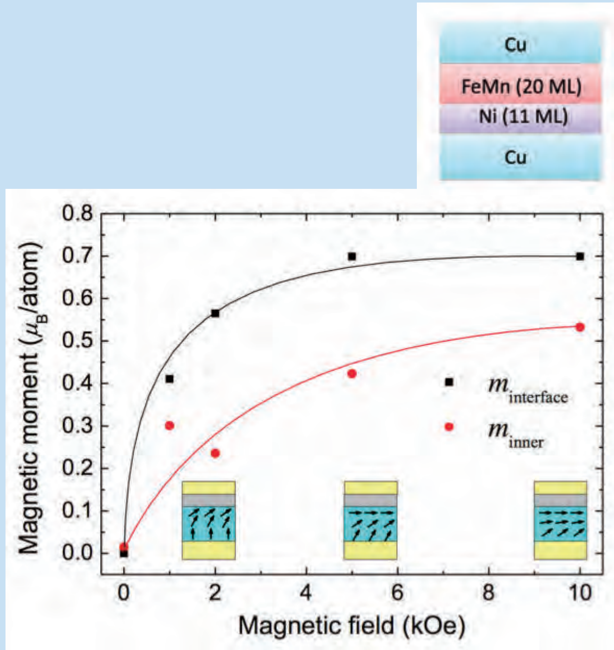

Magnetic field dependence of the depth distribution of the magnetic moment in a multi-layer thin film of Cu/Ni/Fe/Mn/Cu

BL18
Neutron diffraction

Extreme Environment Single-Crystal Diffractometer (SENJU)

Precise and reliable determination of crystal/magnetic structure

Instrument Description

- Determination of hydrogen positions and complicated magnetic structures by highly efficient diffraction measurements.
- Diffraction measurements under multiple extreme sample environments such as low temperature and magnetic field.

Specifications

- Maximum cell length : - 50 Å
- Typical sample size : 0.5 × 0.5 × 0.5 mm³ (crystal structure)
  1 × 1 × 1 mm³ (magnetic structure)
- Detector coverage : −167° to −13°
  +58° to +167°

Sample Environments

- 1-axis/2-axes goniometers (Room temperature)
- 2-axes cryostat (> 4 K)
- 2K cryostat (> 2 K, > 100 mK with dilution unit)
- ^{3}He cryostat (> 300 mK)
- Magnet (< 7 T, > 2 K, dilution unit is available)
- Furnace (< 1500 K)

Instrument Configurations


Outer view of SENJU

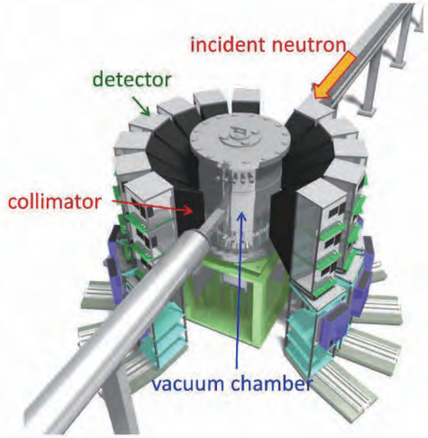

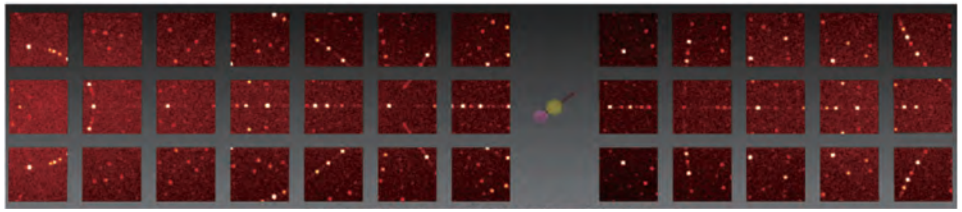
Typical diffraction image obtained by SENJU

CONTACT

Takashi OHHARA
takashi.ohhara@j-parc.jp
JAEA

Ryoji KIYANAGI
ryoji.kiyanagi@j-parc.jp
JAEA

Akiko NAKAO
a_nakao@cross.or.jp
CROSS

Extreme Environment Single-Crystal Diffractometer (SENJU)

Capabilities

- Crystal/magnetic structure determination of a small single-crystal
- Elucidation of structure-function relations under extreme sample environments

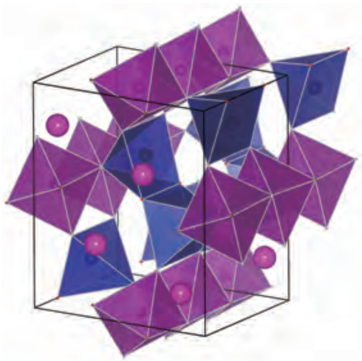

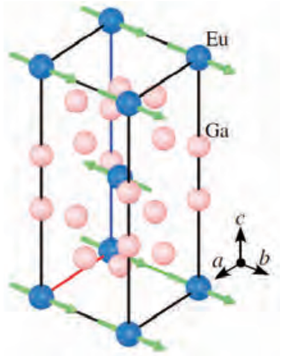

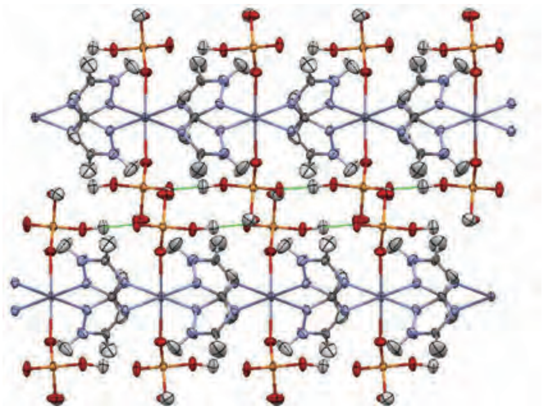

Applications

Double proton transfer coupled spin transition system

Successfully determined accurate positions of hydrogen atoms in hydrogen-bonds of a Fe complex showed the complex is the first temperature-dependent double proton transfer coupled spin transition compound.

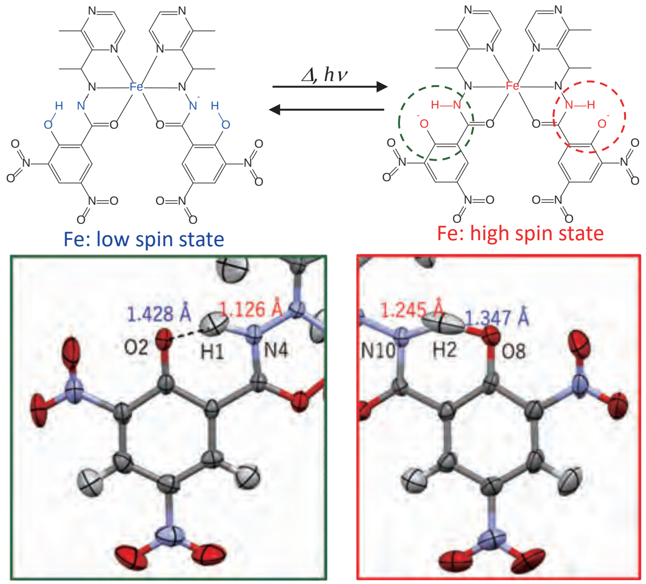

The high spin state phase is the double proton transferred state.

T. Nakanishi et al., Journal of the American Chemical Society 145 19177-19181 (2023).

(©2023 American Chemical Society)

Magnetic structure of a material showing topological Hall effect

Theoretically, the Hall effect manifests itself under a special arrangement of magnetic moments **(topological Hall effect).** However, no experimental evidence had been presented.

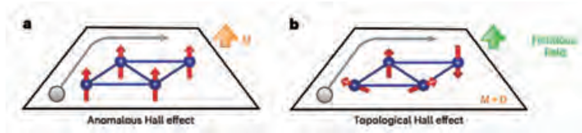

Magnetic structure of CoM_3S_6 (M = Nb, Ta) was elucidated to clarify the origin of the Hall effect observed in those compounds by using SENJU.

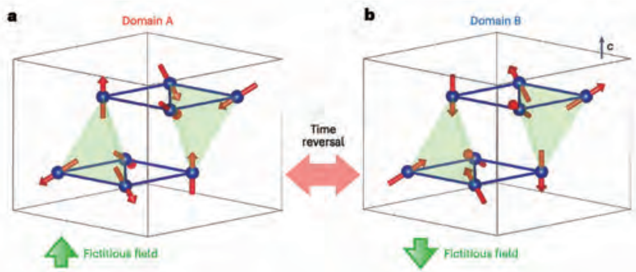

The so-called "all-in-all-out" spin arrangement generates the fictitious magnetic field. The Hall effect in the CoM_3S_6 is induced by the fictitious field and is the "topological Hall effect".

H. Takagi et al., Nature Physics 19 961–968 (2023).

(©2023 American Chemical Society)

Engineering Materials Diffractometer(TAKUMI)

Solving various problems related to stresses and microstructures of various engineering materials

Instrument Description

- Simultaneous meas. of scat. vectors (strains) in two orthogonal dir. or more
- Short time meas. with high accuracy
- Meas. the distribution of lattice strain, etc. by narrowing the gauge and scanning the sample,
- In situ meas. (abundant sample environments: load, temp.)

Specifications

- Resolution $\Delta d/d$: 0.17 - 0.4%
- d-range: 0.05 to 0.29 nm (standard), 0.05 - 0.50 nm (wide range)
- Sample stage: 700 × 700 mm^2, load capacity < 1 t
- Radial collimator: 1 mm, 2 mm, 5 mm
- Data reduction during or after meas.

Sample Environments

- Standard loading mach. (50 kN, ten, comp)
- Induction furnace for high temp loading (1373 K)
- Cryogenic system for loading mach. (15 K - 280 K)
- Hydraulic fatigue mach. (60 kN, <30 Hz)
- High temp loading mach. (30 kN, 1273 K)
- Eulerian Cradle
- Electric field application device, etc.
- Options: dilatation meas., digital image corelation

Instrument Configurations

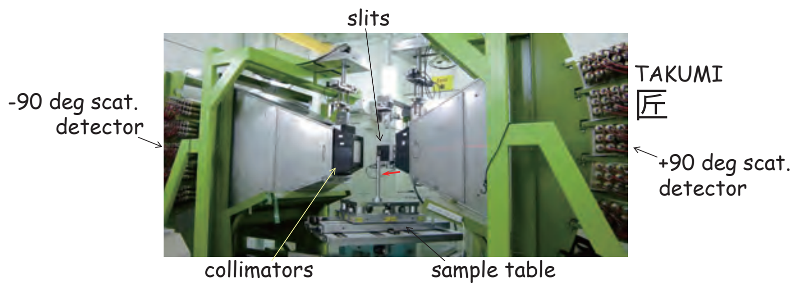


Mapping measurement

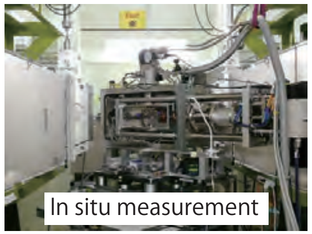
In situ measurement

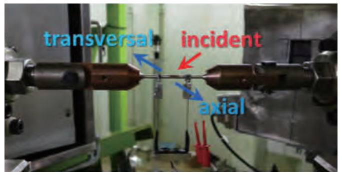

Deformation

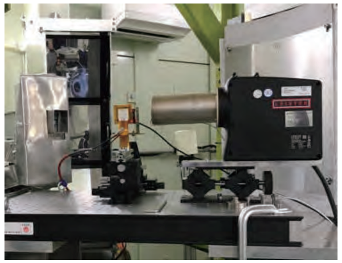
Electric field + temp

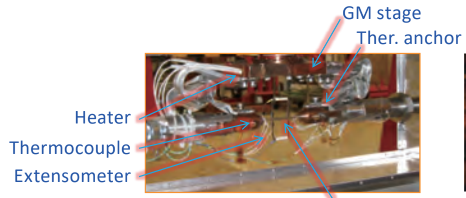

Low-temp + deformation

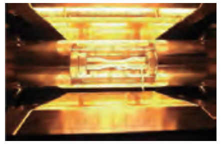
High-temp + deformation

CONTACT

Stefanus HARJO
stefanus.harjo@j-parc.jp
JAEA

Takuro KAWASAKI
takuro.kawasaki@j-parc.jp
JAEA

Wu GONG
wu.gong@j-parc.jp
JAEA

Engineering Materials Diffractometer (TAKUMI)

J-PARC MLF

J-PARC

BL19

Capabilities

- Lattice strain (stress), crystal defects (dislocations, crystallite size, etc.), texture, phase fraction, phase transformation

Mapping measurement

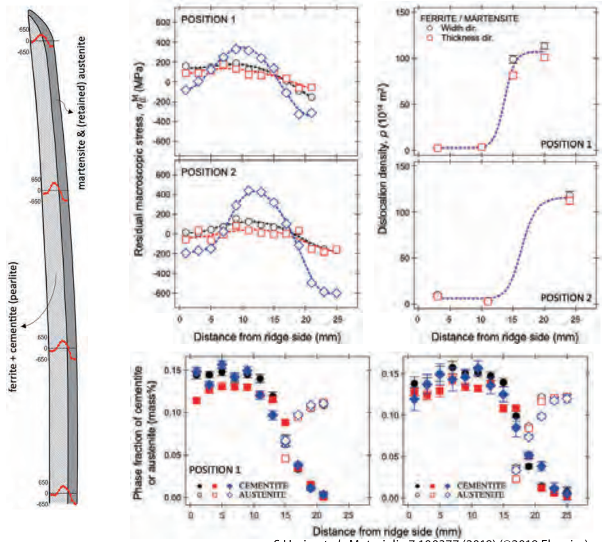

S Harjo *et al.*, Materialia 7 100377 (2019) (©2019 Elsevier)

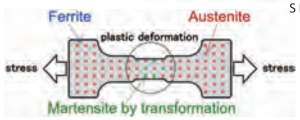

In situ measurement

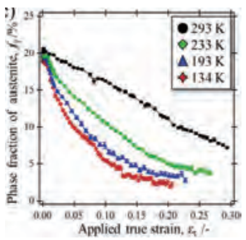

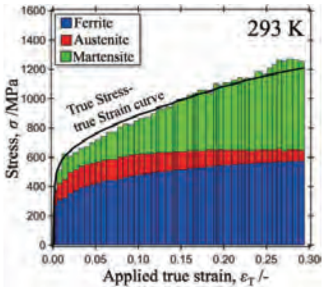

T Yamashita *et al.*, Scripta Materialia 177, 6-10 (2020) (©2020 Elsevier)

Applications

- Deformation mechanism, function expression mechanism by in situ analysis during deformation of metallic materials (RT, low temp, high temp)
- Microstructure control process by in situ analysis during thermo-mech process
- Measurement of residual strain and stress distribution of mechanical parts
- Evaluations of lattice strain and microstructures of non-metallic materials such as rocks, concrete, and ceramics

Microstructure Distribution Inside Japanese Swords

Texture
Inverse pole figure

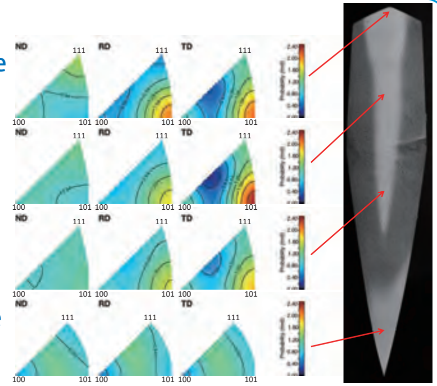

K. Oikawa *et al.*, JSPS Conf. Proc., accepted for publication. (©JSPS)

Degradation of ITER Supercond. conductor

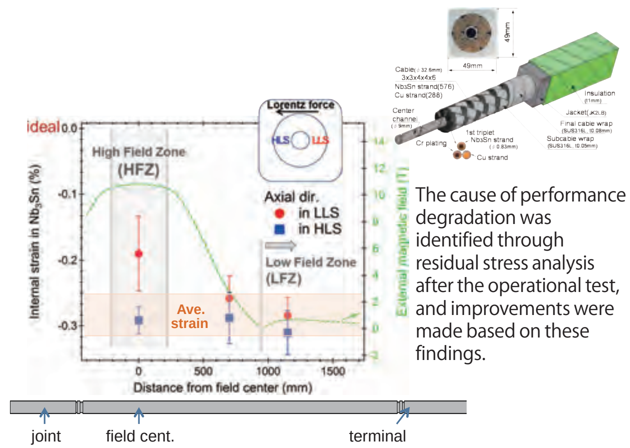

The cause of performance degradation was identified through residual stress analysis after the operational test, and improvements were made based on these findings.

T Hemmi *et al.*, Superconductor Science and Technology 26 084002 (2013) (©2013 IOP Publishing)

The Nb_3Sn superconductor phase received compressive thermal stress during manufacturing process

In situ meas during thermo-mech of steel

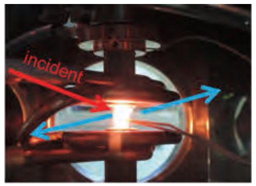

Study of the microscopic structure of metallic materials during thermo-mechanical process

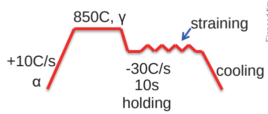

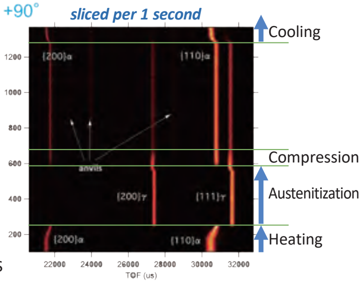

Applying compression promotes the $\gamma \rightarrow \alpha$ transformation

A Shibata *et al.*, Scripta Materialia 165 (2019) 44-49 (©2019 Elsevier)

Manufacturing process simulation

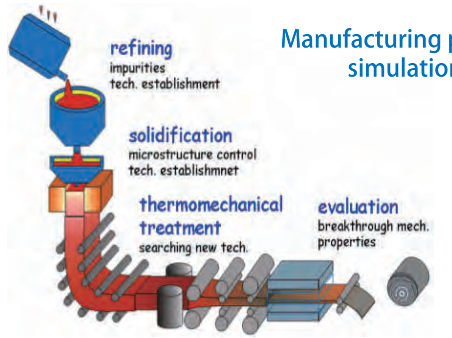

BL20

Neutron diffraction

Ibaraki Material Design Diffractometer(iMATERIA)

General-purpose neutron scattering instrument for quick and high-resolution measurements of diffraction and small-angle scattering in the wide d (lattice spacing) region

Instrument Description

- High-resolution powder diffraction
  - Crystal structure analysis of powder materials
  - Continuous rapid measurement by automatic sample exchange system
- Wide-angle detector arrangement
  - Multiscale structural analysis
  - Crystal orientation (texture) analysis by subdivided banks
  - Local structure (pair distribution function) analysis by total scattering measurements
- Small-angle scattering measurements
  - Nanostructure analysis of multicomponent materials by dynamic nuclear spin polarization

Specifications

- Measurement range: 0.07 < d < 3,000 Å
- Resolution: $\Delta d/d$ ~ 0.16% (High Resolution Bank)
- Typical measurement time:
  - Powder diffraction of cathode materials for LIB: 5~10 min at 900 kW
  - Texture measurement of steel material: 4 min at 900 kW
  - Small-angle scattering of polymer material: 3 min at 500 kW
  - (depending on the composition of the sample, the purpose of measurement, etc.)

Sample Environments

- Sample exchange mechanism (RT, vacuum)
- Vacuum high temperature furnace (RT - 1173 K)
- Cryo-furnace (3 K - RT, RT - 673 K)
- Rapid heating and cooling device (RT - 1273 K, +10 K/s, -20 K/s)
- High temperature universal deformation apparatus (RT - 1273 K, maximum load: 50 kN)
- Sample exchanger for small-angle scattering
- Superconducting magnet for nuclear spin polarization (1.2 K, 7 T)

Instrument Configurations

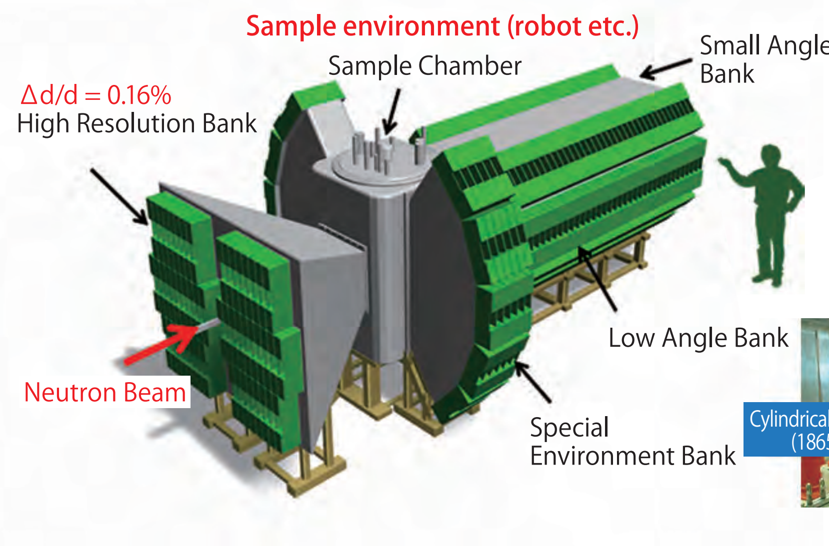

Sample exchange system

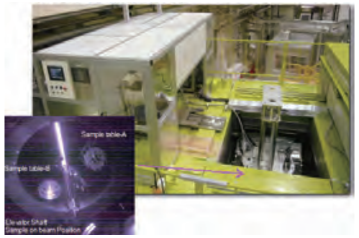

High temperature universal deformation apparatus

In-operando battery measurement system

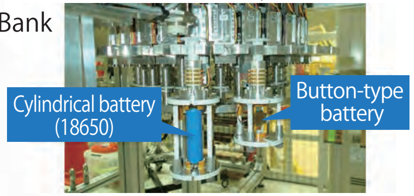

Rapid heating and cooling device

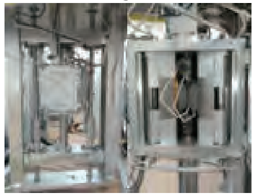

CONTACT

Toru ISHIGAKI
t_ishigaki@cross.or.jp
CROSS

Kazutaka IKEDA
k_ikeda@cross.or.jp
CROSS

Takafumi HAWAI
t_hawai@cross.or.jp
CROSS

Ibaraki Material Design Diffractometer (iMATERIA)

J-PARC MLF

J-PARC

BL20

Capabilities

- Crystal structure
- Local structure of crystalline and amorphous
- Nanostructure and microstructure
- Crystal orientation (texture)

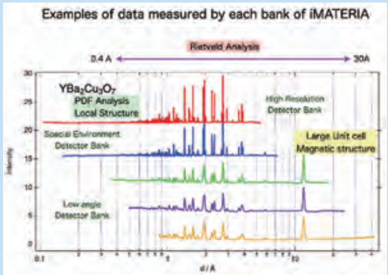

Applications

- Crystal structure of solid electrolyte for all-solid-state lithium-ion batteries
- Crystal structure changes of electrode materials for lithium-ion batteries by in-operando charging and discharging measurement
- Atomic arrangements of photocatalyst coating liquid
- Crystal structure of platinum alternative catalyst for fuel cells
- Structure of high-performance rubber materials with crosslinked network
- Collapse process of detergent foam with surfactants
- Texture of steel materials
- Residual austenite components in steel materials
- Dynamic microstructural changes of steel materials in heat treatment process

Ionic conduction paths in new solid electrolytes for all-solid-state lithium-ion batteries

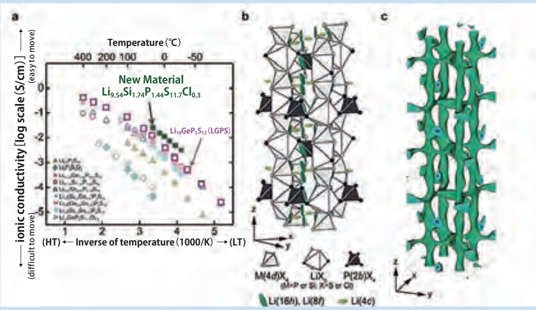

In-operando neutron diffraction measurement during charging and discharging of laminate cell type lithium-ion battery.

Sample holder for laminate type cell

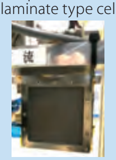

Diffraction pattern changes during charging for stacked battery cells

Charge rate: 0.1C

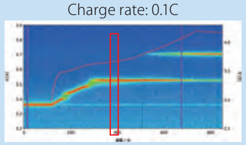

Charge rate: 1C

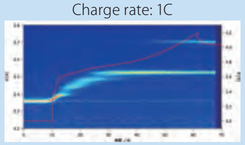

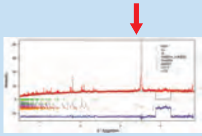

Structural changes in positive and negative electrodes can be analyzed in Rietveld refinement in every minute

In situ neutron diffraction measurement under an environment simulating the microstructure control process of steel materials

Measurement of phase transformation behavior using rapid heating and cooling device

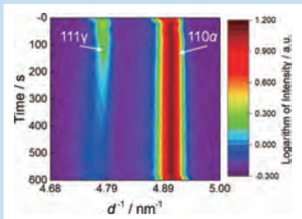

Due to the bainite transformation that occurs during constant temperature holding at 673 K, austenite with a low carbon concentration is gradually consumed, and austenite with a high carbon concentration appears.

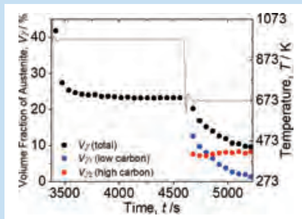

By treating austenite with different carbon concentrations as separate phases, it is possible to quantitatively determine the abundance ratio of both.

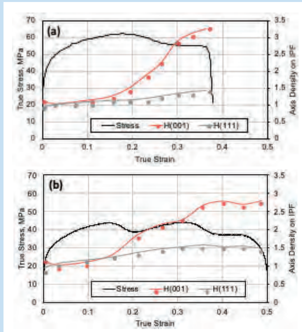

Texture changes using a high temperature universal deformation apparatus

Measurement of changes in (011) and (111) orientation due to tensile deformation at room temperature (a) and high temperature (b)

Observation of texture changes corresponding to stress oscillations observed during high-temperature tensile deformation

In situ small-angle neutron scattering measurements of the collapse process of detergent foam

Utilizes the characteristics of time-of-flight measurement using pulsed neutrons to instantaneously measure neutron scattering in the wide-q range

Development of new surfactants to create detergents with appropriate foam generation and removal properties

Analysis of foam structure and collapse process with different surfactants

There are surfactant micelles in the foam similar to those in the solution

- The foam film thickness does not change significantly
- Observing the drainage process of water in foam

Foaming the surfactant solution with an air pump Then, the bubbles are irradiated with a neutron beam and the collapse process is measured using time-resolved small-angle scattering method.

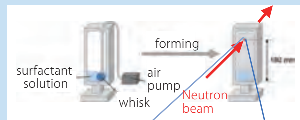

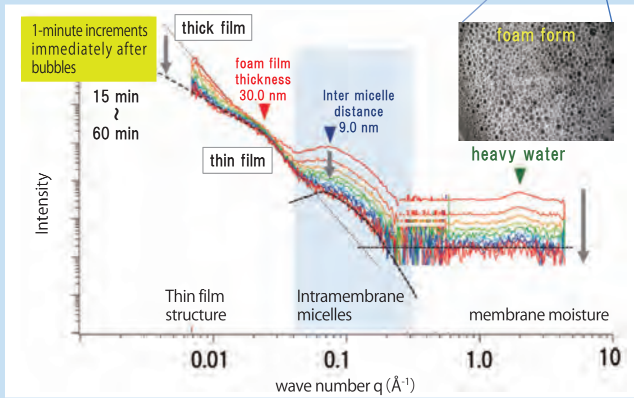

BL21 High Intensity Total Diffractometer (NOVA)

Neutron diffraction

Neutron total diffractometer for structural analysis from crystals to liquids and amorphous materials.

Instrument Description

- Neutron total scattering and powder diffraction measurements using the world's highest intensity
- Measurements over a wide momentum transition space (high real space resolution)

Specifications

- Q range: 0.03 - 100 Å^{-1} (d range: 0.06 - 200Å)
- Q resolution: $\Delta Q/Q$ ~ 0.35 %
- Scattering angle 2θ: 0.7 - 170°
- Standard sample vol.: ∅6 mm×20 mmh (0.6 cc approx.)

Sample Environments

- Auto sample changer (SC)
  No. of sample: 40 (room temperature)
- Auto sample changer with closed cycle refrigerator (TSC)
  No. of sample: 18, Temp.: 20 - 700 K
- Top-Loading cryo-furnace (TLC)
  Temp.: 5 - 700 K
- Fermi chopper for Inelastic scattering exp.
  Reso.: 5 - 20%
- 2K cryostat (MLF common SE)
  Temp.: 1.8 - 300 K
- ^{3}He cryostat (MLF common SE)
  Temp.: 0.3 - 300 K

Instrument Configurations

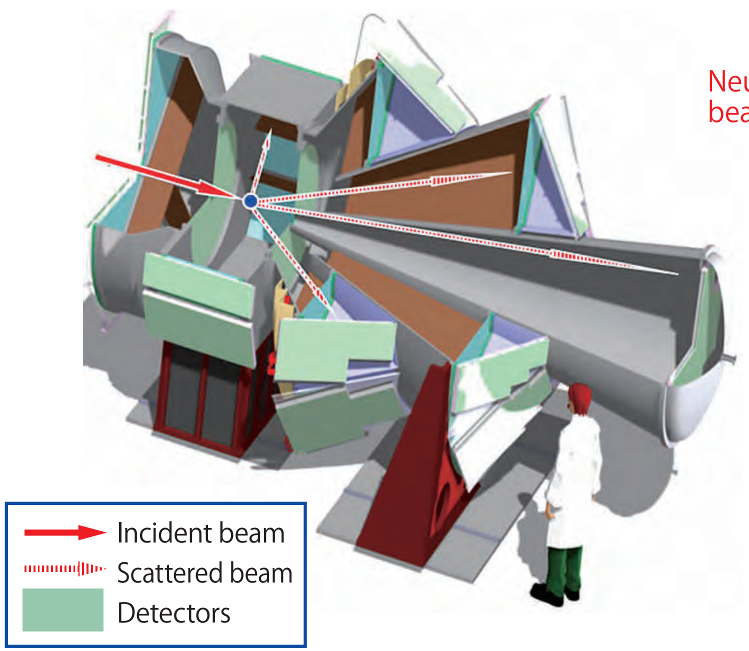

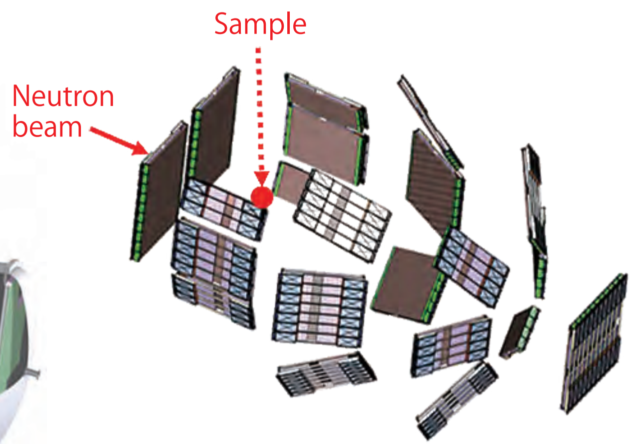

Beam size (max.)
: 20×20 mm^2

^{3}He-gas position sensitive neutron detector
2MPa 1/2 inch 800mm

CONTACT

Takashi HONDA
takhonda@post.kek.jp

Hidetoshi OHSHITA
ohshita@post.kek.jp

High Intensity Total Diffractometer (NOVA)

Capabilities

- Atomic positions, such as hydrogen, and magnetic structure, and changes in these
- Structural changes from the nearest neighbor atom distance to about nm
- Structural analysis of fluctuation systems such as amorphous and liquids

Examples of high-speed measurements

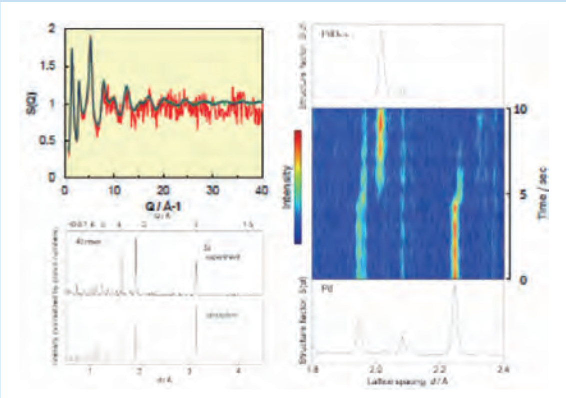

(Upper left) 1sec measurement of SiO_2 glass
(bottom left) 40msec measurement profile of Si powder
(Right) Deuterium absorption process of Pd (10 sec)

Applications

- Crystal and local structure analysis using small amounts of sample
- Short-time observation of structural changes by in situ measurements
- Observation of structural changes by in situ measurements at low/high temperatures・under (gas) pressure
- Local structure analysis of solids・liquids using isotopic substitution

Structural science of H^- conductor Ba-Li oxyhydride

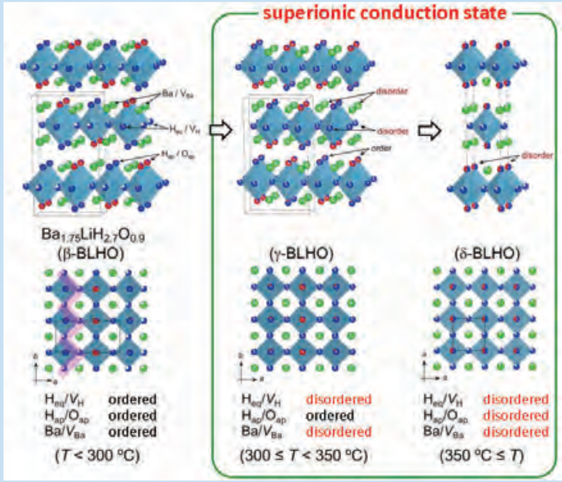

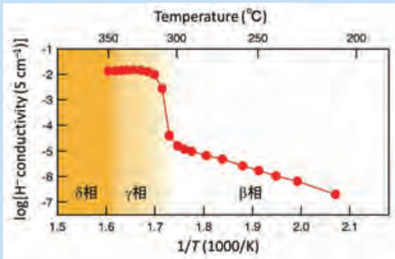

F. Takeiri *et al., Nature Mater.*, **21**, 325 (2022)
(© 2022 Springer Nature).

Local structure of sulfur molecules in CS_2 solution by isotopic substitution

Y. Kameda *et al., Bull. Chem. Soc. Jpn.*, **95**, 1481 (2022)
(© 2022 The Chemical Society of Japan).

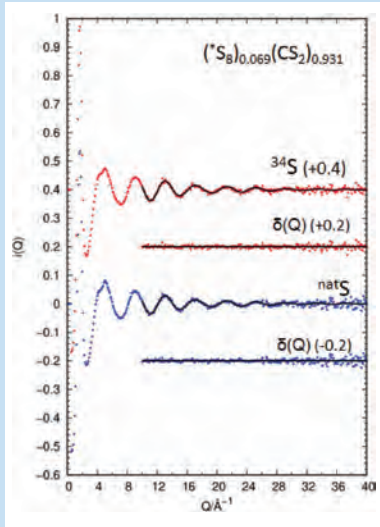

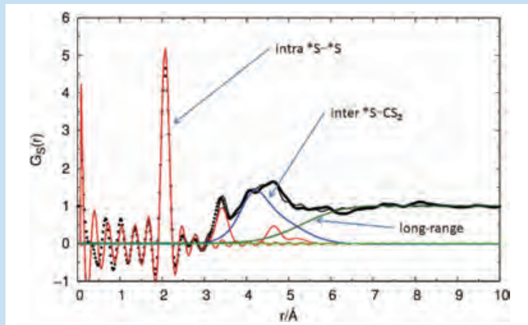

BL22

Neutron imaging

ENERGY RESOLVED NEUTRON IMAGING SYSTEM –RADEN-

Visualization of internal sample shape, crystallographic, elemental, and magnetic information by analyzing the energy dependence of neutron transmission spectra with position resolution

Instrument Description

- Energy-resolved neutron imaging
  - Bragg edge imaging
  - Resonance absorption imaging
  - Polarized neutron imaging
  - Phase contrast/dark field imaging
- Neutron radiography, tomography

Specifications

- Wavelength range: $\lambda < 8.8$ Å (L=18 m, 25 Hz)
- Wavelength resolution ($\Delta\lambda/\lambda$): 0.2%
- Neutron flux @1 MW:
  1.1×10^8 n/s/cm ($E < 1$ MeV, L/D=180)
- Beam size: < 300×300 mm^2
- Spatial resolution: 10 - 300 μm
- Collimator ratio (L/D): 180 - 7500

Sample Environments

- Filter (Pb, Bi, BK7)
- Sample stage
  (Large: capacity 1.0 t, Middle: capacity 650 kg)
- Heater (resistive heating, Infra red lamp)
- ToF 3D polarimetry apparatus
- Neutron Talbot-Lau interferometer
- Hydrogen gas supply/dilution unit

Instrument Configurations

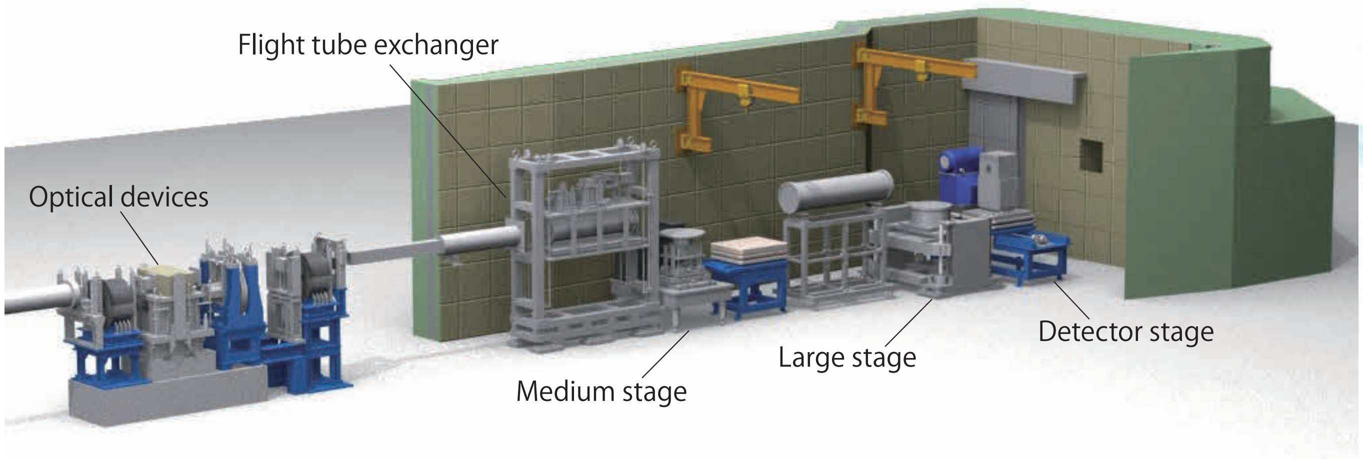

T. Shinohara et al., Rev. Sci. Instrum. 91, 043302 (2020). (©2020 AIP Publishing LLC)

CONTACT

Takenao SHINOHARA
takenao.shinohara@j-parc.jp
JAEA

Tetsuya KAI
tetsuya.kai@j-parc.jp
JAEA

Hirotoshi HAYASHIDA
h_hayashida@cross.or.jp
CROSS

Energy Resolved Neutron Imaging System (RADEN)

Capabilities

- ●Conventional radiography/tomography
  Non-destructive observation, defect inspection, liquid flow
- ●Bragg edge imaging
  Crystallographic information, strain distribution
- ●Polarimetric imaging
  Magnetic field information
- ●Resonance absorption imaging
  Elemental information, temperature distribution

Neutron CT images of a Japanese sword

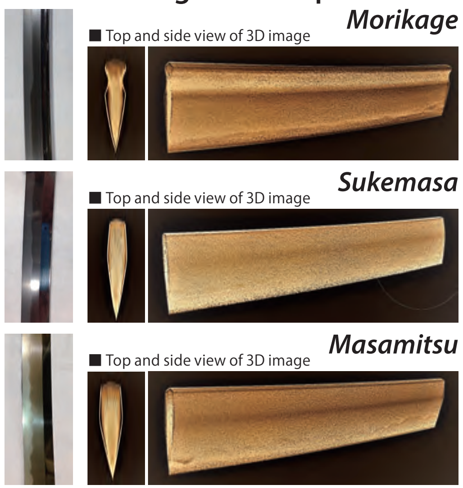

Y. Matsumoto, et al, Materials Research Proceedings 15 (2020) 221-226.
(© 2020 Materials Research Forum)

Neutron CT images of automobile parts

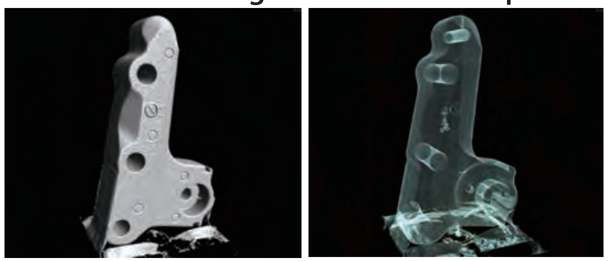

Applications

- ●Neutron radiography/tomography：Observation of energy-related devices (Li ion batteries, fuel cells, water electrolysis, etc.), grease in mechanical bearing, concrete, cultural heritage/archeology (Japanese swords, meteorite, etc.), nuclear engineering.
- ●Bragg edge imaging: steels, metallic alloys, single crystals, cultural heritage/archeology (Japanese swords, meteorite, etc.)
- ●Resonance absorption: Li ion batteries, scintillator materials, nuclear engineering
- ●Polarimetric imaging: electric motors, electric transes, magnetic materials (electric steels, ferritic magnets, etc.)

3D distribution of magnetic field inside a solenoid analyzed by neutron polarimetric tomography

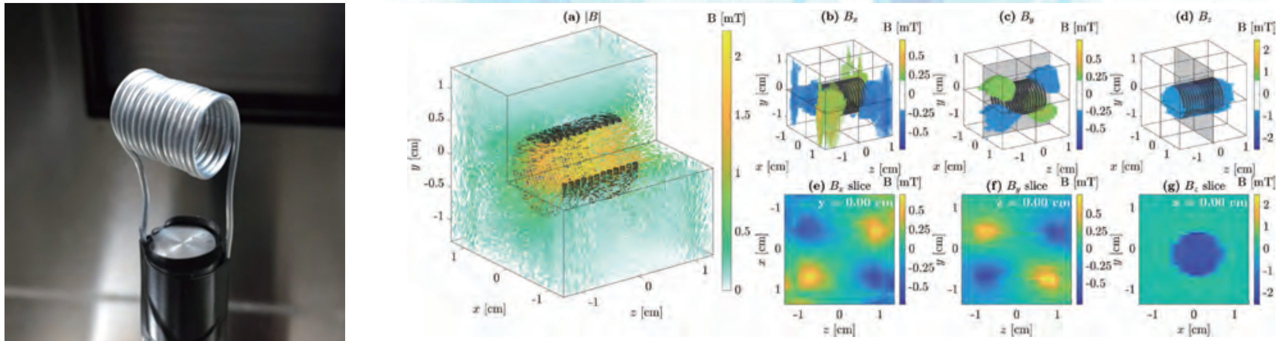

M. Sales *et al.*, J. Phys. D: Appl. Phys. 52, 205001 (2019) (© 2019 IOP Publishing).

Spatial distribution of crystallographic information ofinduction heated gear obtained by Bragg edge imaging

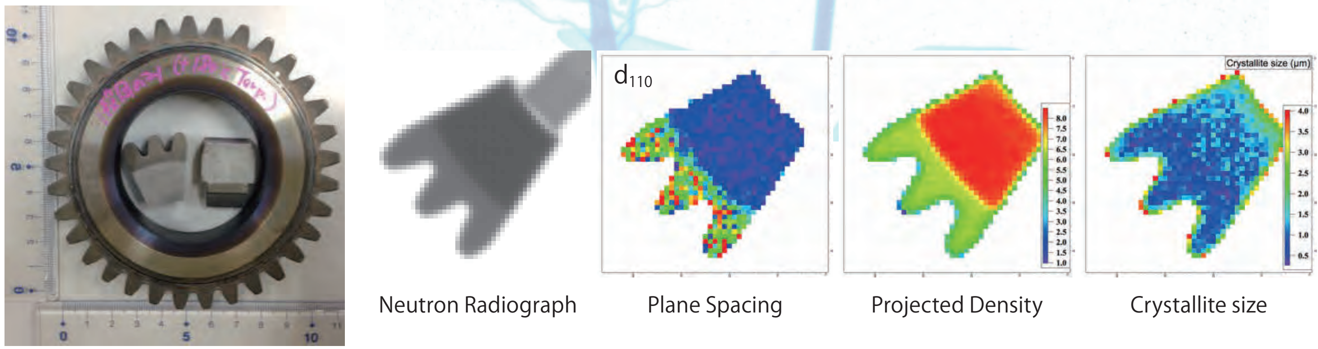

BL23

Quasi-elastic/inelastic neutron scattering

Polarized Neutron Spectrometer (POLANO)

POLANO is a direct geometry chopper spectrometer with polarization options for the study of dynamics in materials such as magnets, superconductors, functional materials, and even liquids, leading to ability to separately observe various degrees of freedom in materials.

Instrument Description

- Reasonable resolution viewing a decoupled moderator
- Wide accessible momentum space
- Relatively higher energy polarization analysis
- Application example
  - Magnetism
  - Strongly correlated electron systems
  - Quantum fluids
  - Vibration of atoms or molecules

Specifications

- Moderator: Decoupled moderator
- Detectors: (hor.) -25˚ - 125˚, (ver.) ± 8˚
- Incident energy: 10 – 1000 meV
- Energy resolution: $\Delta E/E_i \geq 2$ - 4% @E=0
- Momentum resolution ($\Delta Q/k_i$): 1 – 2%
- Beam cross section: 20x20 mm^2 (optimum) – 50x50 mm^2
- Polarization energy: 10 meV < E_i < 40 meV

Sample Environments

- Top-loading GM cryostat (T = 4 –300 K)
- Bottom-loading GM cryostat (T = 7-300 K)
- ^{3}He sorption refrigerator (T = 0.3 K)
- (MLF) 7 T-magnet with ORC
- 10mm, 20mm, 30mm, 40mm, 50mm collimators
- SEOP polarizer and 5.5Q_c bending super mirror analyzer (20˚ of scattering angles)

Instrument Configurations

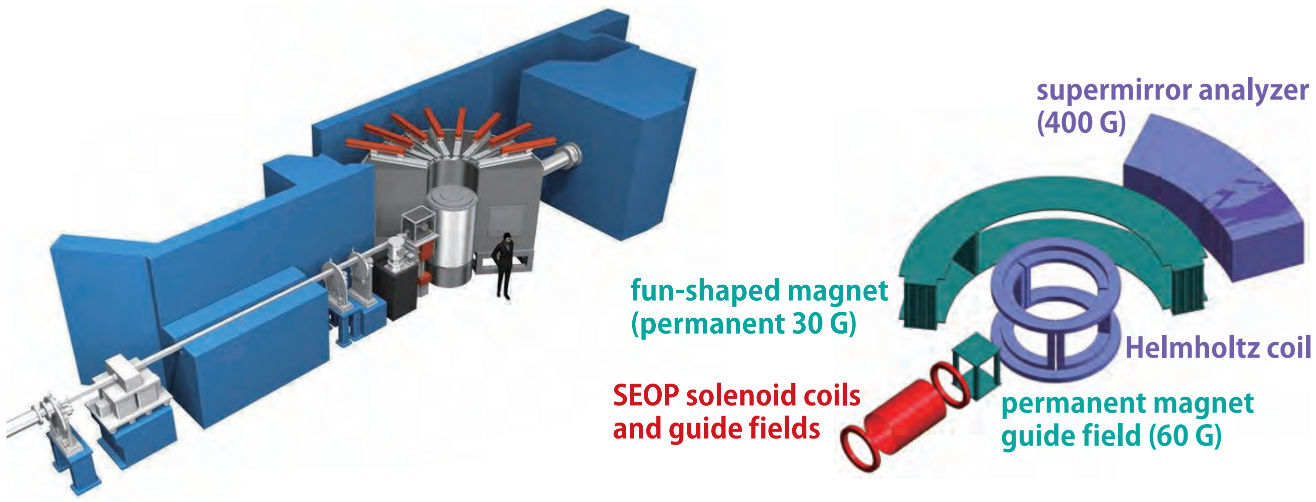

CONTACT

Tetsuya Rex YOKOO
tetsuya.yokoo@kek.jp

Shinichi ITOH
shinichi.itoh@kek.jp

Capabilities

- POLANO is optimized for the measurement of spectroscopies.
- Variety of so-called degrees of freedom in materials, such as atoms, molecules, spins, charges, and orbitals can be detected as a dynamic properties by the POLANO.
- Cross-correlations of the degrees of freedom can be separately observed including coherent/incoherent cross section.

Applications

- Transverse/longitudinal modes separation in quantum spin systems
- Right/left-handedness in chiral materials
- Lattice vibration and spin waves in high temperature superconductivity
- Elementary excitations and orbital waves in orbital-ordered electronic states
- Spin-lattice interactions in multiferroic materials [7)]
- Multipole ordering and hierarchical structures in *f*-electron systems

Degrees of freedom in materials

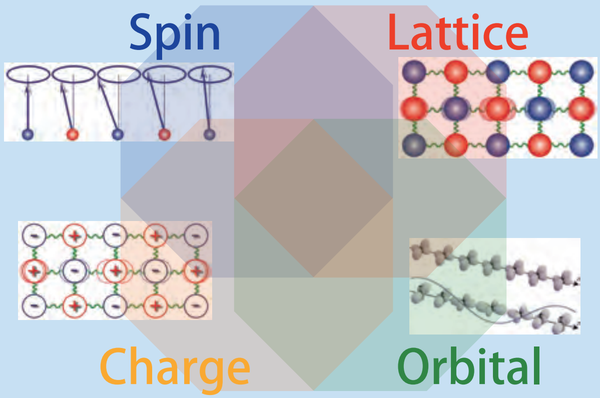

lattice vibration -magnetic fractuation ($YBa_2Cu_3O_{6+d}$)

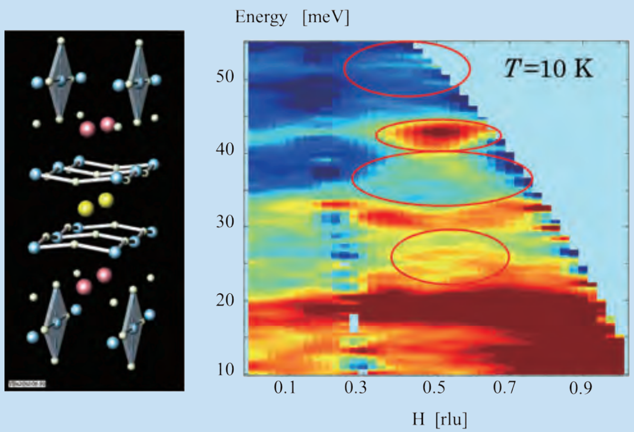

Ovital excitation

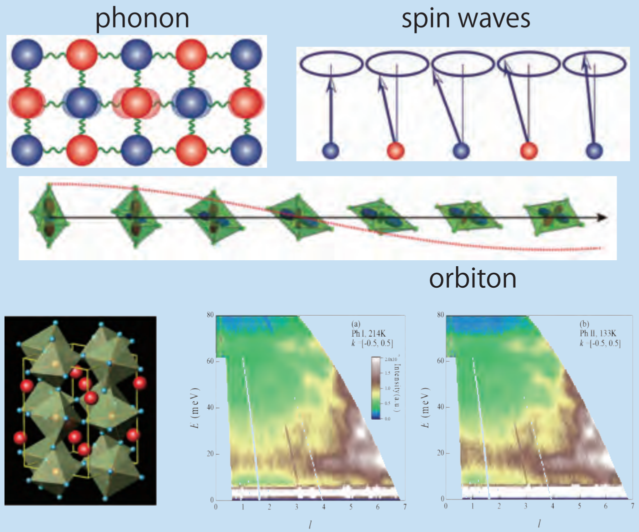

For 7), see Glossary (p. 62).

D1

Muon spin rotation/relaxation/resonance

Muon experiment instrument for materials and life science (Muon D1)

Detecting local magnetic fields in materials by using muon. Muons with a high momentum are available, allowing high-pressure experiments because of the high transmission capability. Negative muon can observe local magnetic fields near nuclei in materials.

Instrument Description

- μSR experimental using pulsed positive or negative muons with variable-momentum.
- Measurements under various complex conditions, such as high pressure and low temperatures, to cover a wide variety of phenomena.

Specifications

- Beam property : μ^+/μ^- 27 - 90 MeV/c
  single-pulse (surface muon) or double-pulse
- Sample Environment: Temp: 0.05 – 1000 K
  Mag. Field: 0 – 0.4 T(along the beam direction)
  0 – 0.01 T (perpendicular to the beam direction)
  Pulsed light-irradiation by a flash lamp

Sample Environments

- Oxford top-loading dilution refrigerator (T = 0.05 – 30 K)
- Oxford microstat (T = 4 – 500 K)
- high-T furnace (T = 300 – 1073 K)

Instrument Configurations

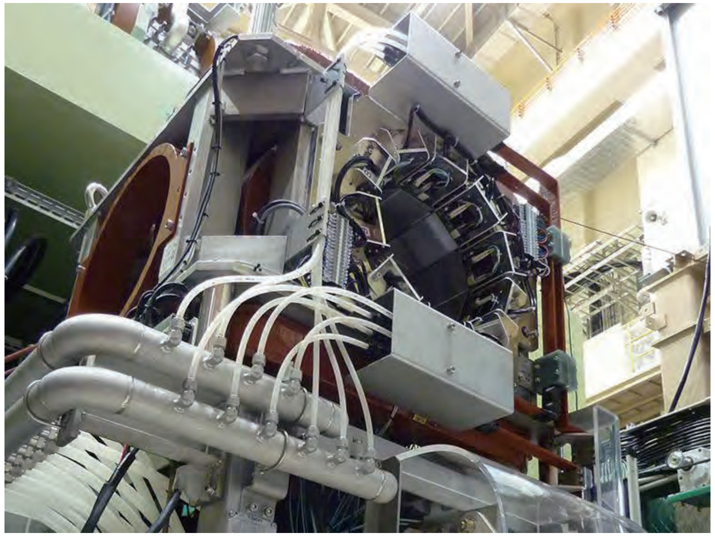

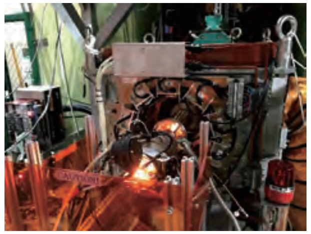

High-temperature Furnace

Dilution Refrigerator

CONTACT

Akihiro KODA
coda@post.kek.jp

Wataru HIGEMOTO
higemoto.wataru@jaea.go.jp

Muon Apparatus for Materials and Life Science Experiments

J-PARC MLF

J-PARC

D1

Capabilities

- Magnetic and electronic states in solids and liquids by observations of internal magnetic field.
- Electronic state of dilute hydrogen in matter.
- Electron, hydrogen and ion dynamics.

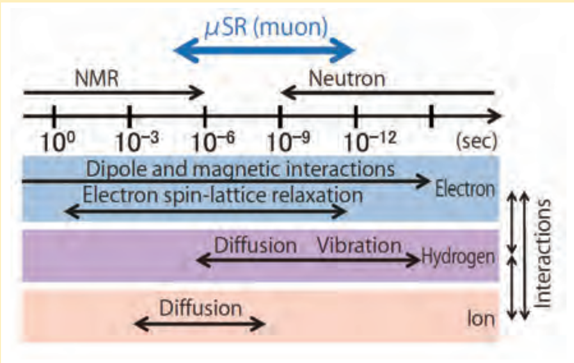

Unique time range: bridging the gap between neutron and NMR sensitivities.

Applications

- Cooper pairing symmetry in superconductors.
- Flux-line lattice in superconductors.
- Electronic structure of hydrogen in semiconductors.
- Magnetism near the quantum critical point.
- Ion diffusion in solids.
- Ion dynamics by negative μSR.

Observing the internal magnetic field by using negative muons.

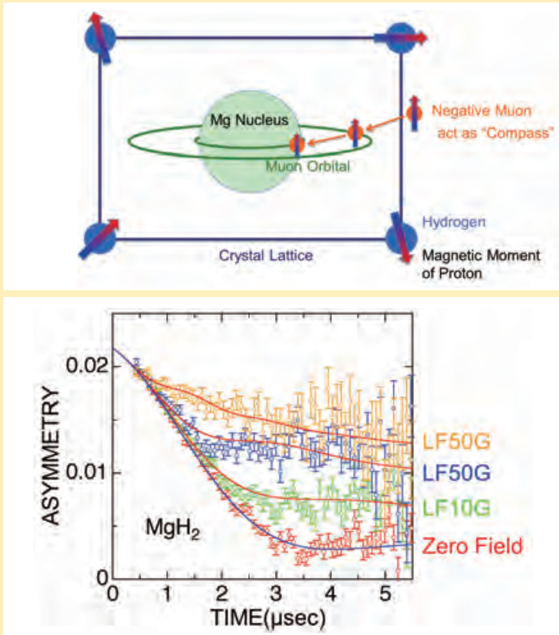

Phys. Rev. Lett. 121, 087202 (2018). (© 2018 Amerian Physical Society)

Ferromagnetic fluctuation in the high-Tc cuprate $[(BiPb)_2Sr_2CuO_{6+d}]$

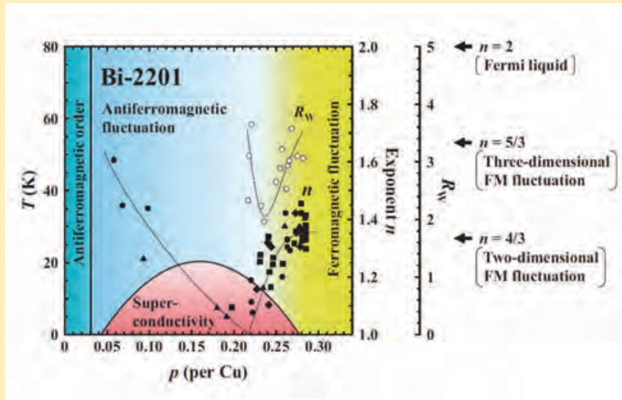

Phys. Rev. Lett. 121, 057002 (2018). (© 2018 Amerian Physical Society)

D2

Fundamental muon physics / Negative muon X-ray elemental analysis

Muon Experimental Area for Basic Science (Muon D2)

Experimental area for research on properties of muons as a particle, structure and reaction of muonic atoms, and non-destructive elemental analysis on archeological or rare specimens using the world's strongest pulsed muons source.

Instrument Description

- Momentum-changeable positive and negative muons with high intensity are available
- Users can bring their equipment for experiments
- Non-destructive elemental analysis with muonic X-rays can be performed

Specifications

● Type	Decay positive・negative muon Surface positive muon
● Momentum	5 - 50 MeV/c　(changeable)
● Intensity	$5.0\times10^{6}\ \mu^{\pm}$/s@50 MeV/c at 1 MW
● Structure	Double bunch 25 Hz Bunch Width　100 ns Interval　600 ns (Single bunch available using kicker)

Sample Environments

- Open space
- Under vaccuum
- He, N_2, or other inert gasses using a kapton window

Instrument Configurations

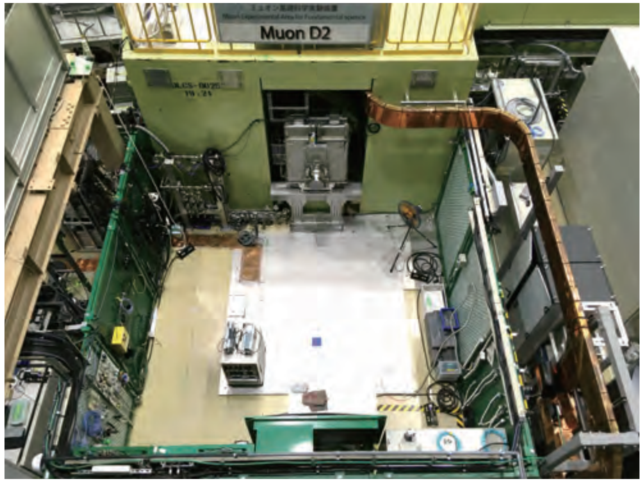

D2 Experimental Area

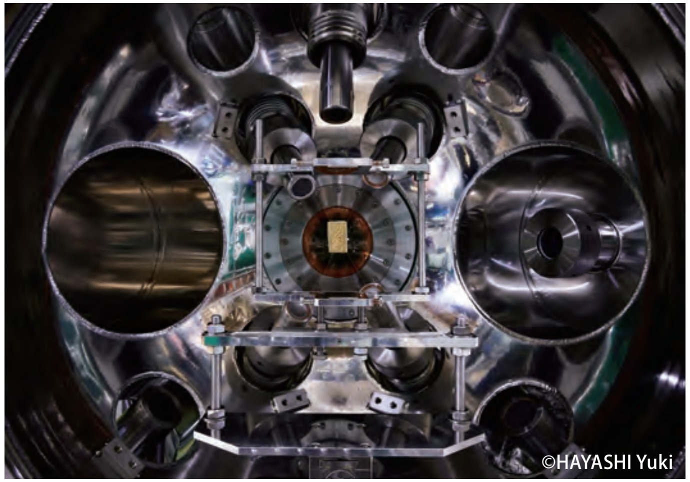

Experimental chamber equipped with Ge detectors featuring a gold coin

CONTACT

Izumi UMEGAKI
umegaki@post.kek.jp

Patrick STRASSER
patrick.strasser@kek.jp

Muon Experimental Area for Basic Science

Capabilities

- Elemental Analysis
- Soft error in semiconductor
- Physical properties of muon

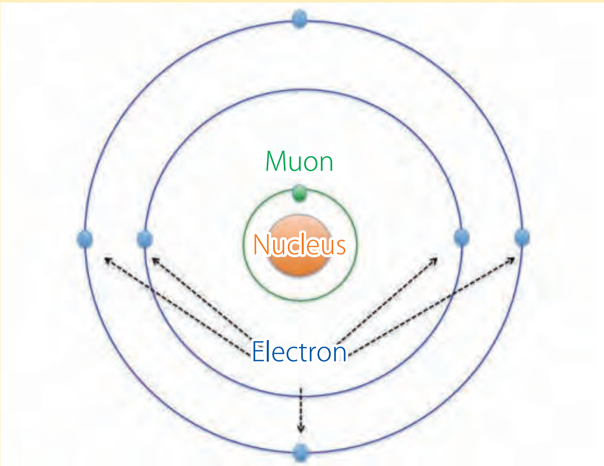

Schematic representation of a muonic atom

Applications

- Reproduction of soft error in semiconductor due to cosmic muon irradiation using muon beam
- Non-destructive elemental analysis (Archeologyical specimens ・ meteorites ・ batteries, etc.)
- Observation of muon rare decay phenomena

Soft error investigated by muon irradiation

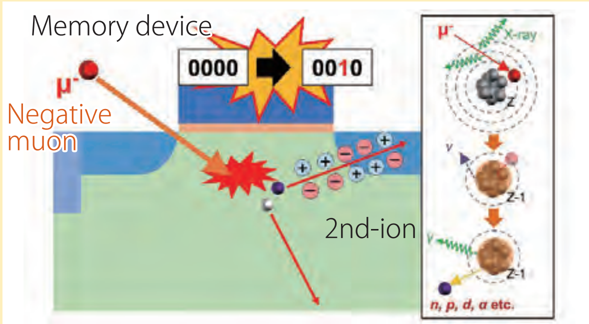

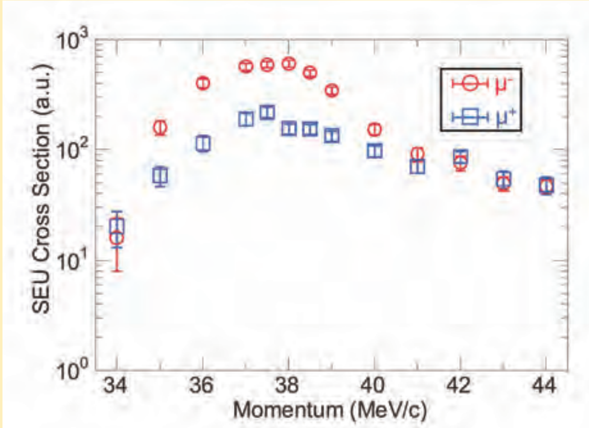

IEEE Transaction on Nuclear Science 65, 1742 (2018). (© 2018 IEEE)

Non-destructive elemental analysis with muonic

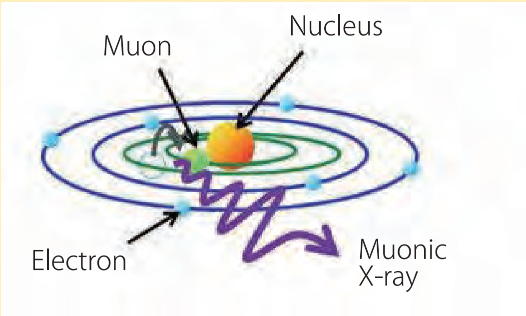

Stone sample from Ryugu asteroid Photo: JAXA

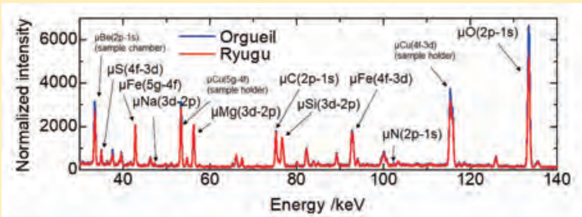

Science (2022), DOI:10.1126/science.abn8671. (©2022 AAAS)

H1

Fundamental muon physics / Negative muon X-ray elemental analysis

High-intensity muon beam for general use (Muon H1)

Various experimental studies such as fundamental physics are performed with high precision and sensitivity using high-intensity pulsed muon beams

Instrument Description

- Positive and negative pulsed muon beams with high intensity and momentum tunability are available.
- User equipment can be brought in for experiments requiring high statistics with long beamtime
- Open space, 6.2m(D)×5.7m(W)×3.5m(H)
- Surrounded by a magnetic shielding
- Area temperature is controlled by packaged air conditioning.

Specifications

- Type of beam: Surface muon or cloud positive/negative muon
- Momentum: 10 ～ 120 MeV/c
- Intensity: 10^8 μ^+/s@28 MeV/c、4×10^7 μ^-/s@50 MeV/c
- Beam structure: Double bunches, 25 Hz
  Bunch width 100 ns, bunch separation 600 ns
- Equipment: Users can install their own equipment.

Sample Environments

- Open space. Users can install their own equipment.

Instrument Configurations

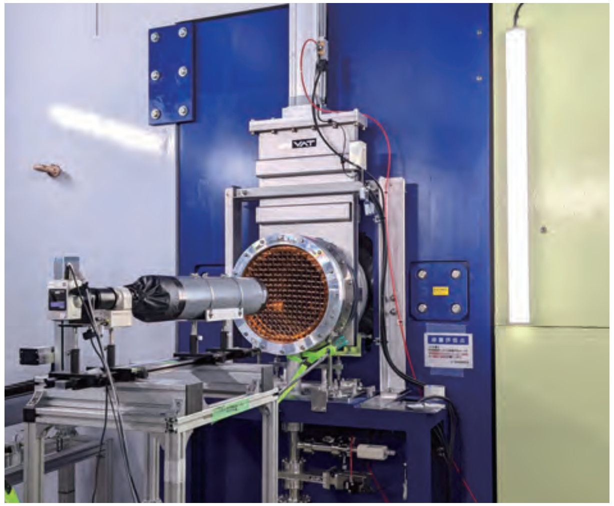

Beam port

CONTACT

Takayuki YAMAZAKI
takayuki@post.kek.jp

Naritoshi KAWAMURA
nari.kawamura@kek.jp

High-intensity muon beam for general use

Capabilities

- Fundamental physical constants of muon (w/ user-prepared equipment)
- New physics beyond the Standard Model of particle physics (w/ user-prepared equipment)

Applications

- Precise measurement of the muonium hyperfine structure
- Search for muon-to-electron conversion

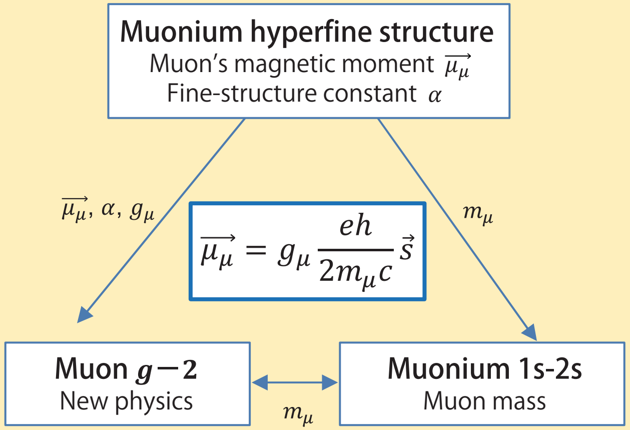

Muon-to-electron conversion

$$\mu^- + (A,Z) \rightarrow e^- + (A,Z)$$

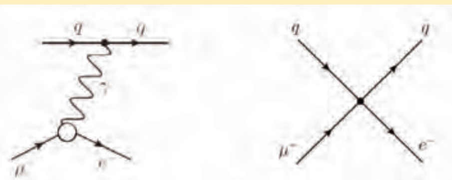

New physics

Precise measurement of the muonium hyperfine structure (MuSEUM experiment)

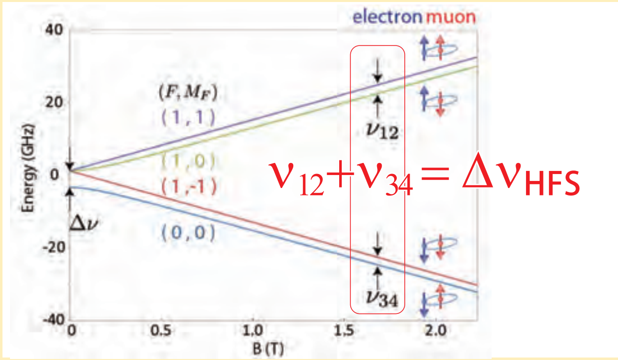

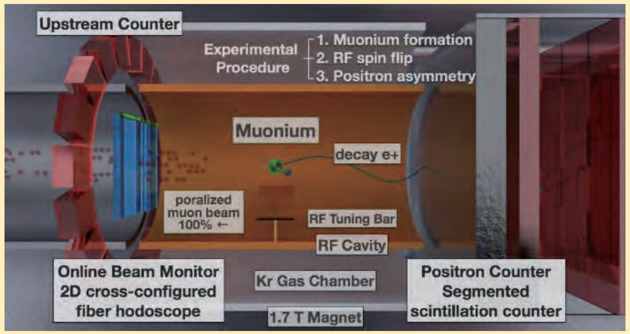

Search for muon-to-electron conversion (DeeMe experiment)

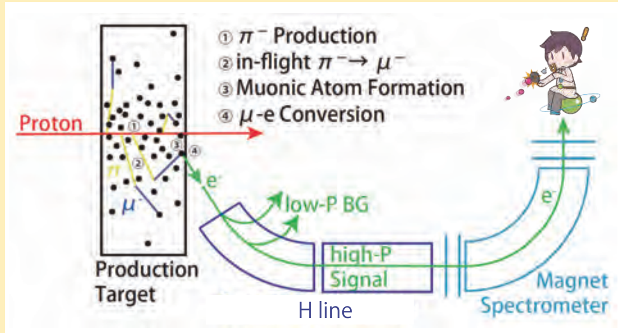

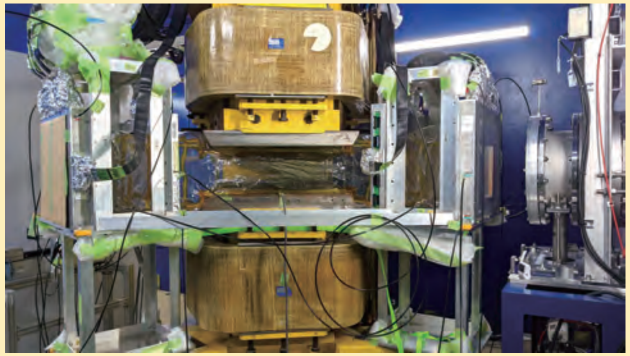

S1

Muon spin rotation/relaxation/resonance

General purpose μSR spectrometer (ARTEMIS)

Muon spin rotation/relaxation/resonance (μSR) measurements for electronic properties of materials and/or electronic state of hydrogen introduced to the material.

Instrument Description

- Positive muons (μ^+) with 27-MeV/c momentum (Surface muon)
- Single pulse- or double pulse-operation can be chosen by using the beam kicker.
- Spectrometer: ARTEMIS (1280 ch detectors)

Specifications

- μSR signal count rates with a flypast chamber @ 800kW
  - ◆Sample with ∅25 mm :
    180 M events/hour (Double pulse)
    90 M events/hour (Single pulse)
  - ◆Sample with ∅10 mm :
    60 M events/hour (Double pulse)
    30 M events/hour (Single pulse)
- Longitudinal magnetic field: max 0.4 T
- Transverse magnetic field: max 12.5 mT (40 mT with μTC magnet)

Sample Environments

- Oxford ^{3}He cryostat (T = 0.3 - 30 K)
- Oxford Microstat (T = 4 - 420 K)
- Furnace (T = 300 - 1073 K)

Instrument Configurations

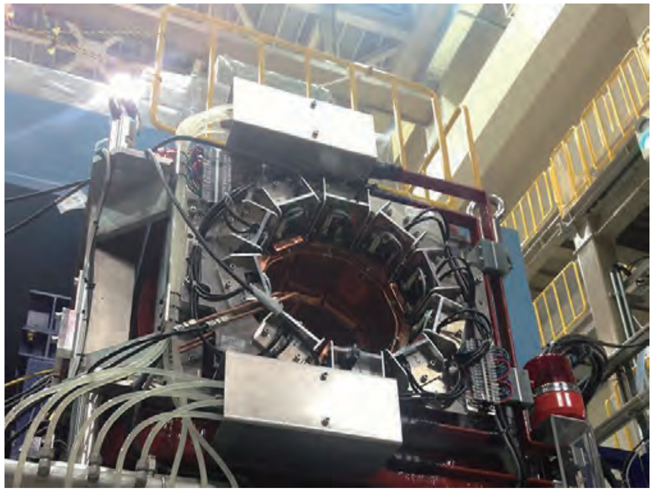

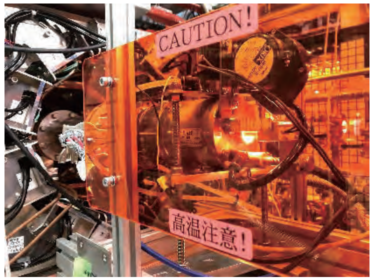

Furnace

^{3}He cryostat

CONTACT

Jumpei G. NAKAMURA
jumpei.nakamura@kek.jp

Shoichiro NISHIMURA
nishimu@post.kek.jp

General purpose μSR spectrometer (ARTEMIS)

J-PARC MLF

J-PARC

S1

Capabilities

- Magnetic and electronic states in solids observed by local magnetic field
- Electronic states of dilute hydrogen in materials
- Dynamics of electrons, hydrogen, and ions

Applications

- Local spin correlations in materials
- Cooper pair symmetry in superconductors
- Flux-line lattice in superconductors
- Electronic state of hydrogen in semiconductors
- Synthesis and reaction processes of magnetic materials
- Ion diffusion behavior in solids
- Analysis of reaction mechanisms in operando measurements

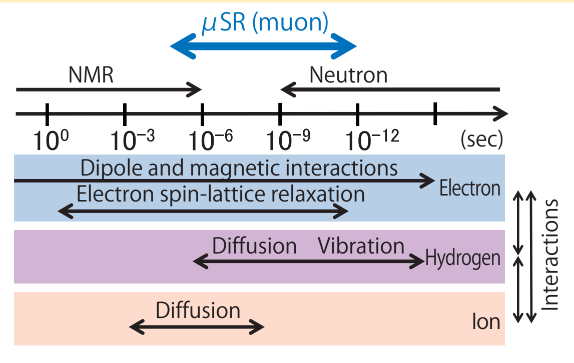

Muon's unique time resolution bridges the gap between neutron and NMR

Desorption reaction process of hydrogen storage materials （MgH_2）

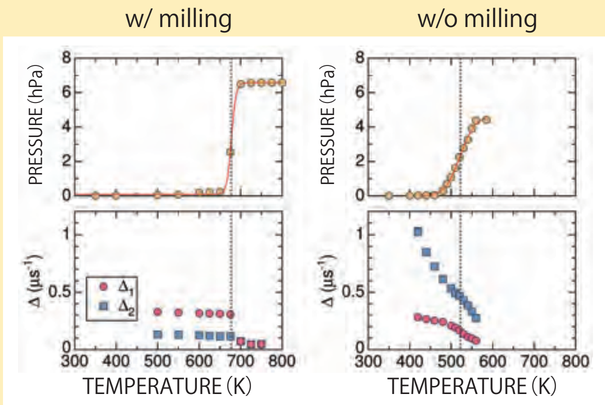

Δ is nuclear field distribution width determined by μSR

Sustainable Energy & Fuels 3, 956 (2019). (© 2019 Royal Society of Chemistry)

Electronic state of hydrogen in semiconductors ($InGaZnO_4$)

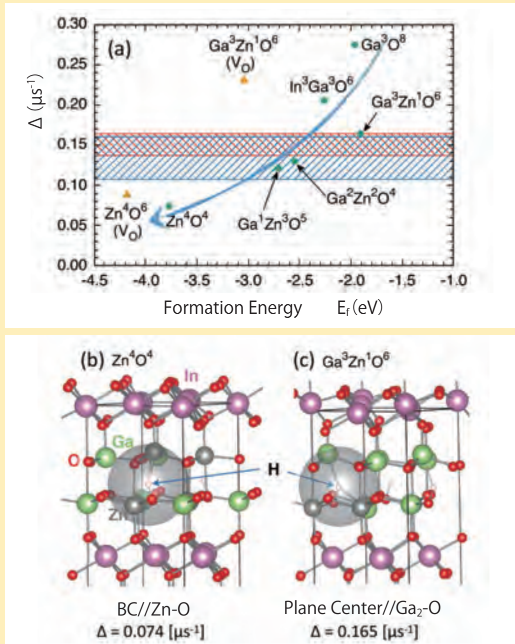

Appl. Phys. Lett. 115, 122104 (2019). (© 2019 AIP Publishing)

S2

Fundamental muon physics / Negative muon X-ray elemental analysis

Muonium Laser Physics Apparatus (Muon S2)

Precise measurement of muonium energy levels using lasers, or ultra-slow muon production by three-photon ionization of muonium

Instrument Description

- Pulsed surface muon (positive) beam available
- Possibility to bring in user equipment and conduct experiments that require high statistics over long beamtimes.
- Completely enclosed area available for laser experiments

Specifications

- Beam performance
  27 MeV/c positive muon
  both single and double pulse modes available
  (requires coordination with S1 area)
- Beam intensity
  ~ 3×10^{6} μ^{+}/s (single pulse) at 760 kW

Sample Environments

- Open space
- Area size
  Length: 5.0 m
  Width: 3.8 m
  Height: 2.8 m
- Utilities
  Cooling water
  Electrical power
  Compressed air & exhaust

Instrument Configurations

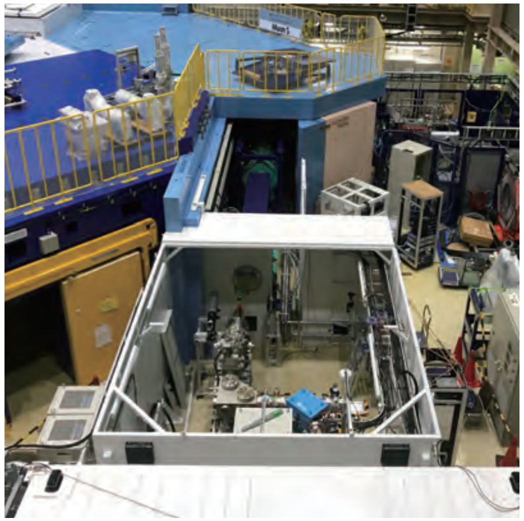

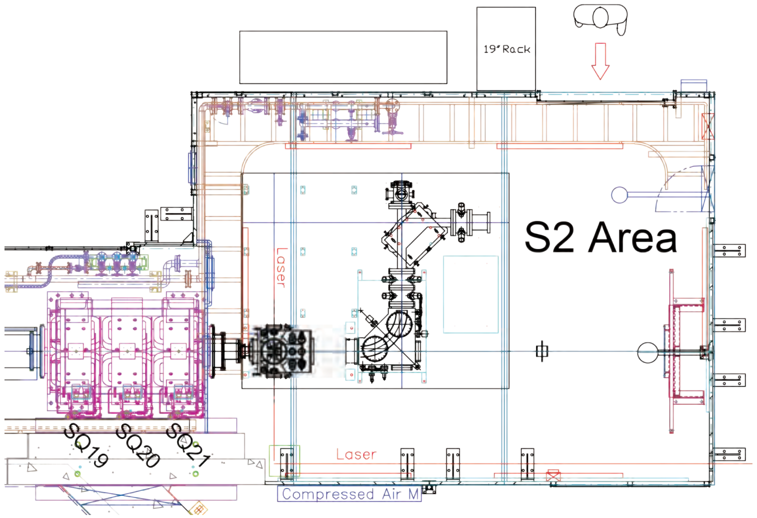

CONTACT

Patrick STRASSER
patrick.strasser@kek.jp

Jumpei G. NAKAMURA
jumpei.nakamura@kek.jp

Muonium Laser Physics Apparatus (Muon S2)

Capabilities

- Generate muonium (an exotic atom consisting of a positive muon and an electron) from slow muons pulled out from an accelerator.
- Irradiate with ionizing lasers (resonant ionization dissociation method) to strip off electrons.
- Generate ultra-slow muons with thermal energy (approximately 0.03 eV).

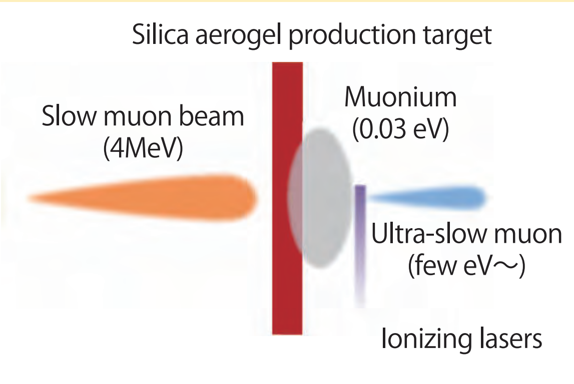

Ultra-slow muon generation

Applications

- Muonium precision laser spectroscopy experiment
- Acceleration of ultra-slow muons using radio-frequency quadrupole linac (RFQ)

Precise measurement of the 1s–2s energy interval in muonium

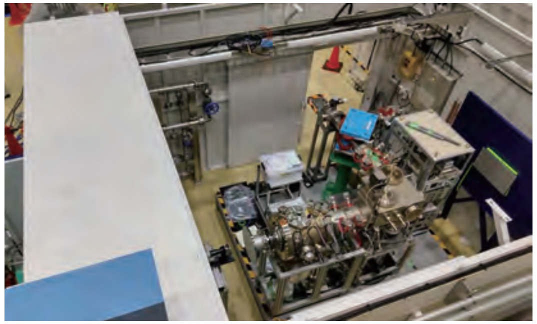

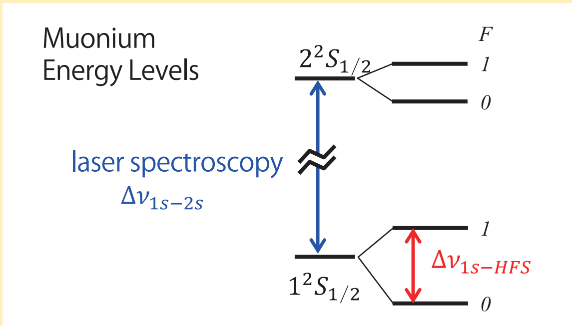

S. Uetake *et al.*, High Energy News **39** (4), 170 (2021) (in Japanese)
(©2021 Japan Association of High Energy Physicists)

Acceleration of ultra-slow muons by radio-frequency quadrupole linac (RFQ)

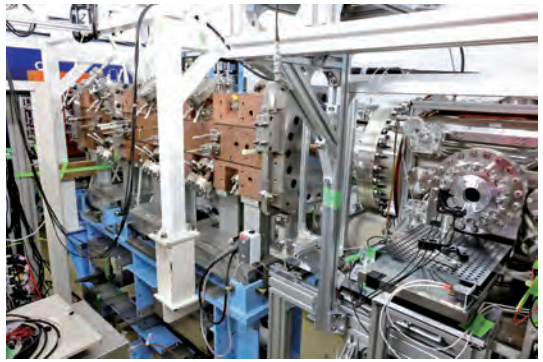

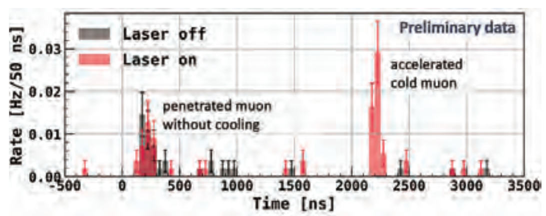

Preliminary experimental results in S2 area (2024)

U1A

Muon spin rotation/relaxation/resonance

Ultra-Slow Muon Microscope (Muon U1A)

A high time-resolution, depth-resolved probe that elucidates surface and interface magnetism with extremely small compasses

Instrument Description

- Ultra-slow muons generated via laser ionization of thermal muonium
- Low- and tunable implantation energies 1/1000 of that of surface muons
- High time resolution comparable to that of continuous beams
- Small beam size that is 1/10 of a typical surface muon

Specifications

- Low-energy positive muons (μ^+)
- Energy: from 0.5 keV to 30 keV
- Energy spread: approx. 50 eV (FWHM)
- Time resolution: 1 ns (Std. dev.)
- Beam size: 1.6 mm (Std. Dev.)
- 512 channels positron detector

Sample Environments

- Helium-flow cryostat (4.2 K - 300 K)
- Static magnetic fields up to 0.14 T
- Current introduction
- Voltage application
- A load-lock chamber for sample transport
- RHEED

Instrument Configurations

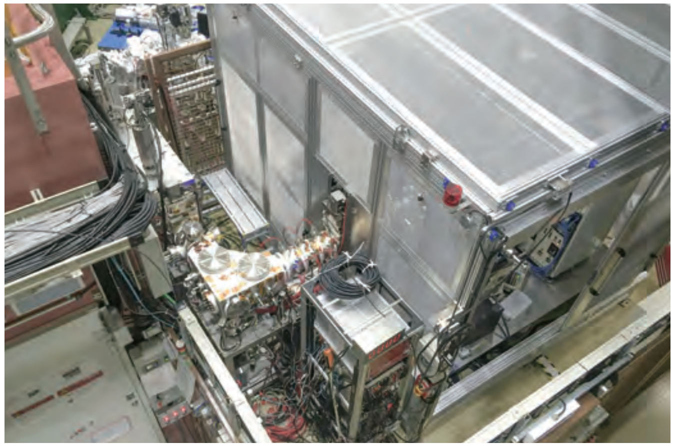

The high-voltage platform

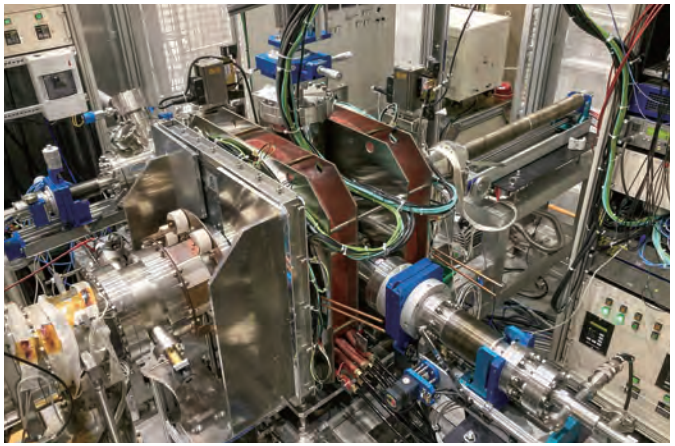

The muon spin spectrometer

CONTACT

Sohtaro KANDA
kanda@post.kek.jp

Yutaka IKEDO
ikedo@post.kek.jp

Ultra-Slow Muon Microscope (Muon U1A)

U1A

Capabilities

- Magnetic and quantum states within solid samples and their depth dependence based on internal magnetic field observations
- Electronic state of trace hydrogen within a material
- Dynamics of electrons, hydrogen, and ions within a material
- Interactions between low-energy muons and materials

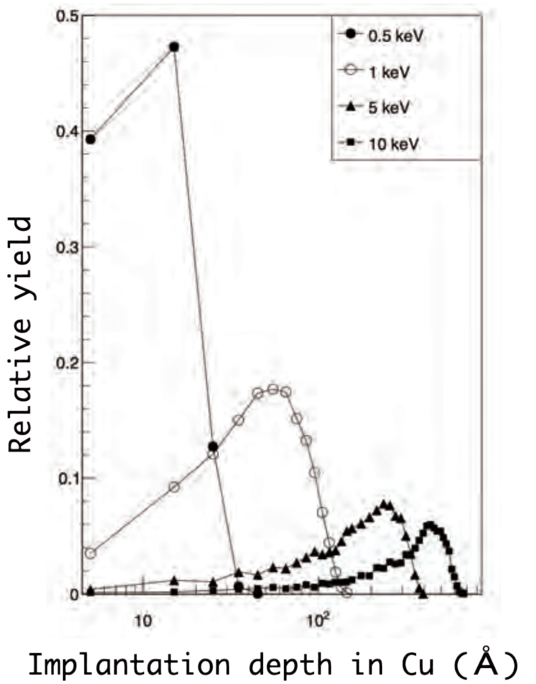

Calculated implantation depth profiles of ultra-slow muons in copper.

Applications

- Magnetic properties of thin-films and micro samples that are difficult to study with conventional μSR.
- μSR measurements that require depth resolution, such as determination of the magnetic field penetration length of a superconductor.
- μSR measurements for selective observation of the interior of materials, such as the study of superconductivity at interfaces.
- Study of elementary processes involving low-energy muons and muonium atoms

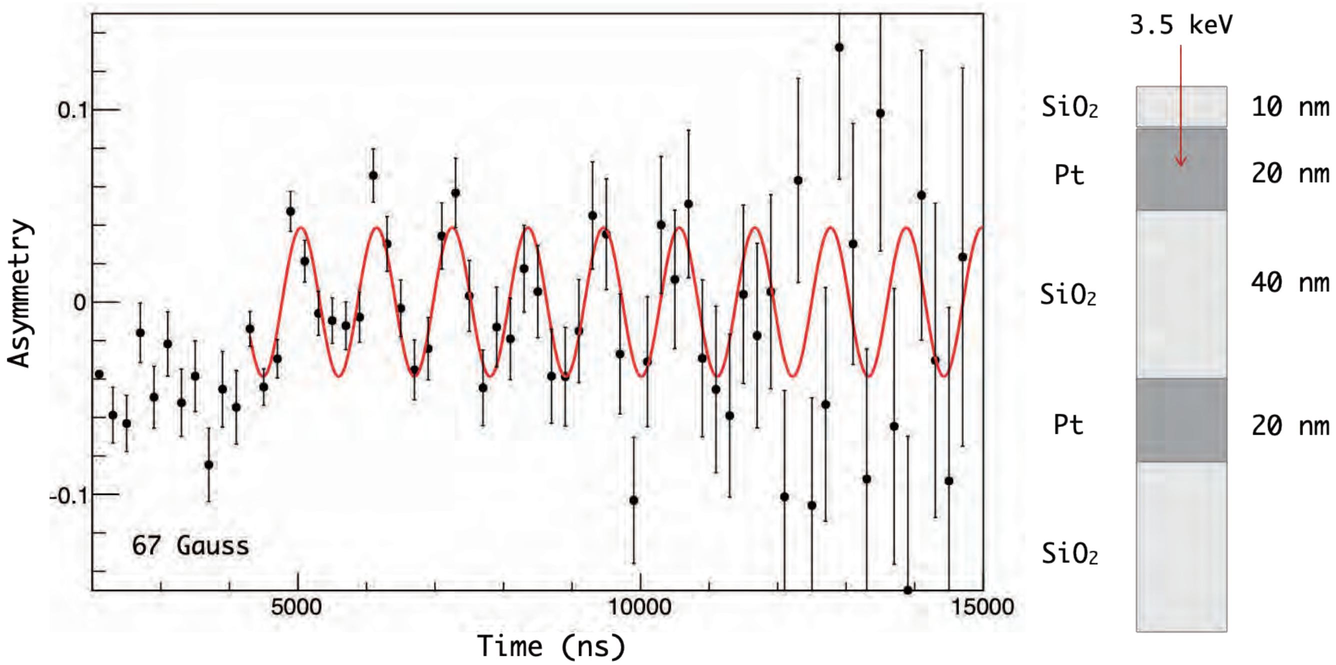

A typical result of USM-μSR with SiO2/Pt/SiO2/Pt multilayer thin-film

For neutron instruments

	Name/description	Specification
Low temperature	GM cryofurnace	Temperature range: 5 - 750 K
	2 K cryostat	Temperature range: 1.7 - 250 K
	^{3}He refrigerator	Temperature range: 0.3 - 300 K
	Dilution refrigerator	Temperature range: 100 mK - 40 K Combinational available apparatus: 7 T superconducting magnet , 2 K cryostat
High temperature	Niobium furnace	Temperature range: room temperature - 1500℃ (in vacuum), room temperature - 1000℃ (He gas atmosphere)
	SANS and WANS furnace	Heater with small windows for SANS Angle range for the incident neutrons: ∅10mm, angle range for the scattered neutrons: ±15° Temperature range: room temperature - 1000℃ (in vacuum), room temperature - 900℃ (He gas atmosphere) Heater with large scattering angles for SANS and WANS Angle range for the scattered neutrons: ±40° Temperature range: room temperature - 800℃ (He gas atmosphere)
High magnetic field	7 T superconducting magnet (vertical magnetic field)	Maximum magnetic field: ±6.85(vertical magnetic field) Temperature range: 3 - 300 K
	Pulsed magnet	Maximum magnetic field: 30 T (maximum) Sample temperature: 3 K (minimum) Repetition rate: one pulse per 1-10 min
Light irradiation	Xenon lamp	300 W
	Mercury lamp	250 W
	LED light source	367 nm (FWHM: 9 nm) , 0.53 W 408 nm (FWHM: 11 nm) , 1.34 W 441 nm (FWHM: 18 nm) , 0.62 W 521 nm (FWHM: 44 nm) , 0.50 W
	Raman spectrometer for simultaneous measurements of Raman scattering and neutron reflectivity	Wavelength of the excitation laser: 785 nm
High pressure	Paris-Edinburgh pressure cell	Opposed anvil device Maximum load 130 tf Temperature: room temperature Maximum pressure: 20 GPa Pressure range depends on the experimental setup. Please consult with the SE staff in advance.
	Syringe pump	For Paris-Edinburgh pressure cell
Stress (tension, fatigue)	Biaxial tensile testing machine	Load capacity: 50 kN Dimensions (mm) of mountable specimen: total length ≧ 130, arm width ≦ 30, thickness = 0.5 - 10
	Material testing machine*	Load: tension/compression 50 kN, 0.01 - 100 mm/min Temperature: room temperature

For neutron instruments

	Name/description	Specification
Soft matter	Rheometer	Temperature range: - 50 to 150℃ Torque: 1 nNm - 200 mNm
	High-precesion gas/ vapor adsorption analyzer	Adsorbate: N_2, Ar, H_2O, D_2O etc.
Humidity	ME240DP/ D2O/H2O mixing vapor generator for contrast variation measurements	Dew point [℃ dp]: (-15 ± 0.2) - (+85 ± 0.2) Maximum flow rate: 3 L/min Available BL: 02, 14, 15, 17
	Humicruise/ Gas flow humidity generator for quick RH change	Dew point [℃ dp]: -36 to +85, ± 1% RH@ 23℃ Maximum flow rate: 1 L/min Available BL: 02, 15, 16, 17

＊ in preparation

For muon instruments

	Name/description	Specification
Low temperature	Mini-Cryo	Temperature range: 5 - 370 K
	Microstat	Temperature range: 4 - 450 K
	Dilution refrigerator	Minimum temperature: 90 mK Sample space: ∅40 mm
	Vertical cryostat	Temperature range: 2 - 300 K
	^{3}He refrigerator	Temperature range: 0.3 - 30 K
High temperature	Furnace	Temperature range: 300 - 1000 K
Magnetic field	Longitudinal field magnet	Magnetic field range: 0 - 0.35 T
	Transverse field magnet	Magnetic field range: 0 - 0.0125 T
	Small transverse field magnet	Magnetic field range: 0 - 0.04 T
	U1A magnet	Magnetic field range: 0 - 0.12 T

1) Frustrated quantum magnet

BL01 / page 6 BL12 / page 26

A magnetic material in which it is not possible to minimize all the interaction energy acting between spins due to geometrical arrangement or competing interactions with opposite effects is called a frustrated magnet.

J-PARC press release https://www.j-parc.jp/c/press-release/2019/10/19000342.html

2) Itinerant magnet

BL01 / page 6

In general, electrons in solids are classified into two types: "itinerant states" in which they spread throughout the crystal and move freely, and "localized states" in which they are bound around atoms.
The f-electrons in rare earth and actinide compounds have properties intermediate between these "itinerant states" and "localized states" and exhibit extremely complex and strange behavior.

SPring-8 press release http://www.spring8.or.jp/ja/news_publications/press_release/2007/070901/

3) Doppler shifter

BL05 / page 13

The BL05 - NOP beamline is equipped with a ultra-cold neutron (UCN) doppler shifter for research on neutron optical devices using UCN and the development of UCN detectors. A UCN doppler shifter is a device that moves a neutron supermirror with high reflectance in the direction of propagation of incident neutrons at 1/2 of the velocity of incident neutrons, causing the neutrons reflected by the supermirror to lose velocity and become UCN.

KENS monthly report https://www2.kek.jp/imss/kens/topics/2014/04/111232.html

4) Superparamagnetism

BL06 / page 16

The magnetic energy of nanoparticles is very small, and the direction of magnetization is easily disturbed by surrounding thermal energy. Therefore, even if each nanoparticle has ferromagnetic magnetization, the direction of magnetization tends to vary among different particles. This state is called superparamagnetism.

SPring-8 press release http://www.spring8.or.jp/ja/news_publications/press_release/2004/040909/

5) Giant magnetovolume effect and negative thermal expansion

BL08 / page 18

The origin of negative thermal expansion is volume contraction accompanying the disappearance of magnetic order, the so-called magnetovolume effect.

Proceedings of 7th Japanese society Meeting for Neutron Science

6) SEOP (spin-exchange optical pumping)

BL10 / page 22

The ^{3}He spin filter is able to polarize neutrons ranging from the cold neutron to the thermal neutron, and because it is a gas, it can be formed into any shape and cover a wide range of neutron scattering angles. In the SEOP (spin-exchange optical pumping) method, the outermost shell electrons of alkali metal atoms such as rubidium are polarized using optical pumping, and 3He nuclear polarization is achieved by spin exchange between these electrons and the ^{3}He atomic nucleus.

KENS monthly report https://www2.kek.jp/imss/kens/topics/2012/12/071914.html

7） Multiferroic material

BL12 / page 26 BL23 / page 46

It is a material in which dielectricity and magnetism are combined through its structure, and magnetic and electrical properties are interconnected, and it is expected to be applied to a variety of electronic devices.

J-PARC reaserch result https://j-parc.jp/researcher/MatLife/ja/result/2012_05.html

8） Skutterudite

BL12 / page 26

The name comes from the discovery of CoAs3, a compound with this structure, in a place (Skutterud) in northwest Oslo, Norway. The chemical formula is RxT4X12 (R: metal, T: transition metal, X: pnicogen). It is known that depending on the combination of elements, materials exhibit various properties such as superconductivity, semiconductivity, and valence fluctuation.

RIKEN press release https://www.riken.jp/press/2011/20111102/index.html

9） Barocaloric effect = pressure caloric effect

BL14 / page 28

The calorific effect is when a material generates heat or absorbs heat due to external factors, such as when a magnetic material undergoes a phase transition from ferromagnetic to paramagnetic due to a magnetic field, or when a dielectric material undergoes a phase transition from ferroelectric to paraelectric due to an electric field. The pressure-caloric effect refers to a phenomenon in which a phase transition accompanied by heat absorption or heat generation is induced by pressure.

J-PARC press release https://j-parc.jp/c/press-release/2019/03/2900

Before applying a proposal to each instrument, please contact the "J-PARC Center User's Office" by email (j_proposal@ml.j-parc.jp).

〇MLF web page: https://mlfinfo.jp/en/

〇J-JOIN web page:
https://www.j-neutron.com/j-join.html

〇 J-PARC Center Users Office
〒319-1106
162-1 Shirakata, Tokai, Naka, Ibaraki
1st floor Aya's Quantum Beam Research Center

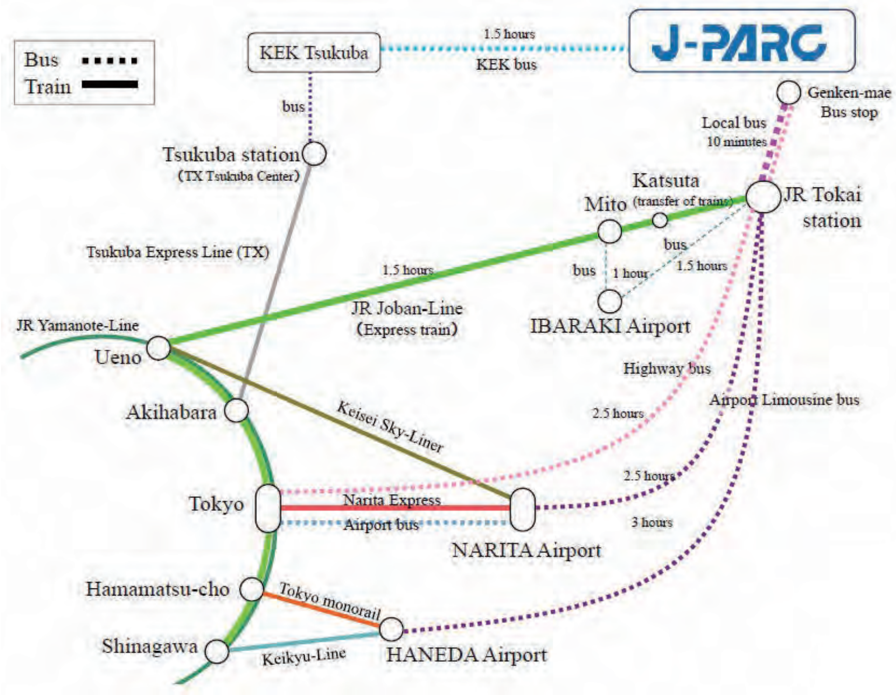

〈J-PARC Materials and Life Science Experimental Facility (MLF)〉

Neutron instruments

Muon instruments

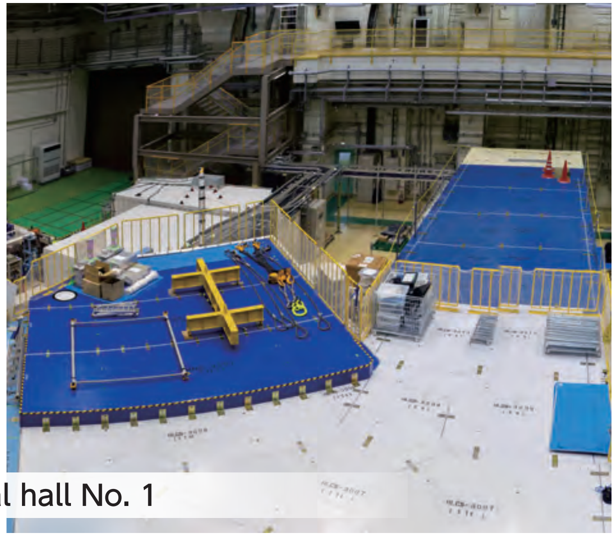

Experimental hall No. 1

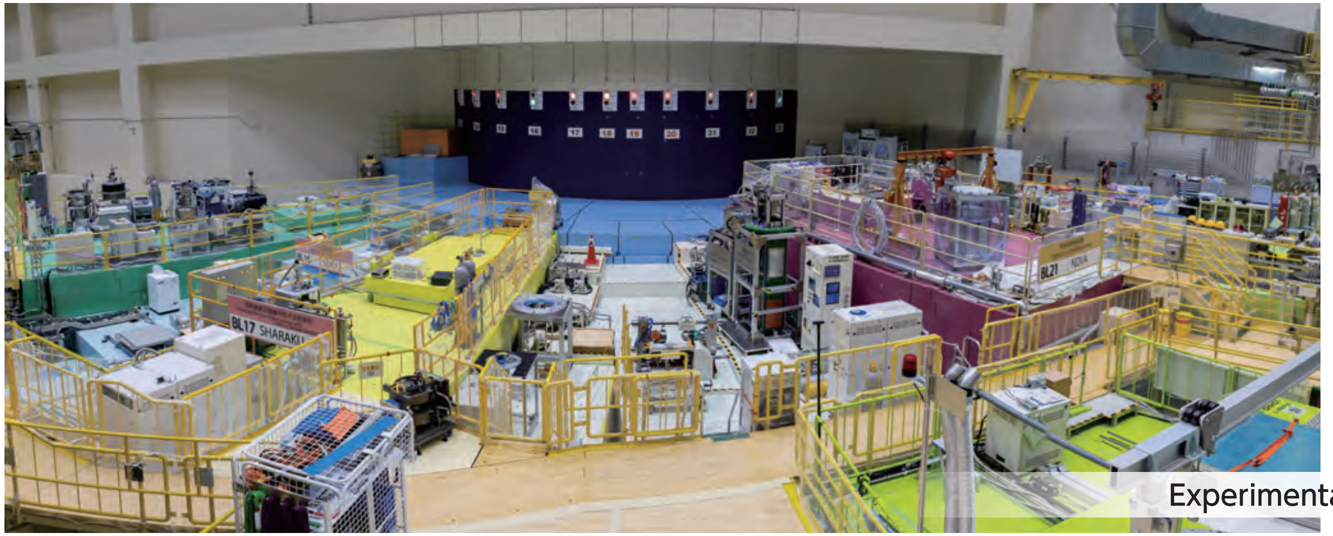

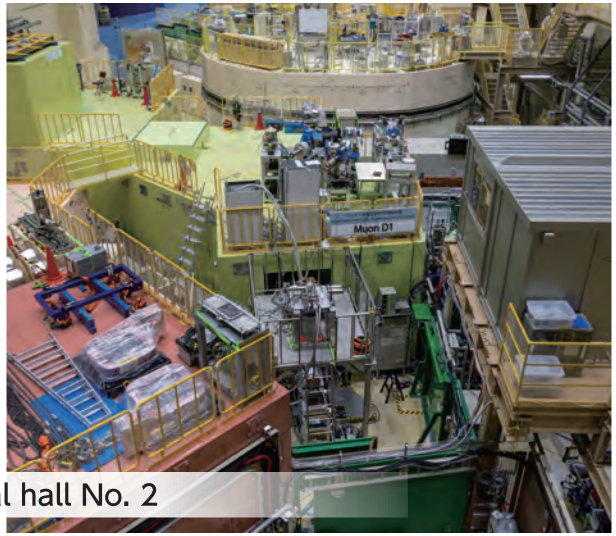

Experimental hall No. 2

CROSS

Copyright©2024

Registered Institution for Facility Use Promotion
General Incorporated Foundation,
Comprehensive Research Organization for Science and Society (CROSS)

162-1 Shirakata, Tokai, Naka, Ibaraki, 319-1106
Aya's Quantum Beam Research Center
Tel. 029-219-5300 (Representative)
URL https://neutron.cross.or.jp/en/

J-PARC

October 2024

photo credit：KEK IMSS